7-1-2015

Improving Satellite-Based Chlorophyll-a Estimating Algorithms in Shallow, Coastal Waters

tara blakey
Florida International University, tblak006@fiu.edu

DOI: 10.25148/etd.FIDC000111

FLORIDA INTERNATIONAL UNIVERSITY

Miami, Florida

IMPROVING SATELLITE-BASED CHLOROPHYLL-A ESTIMATING ALGORITHMS IN SHALLOW, COASTAL WATERS

A dissertation submitted in partial fulfillment of

the requirements for the degree of

DOCTOR OF PHILOSOPHY

in

GEOSCIENCES

by

Tara Blakey

2015

To: Dean Michael R. Heithaus
College of Arts and Sciences

This dissertation, written by Tara Blakey, and entitled Improving Satellite-based Chlorophyll-a Estimating Algorithms in Shallow, Coastal Waters, having been approved in respect to style and intellectual content, is referred to you for judgment.

We have read this dissertation and recommend that it be approved.

_____
Michael C. Sukop

_____
Georgio Tachiev

_____
Dean Whitman

_____
Assefa M. Melesse, Major Professor

Date of Defense: July 1, 2015

The dissertation of Tara Blakey is approved.

_____
Dean Michael R. Heithaus
College of Arts and Sciences

_____
Dean Lakshmi N. Reddi
University Graduate School

Florida International University, 2015

ACKNOWLEDGMENTS

I would like to acknowledge my family and colleagues that provided encouragement and support throughout the duration of the program. I would also like to thank the members of my committee Michael Sukop, Georgio Tachiev, Dean Whitman and especially my major advisor Assefa M Melesse for all their hard work. This work was supported by National Aeronautics and Space Administration's (NASA) WaterSCAPES Fellowship Program and the Florida Education Fund's McKnight Dissertation Fellowship Program.

ABSTRACT OF THE DISSERTATION

IMPROVING SATELLITE-BASED CHLOROPHYLL-A ESTIMATING ALGORITHMS IN SHALLOW, COASTAL WATERS

by

Tara Blakey

Florida International University, 2015

Miami, Florida

Professor Assefa M. Melesse, Major Professor

This work evaluated the improvement to the accuracy of chlorophyll-*a* (chl-*a*) estimating algorithms derived from Sea-Viewing Wide Field-of-View Sensor (SeaWIFS) archives of an optically-shallow, subtropical bay. Preliminary investigation into the *in situ* chl-*a* measurements showed that the fine spatial and temporal resolution currently only available through satellite remote sensing are required to adequately understand the dynamics of coastal chl-*a*. The in situ datasets, however, were found to be useful for developing chl-*a* algorithms by allowing for 1) identification of appropriate times of year for classifying benthic habitats and 2) the assumption of annually invariable bottom reflectance. Benthic type-specific algorithms were developed where benthic class was established through image-based supervised classification of Landsat images of the study area. The overall accuracy of the classifier, using available field data, was 67% and 76% for the two validation years. Although improvement to the accuracy of satellite-retrieved chl-*a* was demonstrated, the accuracy of the improved chl-a estimates remained low. Algorithms tuned to the sparse-low seagrass bottom ($r^2 = 0.234$, mean absolute percent difference (APD) = 71%) performed better than those associated with medium-dense

seagrass (r^2 = 0.332, mean APD = 66%). The positive bias produced by the operational SeaWiFS chl-*a* algorithm was removed through the regionally-tuned algorithms but the residuals of the medium-dense seagrass chl-*a* did suggest a seasonality in the bias of the improved estimates. The accessibility of the studied methodology, in terms of equipment, software and expertise required, and the lack of research into the SeaWiFS archive for multi-temporal analyses of coastal dynamics support continued development of the novel methodology. Atmospheric correction procedures derived specifically for normalizing surface reflectances across images are likely to improve the transferability of image-based classifiers as well as the performance of empirical chl-*a* algorithms. Testing the transferability of image-based optical signatures in space to other study areas is an important next step for this methodology. A well-defined spectral library of image-based classes would improve assessment of global chl-*a* dynamics, which is especially important given global climate change.

TABLE OF CONTENTS

LIST OF TABLES

TABLE PAGE

LIST OF FIGURES

FIGURE PAGE

1 INTRODUCTION

Remote sensing provides synoptic views of the globe and, at this point in time, offers a long-term and frequent record, at moderate spatial resolution. Even when field measurements are available, the coverage of satellite measurements may reduce potential spatial and temporal aliasing (Le 2012). These long-term, synoptic records allow for the evaluation of dynamic, spatially distributed processes such as land-use change detection, coastal erosion and algal blooms to name a few. Although long-term global archives of multi-spectral imagery are now readily accessible, the full temporal extent in terms of length and frequency of acquisition of these archives in the context of thematic land- and benthic-cover type mapping, is not widely utilized (Lyons 2013). These records have been demonstrated to be useful in describing and quantifying interactions between adjacent regions which can be especially instructive for system components that may be exchanged across the landscape scale relatively quickly, like water.

Understanding the seasonality and drivers of global chlorophyll levels in deep water is one such achievement that took advantage of remote sensing records to link processes in topographically adjacent regions, but also to link physical processes (temperature and nutrient upwelling) to chemical processes (ocean primary production). Methods for quantifying chlorophyll from remote sensing in coastal waters, however, have been more elusive as these waters are influenced by terrestrial inputs such as colored dissolved organic matter (CDOM) and detrital particles which may both be falsely interpreted as chlorophyll as all of these constituents absorb blue light strongly (Le 2012). In addition, coastal waters may be optically-shallow so that bottom contamination (reflectance from the benthic habitat) is included in the remotely sensed

reflectance. Despite the inherent difficulty in monitoring coastal chlorophyll levels, spaceborne imagery has been demonstrated to sufficiently track coastal chlorophyll levels so that long-term time-series chlorophyll indicators could be used to support decision making efforts of management agencies that regulate nutrient discharges (Le 2013).

1.1 Background

Long-term trends and short-term variability in spatially distributed coastal chlorophyll levels has the potential to reveal much about the contributing environment including the outcomes of water management practices in the upstream watershed. For example, the Comprehensive Everglades Restoration Plan (CERP) is being undertaken to permit hydropatterns that are more in line with pre-development flows including increased freshwater levels and greater runoff to Florida Bay. While close to half the Everglades water budget was discharged to Florida Bay under pre-drainage conditions, consumptive water use and the construction of canals that drain and redirect water have reduced the percentage of freshwater to only about 20% of the total water in the catchment (Madden 2009). Assessing phytoplankton bloom conditions is essential to ensure that water quality in the southern estuaries is not degraded by CERP implementation. For example, increases in nutrients delivered to the highly oligotrophic system may result in a eutrophic ecosystem with decreased seagrass cover and diminished extent of the high quality benthic nursery habitat necessary to support commercial and recreational fisheries (Boyer 2009).

Florida Bay and the mangrove estuaries of the Whitewater Bay area in South Florida act as the marine receiving-end of the Everglades, one of the largest wetland ecosystems of the world (Boyer 1997). Making up approximately a third of Everglades

National Park, the estuaries of Florida Bay have been well studied with on-going, periodic sampling of water quality and seagrass communities dating back to the late 1980s. Monitoring efforts began after severe water quality problems were observed in the lagoon when remarkable seagrass die-offs, algal blooms and high turbidity were observed in the late 1980s and early 1990s. The bay was not the subject of water quality investigations prior to the die-offs when it was considered to be a viable, healthy and undisturbed ecosystem (Stumpf 1999).

The abundance and distribution of seagrasses in Florida Bay declined by approximately 30% throughout the 1980s and 1990s and the area covered by Everglades National Park is believed to have sustained the greatest losses, estimated at 270 km^2 or 51% of the total regional loss (McPherson 2010). While consensus on the initiating cause of these seagrass declines is lacking, the losses have been linked to phytoplankton blooms and water quality factors, underscoring the importance of monitoring phytoplankton blooms. Phytoplankton blooms decrease light penetration through the water column and can depress seagrass growth, resulting in seagrass decomposition along with the subsequent destabilization of benthic sediments and the release of nutrients which stimulate phytoplankton growth, so that positive feedback loops are possible (Boyer 2009). Seagrass declines in Everglades National Park and greater Florida Bay were accompanied by a cascade of ecological changes including (a) considerable reductions in water transparency resulting from increased phytoplankton abundance and particulate turbidity (b) declines in fish and invertebrate populations and (c) blooms of nuisance macroalgae (McPherson 2010).

The high chlorophyll levels observed mainly in the north- and south- central regions of the bay have been attributed to urban and agricultural anthropogenic changes occurring in South Florida where the most prominent of these changes have been the reduction of freshwater inflow to the bay via the Everglades and general eutrophication of surface waters entering certain regions of the bay via inflows (Phlips 1995). Although the chain of events initiating the mass die-off of seagrass is still not fully understood, water quality deterioration resulting in light limitation is a leading cause of their decline throughout the world (McPherson 2010). Seagrass loss in temperate zones generally comes from increased inputs of nitrogen and phosphorus along more industrialized coasts while in many tropical environments it is primarily caused by sediment discharge into coastal waters due to watershed deforestation and mangrove clearing (Ferwerda 2007). While the role of eutrophication and sedimentation in seagrass loss may differ geographically, associations between anthropogenic land-use changes, water quality, and coastal ecosystem health are undeniable. Therefore, it is important to consider reductions in phytoplankton blooms in the southern estuaries as an indicator of ecosystem restoration success both because blooms could significantly harm these estuaries and adjacent coastal systems and because they occur at the terminus of the entire Kissimmee-Okeechobee-Everglades ecosystem (Boyer 2009).

1.2 Statement of the Problem

Working towards a protocol for assessing Florida Bay water quality that is able to attribute causative factors to past and future ecosystem degradation and support water managers in reducing negative impacts to Florida Bay and similar estuaries is an overlying motivation for the present study. The strength of long term, synoptic data is

only taken advantage of if the methods used to interpret the data are transferrable in time and space.

Few, if any, studies have evaluated improvements to the accuracy of multispectral satellite chl-*a* retrievals in optically shallow water where bottom reflectance is substantial. Le *et al.* (2013) developed a Red-Green-Chlorophyll-Index for multispectral retrieval from estuarine waters achieving uncertainties comparable to those from open ocean waters, but pixels contaminated by bottom reflectance were excluded. Using remote sensing reflectance (R_{rs}) falling outside the transparency window (i.e., $R_{rs}410$ and $R_{rs}670$), Cannizzaro *et al.* (2006) improved chl-*a* algorithm accuracy for optically-shallow water with substantial bottom reflectance. Although the algorithm developed by Cannizzaro was based on wavelengths available from multi-spectral satellite data, that work utilized shipboard and mooring collected reflectances and did not explicitly test the applicability to satellite-based ocean color data.

Therefore, a need for rigorous testing of approaches to solve the problem of bottom contamination in satellite-retrieved data exists. Because the Florida Bay study area is associated with a long record of field studies and *in situ* data on water quality and benthic environments, methods developed here may then be applicable to comparable areas that may not be associated with adequate field data for algorithm development and validation.

1.3 Research Objectives

Consideration of the use of remote sensing to assess variability in water quality in Florida Bay led to the formulation of four research objectives:

- **Research Objective 1** – Understand the spatial and temporal dynamics of chl-*a* concentrations in the study area, including links to water management and other inland activities, as observed from in situ data records.
- **Research Objective 2** – Understand the spatial and temporal dynamics of seagrass and submerged aquatic vegetation (SAV) observed in the study area, including correlations with chl-*a* concentrations, as observed from *in situ* data records.
- **Research Objective 3** – Classify and map seagrass and SAV from space-borne images of the study area through the use of spectral data and information gained from completion of Objectives 1 and 2.
- **Research Objective 4** – Improve on available algorithms for deriving chl-*a* concentration indicators from space-borne imagery in coastal, optically shallow waters, such as those found in the study area.

Chapter 2 documents the work on Objective 1 while Objectives 2 and 3 are covered in Chapter 3 and Objective 4 is covered in Chapter 4. Chapter 5 provides conclusions for the project as a whole. References in Chapters 2 and 3 are formatted for publication in the journals CATENA and Remote Sensing, respectively.

References

Boyer, .J., Kelbe, C., Ortner, P., Rudnick, D. (2009). Phytoplankton bloom status: Chlorophyll a biomass as an indicator of water quality condition in the southern estuaries of Florida, USA. Ecological Indicators, 9, s56-s67.

Boyer, J., Fourqurean, J. (1997). Spatial characterization of water quality in Florida Bay and Whitewater Bay by multi-variate analyses: zones of similar influence. Estuaries, 20, 743-758.

Cannizzaro, J.P., Carder, K.L. (2006). Estimating chlorophyll *a* concentrations from remote sensing reflectance in optically shallow waters. Remote sensing of the Environment, 101, 13-24.

Ferweda, J., de Leeuw, J., Atzberger, C., Vekerdy, Z. (2007). Satellite-based monitoring of tropical seagrass vegetation: current techniques and future developments. Hydrobiologia, 591, 59-71.

Le, C., Chuanmin, H., English, D., Cannizzaro, J., Chen, Z., Feng, L., Boler, R., Kovach, C. (2012). Towards a long term chlorophyll-a data record in a turbid estuary using MODIS observations. Progress in Oceanography, 109, 90-103.

Le, C., Chuanmin, H., English, D., Cannizzaro, J., Chen, Z., Feng, L., Kovach, C., Anastasiou, C., Zhao, J., Carder, K. (2012). Inherent and apparent optical properties of the complex estuarine water of Tampa Bay: What controls light? Estuarine Coastal and Shelf Science, 117, 54-69.

Le, C., Chuanmin, H., English, D., Cannizzaro, J., Kovach, C. (2013). Climate driven chlorophyll-a changes in a turbid estuary: Observations from satellites and implications for management. Remote sensing of Environment, 130, 11-24.

Le, C., Chuanmin, H., English, D., Muller-Karger, F., Lee, Z. (2013). Evaluation of a chlorophyll-a remote sensing algorithms for an optically complex esturay. Remote sensing of Environment, 129, 75-89.

Lyons, M., Roelfsema, C., Phinn, S. (2013). Towards understanding temporal and spatial dynamics of seagrass landscapes using time-series remote sensing. Estuarine Coastal and Shelf Science, 120, 42-53.

McPherson, M., Hill, V., Zimmerman, R., Dierssen, H. (2010). The optical properties of Greater Florida Bay: Implications for seagrass abundance. Estuaries and Coasts, 34, 1150-1160.

Phlips, E.J., Lynch, T., Badylak, S. (1995). Chlorophyll a, tripton, color and light availability in a shallow tropical inner-shelf lagoon, Florida Bay, USA. Marine Ecology Progress Series, 127, 223-234.

Stumpf, R.F., Frayer, M., Durako, M., Brock, J. (1999). Variations in water clarity and bottom albedo in Florida Bay from 1985 to 1997. Estuaries, 22, 431-444.

2 TOWARD CONNECTING SUBTROPICAL ALGAL BLOOMS TO FRESHWATER NUTRIENT SOURCES USING A LONG-TERM, SPATIALLY DISTRIBUTED, IN SITU CHLOROPHYLL-A RECORD

Blakey T, Melesse A, Rousseaux C (2015). Toward connecting subtropical algal blooms to freshwater nutrient sources using a long-term, spatially distributed, in situ chlorophyll-*a* record. CATENA, 133, 119-127.

Abstract

Harmful algal blooms are increasing in tropical estuaries which can have complex morphologies and hydrologic regimes while being less well studied than temperate estuaries. Spatial and temporal patterns of algal bloom occurrence in Florida Bay were examined to evaluate the potential contribution of the various freshwater inputs to the subtropical bay as nutrient sources. Monthly water quality data, from 1989 to 2009, at 28 sampling stations across the bay were analyzed at the station-month level, aggregated into hydrologic Zones of Similar Influence and based on annual rainfall seasons. The Zones of Similar Influence are linked to the geomorphology of the bay with western areas being more directly connected to the Southwest Florida Shelf waters than eastern areas. Correlation analysis suggested that inputs of phosphorus were the predominant factor in the initiation of elevated chlorophyll a (chl-*a*) levels but was also consistent with higher nitrogen limitation in western Florida Bay as reported in literature. Differences in mean monthly chl-*a* indicated a seasonality of algal blooms with elevated chl-*a* concentrations following heavy precipitation months for stations in the north-central and western areas of the bay where algal blooms have been re-occurring. Differences in stations' chl-*a* concentrations showed stations to the northwest as having significantly higher concentrations than more interior stations during the dry season but not during the rainy season (when algal blooms are occurring). Mapping the sampling stations atop the

bathymetry of Florida Bay highlighted the importance of coastal morphology in evaluation of potential nutrient pathways for estuarine algal bloom sources. The specific factors resulting in the seasonal cycles of blooms remained unresolved but portions of the bay and times of year were identified as important areas for further research. This study indicates that illustrating the interplay of geomorphology and winds and rains at fine temporal and spatial resolution is required to describe nutrient circulation for systems with complex morphologies such as those associated with reefs, island matrices and headlands.

Key words: tropical environment; eutrophication; Chl-*a*; Florida Bay; nutrients; algal blooms

2.1 Introduction

Tropical harmful algal blooms (HABs) are increasing in frequency and intensity, and are substantially affecting marine communities, as a result of increased coastal eutrophication, changes in oceanic climate and enhanced long-distance dispersal in ballast water (Bauman et al., 2010). While human activity has significantly altered water discharges throughout the world, the impacts within any particular estuarine system depend critically on the nature of the coastal sea such as its flushing characteristics (Jickells et al., 2014). The complex morphology associated with reefs, island archipelagos, capes and headlands can play an important role in determining the ecological function of coastal waters. Regions inshore of reef and island matrices are isolated by varying degrees from adjoining offshore oceanic waters, potentially leading to localized physical and biogeochemical processes and to large variations in the function of planktonic ecosystems over small spatial areas (Jones et al., 2014). Control of HABs in these types of systems,

therefore, depends on information of adequately fine scale and resolution in order to determine the influence of the complex morphologies on water mass properties.

Florida Bay is recognized for its productivity, diversity and role as a marine nursery (Butler et al., 1995). Bounded on the east and south by the Florida Keys and to the west by the Gulf of Mexico on the southwest Florida shelf, the bay is a critical part of a complex system involving freshwater marshes, mangrove ecotones and islands, seagrass meadows and coral reefs. The Florida Bay-Everglades ecosystem is unique among North American estuaries because of its carbonate sedimentary environment, restricted tidal regime and subtropical climate (Sutula et al., 2003). Tropical and subtropical estuaries are typically dominated by calcium carbonate sediment, as opposed to silicate or clay-dominated sediments of temperate coastal regions (Koch, 2001), which generally leads to phosphorus limitation as calcium carbonate scavenges phosphate from seawater (Brand, 2002).

In the late 1980s, algal blooms began to be documented as a new threat to Florida Bay, especially in association with ecosystem degradation and decline in commercially important species including seagrass, corals and sponges as well as fish and lobster (Butler et al., 1995; Phlips et al., 1999). Prolonged pico-cyanobacterial blooms are believed to now threaten the ecological health of this system (Gilbert et al., 2009) and many genera of cyanobacteria are known to produce toxic compounds (O'Neil et al., 2012). While HABs have been re-occurring into the present in western and north-central regions of the bay, the direct chain of events leading to the initiation and persistence of HABs in the estuary remains unclear (Butler et al. 1995; Brand, 2002; Richardson, 2002; Boyer et al., 2009; McCarthy et al., 2009) as in other tropical estuaries around the world (Bauman et al., 2010). Of particular interest is the source of nutrients for these blooms. Uncertainty about the

specific factors leading to the HABs limits the management of the estuary and could allow for eutrophication here and in other estuaries experiencing similar problems.

While spring phytoplankton blooms are ubiquitous in temperate coastal systems, phytoplankton blooms in fall and summer have gained attention in recent years as a consequence of their increasing recurrence (Guinder et al., 2013). These events have been related to climate trends such as changes in rainfall (Briceño and Boyer, 2010) and temperature (McCarthy et al., 2009) and to anthropogenic disturbance (Gilbert et al., 2009), however the underlying causes remain a matter of debate. Importantly, there is consensus that HABs are complex events, typically not caused by a single environmental driver but rather multiple factors occurring simultaneously (O'Neil et al., 2012). Assessing the systematic effect of factors influencing the occurrence of fall HABs in Florida Bay can provide information that is relevant to other estuaries facing eutrophication especially since considerably less is known about how tropical coastal ecosystems function compared to their temperate counterparts (Gilbert et al., 2009).

The objective for this work was to evaluate the spatial and temporal dynamics of chlorophyll-*a* (chl-*a*) concentrations, indicative of phytoplankton biomass, in the study area using a 20 year-long in situ data record. Chl-*a* concentrations from 28 stations divided in 6 zones were analyzed. Correlations between chl-*a,* at the resolution of monthly measurements at individual stations, and potential driving forces were tested and then assessed in light of the study area's morphology and hydrologic regime. The chl-*a* concentrations were compared across stations and months to assess the magnitude and timing of algal bloom occurrence in relation to location. Completion of these objectives is expected to provide information that will be useful in assessing the causes of tropical algal

blooms through the identification of seasonal patterns in phytoplankton biomass and by substantiating connections with potential nutrient sources.

2.2 Methods

2.2.1 Study Site

Florida Bay (Fig. 1) is a shallow lagoon located off the southern tip of the Florida peninsula with depths of less than 4 meters throughout (Phlips et al., 1995). It is bounded by the Everglades to the north and is open to the Gulf of Mexico along its western margin. The main line of the Florida Keys, a Pleistocene reef, separates Florida Bay from the Atlantic Ocean (Boyer, 1997; Wanless and Tagett, 1989).

South Florida's subtropical climate can be subdivided into dry (November through May) and wet (June through October) seasons (Steinman et al., 2002). The annual average precipitation for South Florida (Lake Okeechobee and south) for 1976-2001 was 132 cm (52 in). In Florida Bay, the lowest mean monthly temperature occurs during the dry season (20^{o}C in January) and the highest monthly mean temperature coincides with the wet season (28^{o}C in August) (Briceño and Boyer, 2010).

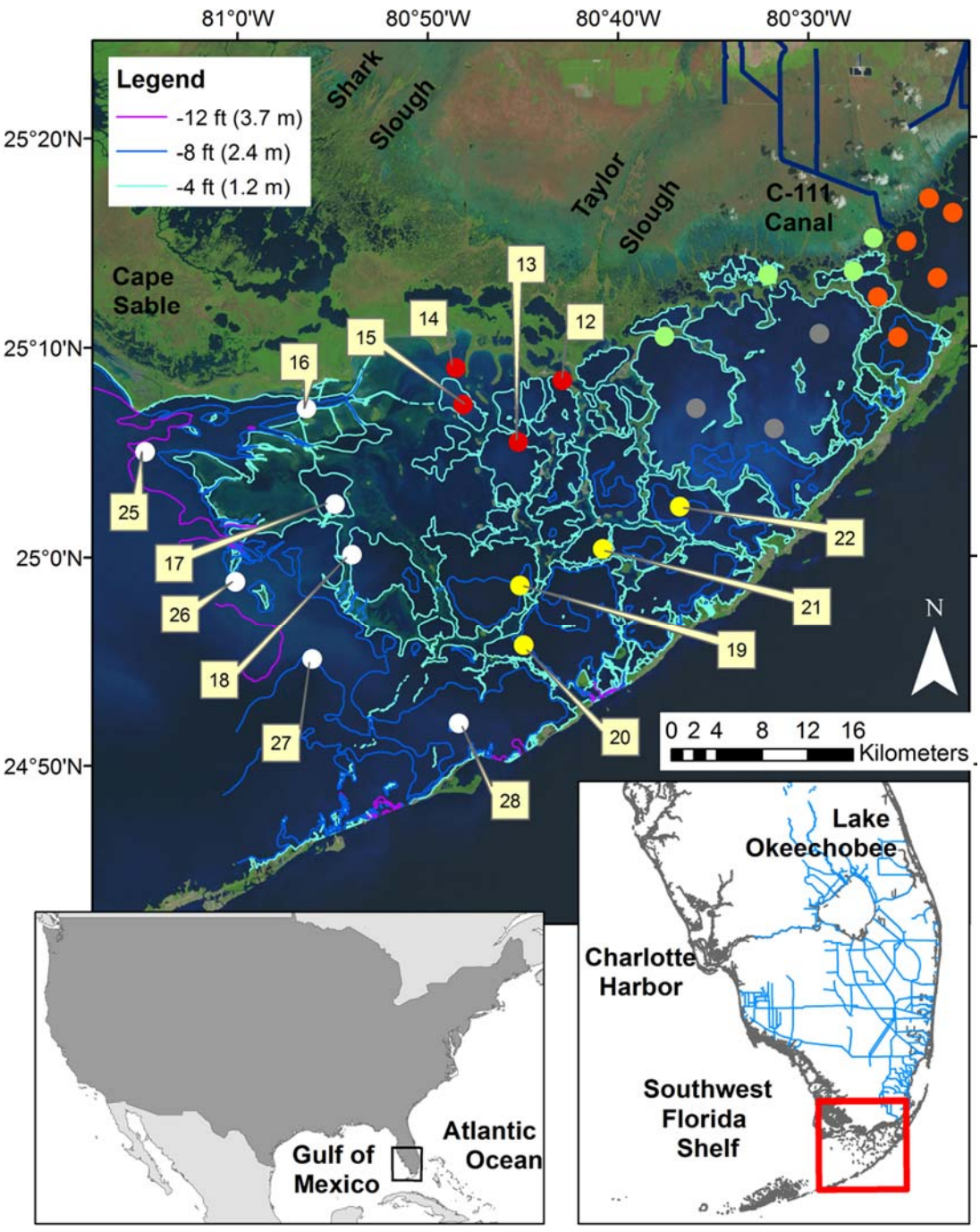

Figure 2.1 April 12, 1998 Sea-Viewing Wide Field-of-View Sensor (SeaWIFS) image of study area showing Florida Bay water depth contours and sampling stations. Color groupings indicate the different Zones of Similar Influence with orange circles for Florida Bay East (FBE), green for North Bay (NB), grey for Florida Bay East Central (FBEC), red for Florida Bay Central (FBC), yellow for Florida Bay South (FBS) and white for Florida Bay West (FBW). Station numbers are included for reference for central and western bay stations.

Florida Bay is at the downstream end of the Kissimmee River-Lake Okeechobee-Everglades watershed and can therefore be affected by any changes that occur in that hydrological system (Brand, 2002). The Everglades, one of the largest freshwater wetlands in North America, are highly oligotrophic with phosphorus (P) being the limiting macronutrient (Childers et al., 2002). The two important drainage areas making-up the remaining wetlands of the Everglades are Taylor Slough in the southeast and the much larger Shark Slough to the north and west.

Changes in the timing and magnitude of water entering the Everglades have been caused by anthropogenic development in South Florida, where a vast network of levees, pumps and canals now cover South Florida. The majority of freshwater that historically flowed from Lake Okeechobee south through the Everglades has been diverted to the Atlantic Ocean and Gulf of Mexico by a network of 2,400 km of canals (SFNRC, 2012).

2.2.1.1 Florida Bay Hydrogeology

Florida Bay is made up of ecologically disparate basins (varying in sediment type, sediment depth, and benthic vegetation) that are structurally defined by a network of mudbanks (Phlips et al., 1995). The banks are broad with gently sloping flanks and cover a majority of the area in the western portions of the bay whereas banks in the eastern portions of the bay are narrow and discontinuous with steep windward flanks (Taylor and Purkis, 2012; Wanless and Tagett, 1989). Direct freshwater runoff into Florida Bay is largely restricted to the northeast portions where Taylor Slough and the C-111 canal drainage basins meet the estuary.

In Florida Bay, the hydrology of the system dominates the ecological and geochemical dynamics (Gilbert et al., 2009) with the various regions of the bay being

associated with differing hydrologic regimes and therefore differing geochemical dynamics. The network of mudbanks impedes water circulation within the bay as well as tidal exchange with the adjacent Gulf of Mexico and Atlantic Ocean (Briceño and Boyer, 2010). The southeastward flow connecting the Gulf and Atlantic entrains freshwater outflows from the Everglades' Shark Slough and results in a low salinity band extending along the coast and into northwestern Florida Bay (Lee et al., 2002). Shelf waters are periodically directed into the bay interior by prevailing currents (Gilbert et al., 2009; Briceño and Boyer, 2010). Being semi-isolated, the central and eastern basins have longer residence times than the more open southern or western regions (SFNRC, 2012). Seasonal variations in wind direction and magnitude were shown by Lee and Smith (2002) to lead to predictable changes in the direction and volume of flow through the middle Keys at the south of Florida Bay.

Groundwater is gaining increasing attention as a source of inputs to the Everglades and Florida Bay. The Biscayne aquifer, which extends from Palm Beach County and underlies Florida Bay and the Florida Keys (Chen et al., 2010), is one of the most productive karst aquifers in the world with its thickness increasing in a southeasterly direction from a feather edge in northwestern Shark Slough to over 65 m thick along the southeastern coastline (Price et al., 2006). Salt water intrusion into the porous aquifer creates a mixing zone where the more dense seawater mixes with the less dense, inland freshwater. Several studies have found brackish groundwater discharge to occur in the mixing zone (Spence, 2011). The position and extent of the mixing zone and the flux of its associated brackish groundwater discharge are governed by many factors such as rainfall, groundwater withdrawals, irrigation, evapotranspiration, waves, and changes in sea level

(Price et al., 2006). Significant exchange has also been documented from the aquifer beneath the Florida Keys into Florida Bay due to differences in surface water levels between the bay and Atlantic Ocean that occurs on the tidal cycle (Chen et al., 2010).

2.2.1.2 Florida Bay Algal Blooms

Florida Bay has historically had a clear water column supporting low phytoplankton biomass (Richardson, 2009) whereas, in more recent times, algal blooms have been re-occurring in the northwestern and north-central portions of the bay. Boyer and Fourqurean (1997) found that median chl-*a* concentration was not significantly different in western and central portions although the phytoplankton communities differed. Phytoplankton community composition has been typically dominated by centric (*Rhizosolenia* spp.) and pennate diatoms (*Cocconeis, Navicula*, and *Surirella* sp.) in the west whereas blooms in the central and, occasionally, eastern areas of the bay have been dominated by the pico-cyanobacteria *Synechoccus* spp. (Gilbert et al., 2009). In laboratory experiments on interspecific differences between the cyanobacteria and diatom species from Florida Bay, Richardson (2009) found that *Synechococus* spp. had an advantage in nutrient competition while diatoms were associated with superior maximum growth rates. *Synechococus* spp. has also been documented to thrive at low irradiances, resist viral infection, adapt to salinity variations (McCarthy et al., 2009) and be associated with low grazing losses (Richardson, 2009).

The western Florida Bay blooms, dominated by open water shelf species, have been known to occur from late summer/fall to winter (Richardson, 2009; Vargo et al., 2009). Central-zone blooms tended to originate in the north-central region in the summer, spreading principally into the south-central region as the bloom grows during the fall, and

dissipating during the winter to spring period by shrinking to a small bloom located in the north-central zone (Richardson 2009).

The central basins' large blooms of *Synechoccus* spp. occurred in an area of transition between P and N limitation (Gilbert et al., 2009). The spatial gradients of P and N have been hypothesized to reflect their west Florida shelf and freshwater runoff source waters, respectively (Richardson, 2009; Brand, 2002).

The *Synechoccus* spp. blooms in Florida Bay were most pronounced in the mid-1990s (Gilbert et al., 2009). Inter-annual trends in phytoplankton biomass have been explained by variations in climatic conditions. Briceño and Boyer (2010) showed a general decline in phytoplankton biomass across the bay, at least until 2005, that was explained by a regime system shift from below average to above average rainfall centered around 1994-1995. The generalized decline was interrupted by regionally specific, sudden increases in chl-*a* that were correlated with hurricane events. Similar results were found by Le et al. (2013) in Tampa Bay, Florida where, on average, river discharge could explain ~60% of the seasonal changes and ~90% of the inter-annual changes in the chl-*a* record, with the latter mainly driven by climate variability (e.g. El Niño and La Niña years) and anomaly events (e.g. tropical cyclones).

Algal blooms have been studied more intensively for the greater southwest Florida shelf than for Florida Bay in particular with most of the studies focusing on the region between Tampa Bay and Charlotte Harbor where *Karenia brevis* blooms occur almost annually (Heil et al., 2007). For this larger region, Heil et al. (2007) found N limitation in the northern areas and P limitation south of the Shark River with phytoplankton community composition varying along the same gradient from a cyanobacteria- and dinoflagellates-

dominated community in the vicinity of Tampa Bay and Port Charlotte to a diatom-dominated community in the southern part of the shelf.

2.2.2 Dataset

A network of water quality monitoring stations, the South Florida Water Quality Management Network, was established in Florida Bay by the Southeast Environmental Research Center at Florida International University. Water column measurements and samples were collected every other month from July 1989 to December 1990, monthly from March 1991 to September 2008 (Briceño and Boyer, 2010) and in June 2009 at selected stations. The data is available from the Center's website at serc.fiu.edu/wqmnetwork/SFWMD-CD/Pages/DataDL.htm (accessed May 31, 2013). Field measurement of chl-*a*, salinity (surface and bottom), temperature (surface and bottom), dissolved oxygen (surface and bottom), turbidity, and nutrient concentrations (NOx, NO_3, NO_2, NH_4, TN, DIN, TON, TP, SRP, TOC) were conducted at the 28 water quality stations distributed across Florida Bay (Table 2.1).

Table 2.1 Span of monthly chl-*a* measurements from the South Florida Water Quality Management Network at study stations

Span of chl-*a* measurements	Stations
Dec 89 – Jul 09	13, 15, 16, 17, 18
Dec 89 – Sep 08	4, 5, 8, 9, 23, 25
Apr 90 – Sep 08	19, 20, 21, 26, 27, 28
Aug 90 - Sep 08	24
Mar/Apr 91 – Sep 09	12, 14
Mar/Apr 91 – Sep 08	1, 2, 3, 6, 7, 10, 11, 22

Surface salinity was measured using a combination salinity-conductivity-temperature

probe (Boyer and Fourqurean, 1997). Details on sampling methodology and laboratory analysis for chl-*a* and nutrients were described by Boyer and Fourqurean (1997) and Briceño and Boyer (2010).

2.2.3 Statistical Analyses

Measurements of chl-*a* were assumed to be representative of phytoplankton concentrations. There is a long history of the application of chl-*a* as an indicator of photoautotrophic biomass and as an index of the productivity and trophic condition of estuaries, coastal and oceanic waters (Boyer et al., 2009). Correlation coefficients between chl-*a* and nitrogen (DIN and TON), phosphorus (TP) and salinity were calculated for each station's entire monthly dataset on untransformed data points.

Data analysis was completed through SPSS statistical software beginning with exploration of the data distributions and summary statistics. A logarithmic (base 10) transformation was applied to the chl-*a* data grouped by month for each station to reduce positive skews in those groupings so that the distributions more closely approximated the normal distribution. Histograms and Q-Q plots were visually inspected to validate the normality assumption.

Differences in the spatial and temporal distribution of the log-transformed algal bloom indicator were tested through ANOVA analyses and by testing for significant differences in pairwise comparisons where warranted. ANOVA was performed to test the null hypothesis of no difference in means (1) across the 12 months at each station and (2) across the 11 stations in areas of the bay associated with HABs for each month. Significant differences within groups (rejection of null hypothesis) were indicated through ANOVA *F* test and a 95% confidence interval. Pairwise comparisons were employed to identify the

differences if the null hypothesis was rejected. For pairwise comparisons, Tukey's test (*Q* statistic) was applied when variances were assumed equal while Dunnet's T3 test (studentized maximum modulus) (Day and Quinn, 1989) was performed for groups with unequal variance based on the Levene statistic for unequal variances across groups. Pairwise comparisons were considered significant at the 95% confidence level.

While analysis focused on evaluation of the data at the scale of an individual month and station, Zones of Similar Influence (ZSI) were also considered in order to simplify the analysis. Since water quality at a specific site is the result of the interaction of a variety of driving forces, including oceanic and freshwater inputs and outputs, sinks and internal cycling, it is reasonable to assume that contiguous groups of stations with similar water quality were the result of comparable interactions (Boyer and Fourqurean, 1997). Indeed, statistical methods varying in the temporal range and resolution of inputs as well as in the factors involved seem to agree on general subdivisions in Florida Bay represented by the ZSI (Boyer and Fourqurean, 1997; Phlips et al., 1999; Briceño and Boyer, 2010). The six ZSI regimes referenced in this study were those derived by Briceño and Boyer (2010) as (1) North Bay (NB), (2) Florida Bay East (FBE), (3) Florida Bay East Central (FBEC), (4) Florida Bay South (FBS), (5) Florida Bay Central (FBC), and (6) Florida Bay West (FBW) as shown in Figure 2.1. The ZSI were defined through principle component analyses conducted on the South Florida Water Quality Management Network's sample data from 1989 to 2007. Both the mean and standard deviation of the factor scores were then used as independent variables in a cluster analysis to aggregate the 28 stations into the 6 ZSI. The

ZSI mimic the divisions of Florida Bay defined by benthic plant communities and by

phytoplankton communities (Briceño and Boyer, 2010).

2.3 Results

The results indicated a seasonality within the 20 years of in situ data that was also illustrated by plots showing mean monthly chl-*a* for the ZSIs with mean salinity, TP and TON (Fig. 2) which were all shown to be significantly correlated with chl-*a* at half or more of the Florida Bay stations. The following inferences are based on interpretation of Figure 2.2: (1) while mean chl-*a* concentrations over the in situ data record did not vary substantially across months in eastern zones, chl-*a* was seasonally variable in FBW and FBC, (2) salinity decreased with the progression of the rainy season (Jun-Nov) and increased as the dry season progresses (Dec-May), (3) TP was inversely related to salinity with TP concentrations increasing over the duration of the rainy season, and (4) similar to TP, TON was inversely related to salinity in interior bay zones; however, TON peaking in these zones occurred early in the rainy season and dissipated by the end of the rainy season. The annual patterns in chl-*a* and TP were linked to seasonal changes in precipitation and wind regimes as discussed in following sections.

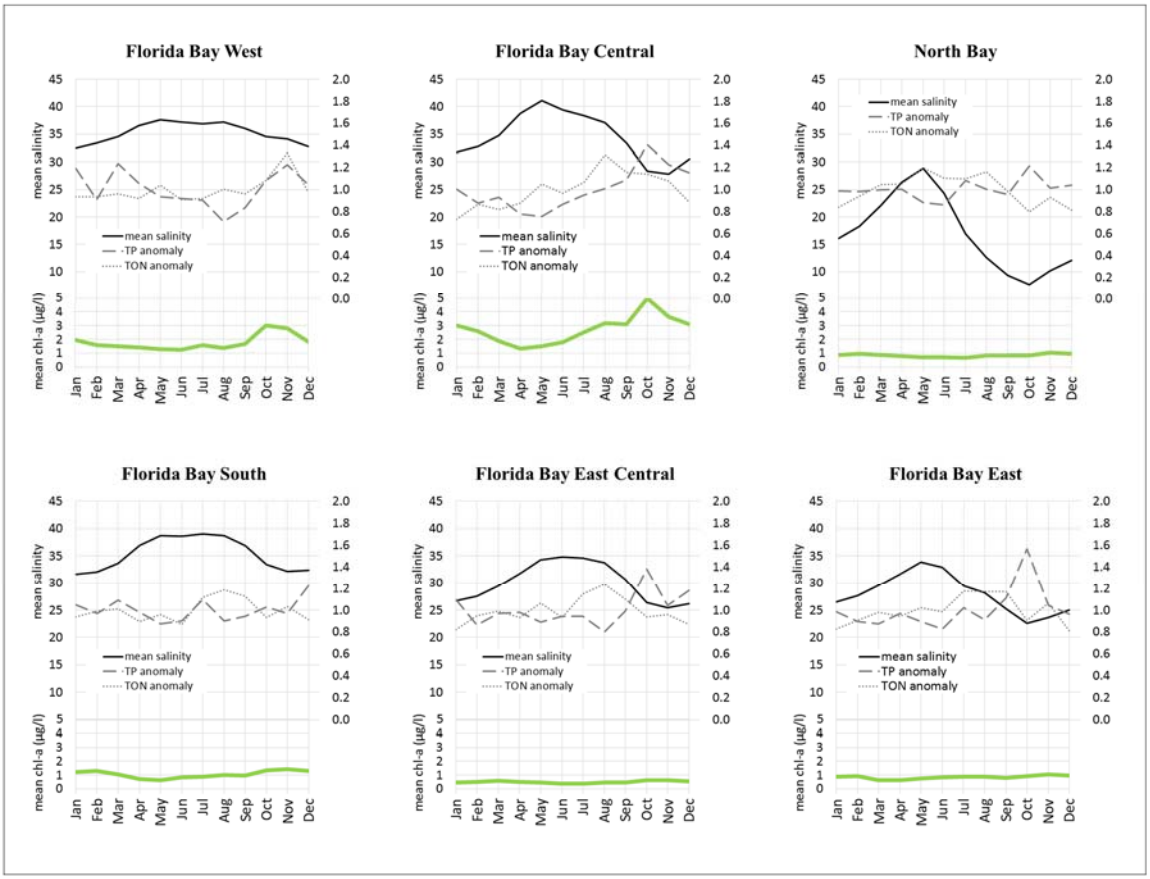

Figure 2.2 Mean monthly chl-*a* for each Florida Bay Zone of Similar Influence with mean salinity also plotted along the primary y-axis. Anomalies in TP and TON, calculated as the monthly mean divided by the overall mean for the ZSI, are plotted on the secondary y-axis.

2.3.1 Correlation Analysis

In general, stations' chl-*a* levels exhibited significant positive correlations with TP throughout the bay, significant positive correlations with TON towards the west and south of the bay, and significant negative correlations with surface salinity in the western and central areas of the bay (Table 2.2 and Figure 2.3). Correlations between chl-*a* and DIN were low to insignificant at most stations, with some exceptions described below.

Table 2.2 Correlation between chl-*a* and nitrogen (DIN and TON), phosphorus (TP) and salinity at each station. Correlations significant at 95% are shown in bold, insignificant correlations are marked with an asterisk.

	Station	Water Depth (m)	DIN (ppm)	TON (ppm)	TP (ppm)	Surface Salinity (ppt)
North Bay	7	0.9	-0.020*	0.013*	**0.252**	**0.249**
	8	1.6	0.073*	-0.073*	**0.312**	-0.024*
	10	1.4	**-0.296**	0.133*	**0.288**	**-0.346**
	11	1.6	**0.416**	0.072*	0.112*	**-0.161**
Florida Bay East	1	2.2	-0.112*	0.056*	**0.574**	0.059*
	2	1.3	-0.117*	0.042*	**0.571**	0.063*
	3	1.9	-0.133*	-0.049*	**0.686**	0.049*
	4	2.8	**-0.146**	0.008*	**0.463**	0.065*
	5	2.5	-0.109*	-0.005*	**0.471**	0.072*
	6	1.9	0.100*	-0.034*	**0.426**	-0.055*
Florida Bay East Central	9	1.7	**0.238**	**0.185**	**0.199**	0.050*
	23	1.8	**0.311**	0.120*	**0.159**	-0.023*
	24	1.7	**0.424**	0.114*	**0.145**	0.056*
Florida Bay Central	12	1.1	-0.087*	**0.378**	**0.595**	-0.131*
	13	2.0	**-0.191**	**0.338**	**0.466**	**-0.273**
	14	0.9	**-0.145**	**0.372**	**0.446**	**-0.350**
	15	1.4	-0.124*	**0.492**	**0.633**	**-0.358**
Florida Bay West	16	2.8	**0.168**	**0.264**	**0.364**	**-0.290**
	17	1.8	0.096*	**0.400**	**0.674**	**-0.351**
	18	2.4	0.087*	**0.517**	**0.623**	**-0.279**
	25	3.6	**0.163**	0.099*	**0.342**	**-0.316**
	26	3.4	**0.315**	**0.215**	**0.235**	**-0.332**
	27	3.1	**0.172**	**0.400**	**0.388**	**-0.291**
	28	2.6	**0.140**	**0.287**	**0.264**	**-0.195**
Florida Bay South	19	2.6	**-0.302**	**0.442**	**0.636**	**-0.201**
	20	2.8	-0.120*	**0.456**	**0.451**	-0.055*
	21	2.3	-0.122*	**0.469**	**0.500**	0.028*
	22	2.5	0.048*	**0.417**	**0.310**	0.103*

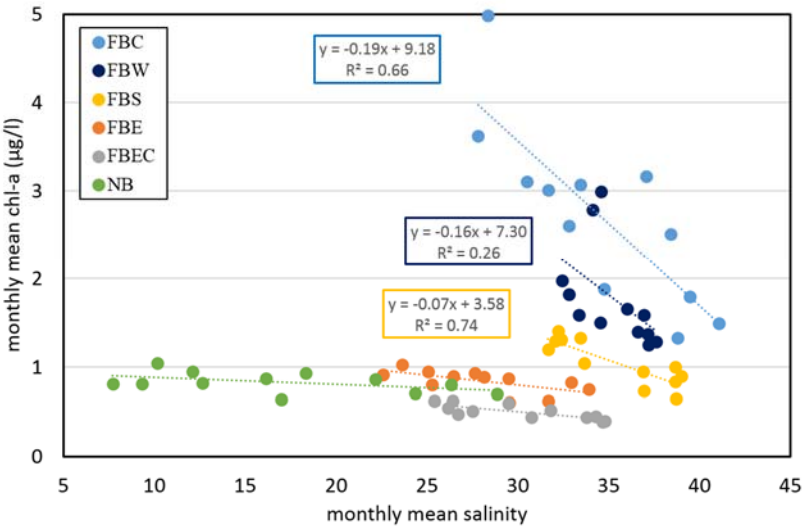

Figure 2.3 Monthly mean chl-*a* plotted against monthly mean salinity for each Florida Bay Zone of Similar Influence showing a negative relationship between chl-*a* and salinity. Linear trendlines and associated R^2 values are included for zones in central and western areas of the bay (FBC, FBW and FBS) where algal blooms have been re-occurring.

Stations in NB exhibited significant correlations between chl-*a* and TP and with surface salinity although only the correlations with TP were consistent in sign. Significant correlations between TP and chl-*a* had positive correlation coefficients ranging from 0.252 to 0.312 for NB stations.

All stations in FBE showed positive, significant correlation between TP and chl-*a*, with coefficients ranging from 0.426 to 0.686. For FBE, the correlation between chl-*a* and either TON or salinity was not found to be significant at any station.

As in FBE, no significant correlation between chl-*a* and salinity was found at FBEC stations. In FBEC, the highest correlation coefficients observed were between chl-*a* and DIN (0.238 to 0.424) which were significant for all three FBEC stations. Within FBEC, all stations showed a significant positive correlation with TP (0.145 to 0.199) while the correlation to TON was generally insignificant (0.144 to 0.185).

All FBS stations demonstrated significant positive correlation between chl-*a* and both TP and TON (0.310 to 0.451 and 0.417 to 0.469, respectively) while correlation coefficients for chl-*a* and salinity were generally insignificant. Only station 19, the FBS station closest to Cape Sable, showed a significant correlation between chl-*a* and surface salinity (-0.201) in this ZSI.

FBC stations displayed correlations similar to those described for FBS, with significant, positive correlations between chl-*a* and both TP and TON (0.446 to 0.633 and 0.338 to 0.492 respectively) at all stations. Significant correlations between chl-*a* and salinity were consistently negative (-0.273 to -0.358 and -0.145 to -0.191) for stations in FBC.

Stations in FBW also exhibited significant positive correlations between chl-*a* and both TP and TON (0.235 to 0.674 and 0.099 to 0.517 respectively) although, unlike FBS and FBC, chl-*a* concentrations at FBW stations also demonstrated significant positive correlations with DIN (0.140 to 0.315). Like in FBC, stations in FBW showed consistently negative correlations between chl-*a* and salinity (-0.195 to -0.351).

2.3.2 Differences Across Months by Station

While significant differences in monthly chl-*a* indicated a seasonality of phytoplankton biomass in the western areas of the bay, no such seasonality was evident in eastern areas where algal blooms are much less prevalent. Based on the ANOVA, the two easternmost ZSIs (FBE and FBEC) showed no significant differences in monthly chl-*a*. Stations in NB, FBC, FBS and FBW exhibited significant differences in monthly chl-*a* concentrations based on the ANOVA analysis and a 95% confidence interval (Table 2.3). The pairwise comparisons showed chl-*a* concentrations in western parts of the bay were

higher at the end of the rainy season than during or at the end of the dry season ($p<0.05$) as shown in Table 2.4.

Table 2.3 ANOVA F and p-value for each station where the null hypothesis was rejected in comparison of mean chl-*a* across months. While Stations 17, 28 and 20 indicated a difference across mean monthly chl-*a* through the ANOVA analysis pairwise comparisons did not reveal significant differences between any pair of months at these stations.

	Station	ANOVA F	p-value
North Bay	7	3.237	0.000
	11	2.925	0.001
Florida Bay West	16	2.219	0.015
	17	1.989	0.031
	18	3.912	0.002
	27	2.828	0.002
	28	2.522	0.006
Florida Bay Central	13	2.812	0.002
	14	4.680	0.000
	15	4.322	0.000
Florida Bay South	19	5.050	0.000
	20	1.848	0.048

Table 2.4 Significant differences ($p<0.05$) in pairwise comparisons of monthly chl-*a* by station for central and western Florida Bay. The rows list, for a station, each month indicated as having significantly higher chl-*a* than other times of the year. The months with higher chl-*a* concentrations range from the middle of the wet season (Aug) until immediately following wet season (Dec). All months associated with lower chl-*a* are during the late dry season to mid wet season.

	Station	Higher concentration month	Lower concentration month						
			Mar	Apr	May	Jun	Jul	Aug	Sep
			(late dry season)			(early-mid wet season)			
Florida Bay Central	13	Oct		X		X			
	14	Aug		X	X				
		Oct	X	X	X		X		
		Nov		X					
		Dec		X					
	15	Sep		X					
		Oct	X	X	X	X			
		Nov		X					
Florida Bay West	16	Nov				X			
	18	Oct		X				X	
		Nov		X				X	X
	27	Oct		X	X				
Florida Bay South	19	Oct		X					
		Nov	X	X	X	X		X	X
		Dec		X		X		X	X

In FBC, three of the four sampling stations demonstrated significant differences among monthly chl-*a* with higher concentrations at the end of the rainy season than at the end of the dry season. For example, Station 14 showed significantly higher chl-*a* concentrations in October than in March, April, May (pre-rainy season) and July (early rainy season).

In FBW, stations 16, 18 and 27 exhibited significant differences in pairwise comparisons with chl-*a* concentrations in October and/or November (at the end of the rainy season) being higher than during months earlier in the rainy season.

In FBS, only station 19, exhibited significant differences in the pairwise comparisons with concentrations in October (wet season) higher than those in April (dry season) and concentrations in November and December being significantly higher than in months spanning from the end of the dry season through the beginning of the wet season.

2.3.3 Differences Across Stations by Month

For ANOVA analysis across stations by month, conducted on FBC and FBW stations only, differences between stations were identified for all months with the locations of these differences varying each month indicating a seasonal shift in the geographic distribution of chl-*a* in Florida Bay as shown in Table 2.5.

Table 2.5 ANOVA F for differences in chl-*a* across central and western stations each month (all $p<0.001$) and significant ($p<0.05$) pairwise comparisons organized by station with higher concentration.

Month	ANOVA F	Station(s) with significantly lower chl-*a* concentrations									
		12	13	14	15	16	17	18	25	26	27
Jan	3.58			28	28	28			28	28	
Feb	3.80								27		
				28		28			28		
Mar	6.88					17					
						18					
						27			18		
		28	28	28	28	28			28	28	
Apr	10.23					13			13		
						15					
						17			17		
						18			18		
						27			27		
		28	28	28	28	28	28		28	28	
May	10.17					12					
						13					
						15					
						17			17		
						18			18		
						27			27	27	
			28	28	28	28	28	28	28	28	
Jun	6.23			18							
				27		27					
		28	28	28	28	28	28		28	28	

Month	ANOVA F	Station(s) with significantly lower chl-*a* concentrations									
		12	13	14	15	16	17	18	25	26	27
Jul	3.76				28	28			28	28	
Aug	11.98			12							
				13							
				17							
				18	18	18			18		
				25						18	
		18	18	27	27	27				27	
		28	28	28	28	28			28	28	
Sep	12.81			17	17	17			17		
		18	18	18	18	18			18	18	
		27	27	27	27	27			27	27	
		28	28	28	28	28			28	28	
Oct	5.69			27	27						
		28	28	28	28	28			28	28	
Nov	6.61			12		12					
			28	28	28	28		28	28	28	28
Dec	6.61			17		17					
				18		18					
				27		27			17		
				28		28			18	18	

The months exhibiting the least amount of significant differences in chl-*a* levels across stations in FBC and FBW (when most of these stations have equivalent levels of chl-*a*) are in winter (January, February) after the rainy season and in summer (July) at the beginning of the rainy season.

Stations 28, 27 and 18 were associated with chl-*a* concentrations that were less than at other stations in FBC and FBW for good portions of the year (12, 10 and 7 months, respectively).

Stations 16 and 14 were associated with chl-*a* higher than at other stations in FBC and FBW for good portions of the year (11 months each). While concentrations in these stations were often significantly higher than at other stations these are the only two stations that were never associated with lower chl-*a* than another station in any month. Station 16 chl-*a* was significantly higher than at most tested stations, including stations from FBC, in

April and May (during low chl-*a* months). Concentrations at station 16 for other months of the year, however, do not show the same number of significant differences with other stations, especially in consideration of FBC stations. In August (beginning of high chl-*a* months in FBC) station 14 chl-*a* was significantly higher than at most tested stations including other stations within FBC, although this pattern did not hold for other months in the year.

2.4 Discussion

Correlation analysis showed TP to be significantly correlated with all but one station in the bay (as opposed to around 50% of stations for other factors tested) suggesting that inputs of phosphorus are the predominant factor in the initiation and persistence of elevated chl-*a* levels, especially in the central, western and southern basins where correlation coefficients are around or above 0.5 for most stations (the strength of this correlation was also relatively high at Florida Bay East stations). The observed strengthening of correlations between chl-*a* and nitrogen (TON) from east to west support a nitrogen source from east (with higher nitrogen limitation in west), such as Taylor slough inputs, as reported in literature (Briceño and Boyer, 2010; Melesse et al, 2008; Brand, 2002). Compared to the east coast of Florida and eastern Florida Bay, phosphorus concentrations tend to be high along the southwest coast of Florida and in northwest Florida Bay south of Cape Sable (Brand, 2002). Correlations between chl-*a* and TP were, nonetheless, stronger than with DIN or TON in the western ZSIs that are associated with HAB's (FBC, FBW), except at the southernmost stations - 27 and 28 where phytoplankton biomass is generally low for these ZSI's and may be transported from the north by wind and currents. For FBC and FBW, surface salinity was significantly negatively correlated

with chl-*a* levels at all but one station, indicating a freshening of the water column at the time of the occurrence of HABs and supporting a freshwater link to the source of TP.

The stations furthest from the Florida Peninsula (28, 27 and 18) were associated with chl-*a* concentrations less than at other stations in FBC and FBW suggesting that these locations are the least connected to HAB nutrient sources. Two stations in the northwest of the bay, stations 16 and 14, appeared to be most connected to nutrient sources. A shift in either nutrient delivery or other mechanisms controlling algal blooms is indicated in August, at the onset of the elevated chl-*a* period, when chl-*a* concentrations at station 14 are greater than at eastern FBC stations but not significantly different from those at station 16 to the west.

Testing for differences in monthly chl-*a* concentrations by site revealed that stations within zones associated with recurring HABs (FBC, FBW) exhibited monthly differences in the chl-*a* levels while stations in the other zones generally showed no significant difference in chl-*a* across months. Stations in FBC and FBW exhibited significantly greater chl-*a* levels at the end of the rainy season (October and November) compared to levels at the end of the dry season (April through June). These results support the hypothesis that wet season rainfall is an impetus for the delivery of nutrients to the bay, however, the proportion of nutrients delivered through runoff versus groundwater discharge remains unclear.

As illustrated by satellite imagery and the bay's bathymetry (Fig. 1), potential sources of phosphorus need to be reconciled with the geomorphology of the bay and

other study area characteristics such as seasonal water levels, winds and currents which

govern nutrient inputs distinctly in each region of the bay.

Inspection of the bay's bathymetry in the context of seasonal wind patterns do not preclude marine inputs from the Gulf of Mexico as the source of nutrients fueling algal blooms even though chl-*a* levels were negatively correlated with salinity. Phosphorus carried by long-shore currents from the Central Florida coast (Rudnick et al., 1999) may mix with Shark Slough discharges throughout the rainy season in the Gulf of Mexico. The wide shallow shelf of southwest Florida receives contributions from several Florida rivers, including the Caloosahatchee which drains Lake Okeechobee (Zanardi-Lamardo et al., 2004) and Peace River which empties into Charlotte Harbor. In fall, winds toward the south become more prevalent perhaps increasing flow from the southwest Florida shelf toward the interior of the bay coincident with the rainy season runoff. In this case, terrestrial nutrients from Central Florida could be transported along the shelf and directed into the study area providing fuel for the algal blooms. Marine delivery of terrestrial nutrients into the study area was supported by an analysis of the sediments in Florida Bay where total organic phosphorus (TOP) in western sediments were found to be mainly terrestrial while the sediments from central and eastern Florida Bay were primarily influenced by autochthonous TOP (Kang and Tefry, 2012).

Negative correlations with salinity, significantly higher chl-*a* concentrations at stations nearest to the coast (i.e. station 14, 16) and significantly higher chl-*a* levels at the end of the rainy season may, alternatively, be explained by a groundwater source of phosphorus. Brackish groundwater of the southern Everglades contain elevated calcium concentrations and concentrations of TP that exceeds those in both local fresh groundwater and intruding seawater so that it has been proposed that the enhanced productivity of the freshwater-

marine ecotone of the coastal Everglades is attributable to brackish groundwater delivered nutrients as opposed to either freshwater or marine end member (Price et al., 2006). Indeed, TP measured in the Gulf of Mexico was found to be higher than in the freshwater wetlands of Shark Slough but much lower than in the coastal mangrove zone during the wet season (Rudnick et al., 1999). Increased salinity in the mixing zone would cause desorption of phosphorus from the limestone of the aquifer (Brand, 2002). As the rainy season progresses each year, brackish groundwater may discharge under the bay or closer to the coast than during the dry season so that less phosphorus is trapped by wetlands before being exported to the bay.

Anthropogenic sources from the Florida Keys have been implicated as nutrient sources for Florida Bay algal blooms, although the keys are generally downstream from the location of HAB occurrences. Minimum outflow from the bay to the Atlantic occurred in fall, coincident with elevated chl-*a* concentrations, when winds toward the west and southwest were more frequent and inflows to Florida Bay from the middle keys area can persist for several days (Lee et al., 2002). A Florida Keys source of nutrients is not supported by the examination of chl-*a* concentrations across stations, though, which showed stations closest to the keys were associated with relatively low chl-*a* levels.

2.5 Conclusion

The results of this analysis provided details on spatial and temporal trends in HAB dynamics and placed emphasis on specific directions for further research, but were not able to fully detail the nutrient sources and circulation pathways responsible for the seasonal pattern in phytoplankton biomass. It is evident that one-dimensional mixing diagrams, useful in river dominated estuaries of the temperate zone, are inappropriate for studying

nutrient behavior in these systems (Boyer and Fourqurean, 1997) with multidimensional connections to terrestrial inputs.

While the dataset represents 20 years of monthly data collected across the breadth and width of the bay, the data is still not continuous enough in time and space to differentiate between potential nutrient sources that are affected by a multitude of variables simultaneously. The connection between Florida Bay and the terrestrial ecosystems of South Florida is diffuse and, therefore, poorly understood. The hydrodynamics within the bay are complex and vary by season (Rudnick et al., 1999; Gilbert et al., 2009) thereby obscuring the predominant source of nutrient inputs to the bay. The importance of winds in the region contributes to the complexity, since the magnitude and direction of winds is highly variable. Coastal geomorphology along with seasonal changes in the direction of winds and magnitude of rain and evapotranspiration are factors that require increased study at appropriately fine spatial and temporal resolution in order to describe the pathways for nutrients entering the bay.

These results point to the utility of regional hydrogeologic characterizations, that can be employed together with geographic information systems (GIS), in tracking hydrologic inputs in complex and dynamic systems. A fine spatial and temporal resolution can illustrate small scale differences which may be indicative of diffuse or subtle processes where these processes may ultimately dictate nutrient circulation. With these tools, inputs from groundwater and surface runoff sources may be distinguished from each other by evaluating a more comprehensive and evolving picture of resulting algal blooms in conjunction with data on coincident winds and rain.

Remotely-sensed, satellite imagery provides an opportunity to adequately represent the hydrology and nutrient pathways of the study area. Remote sensing provides synoptic views of the region and at this point offers a long ranging and frequent record, at moderate spatial resolution. Even when field measurements are available, the coverage of satellite measurements may reduce potential spatial and temporal aliasing (Le et al., 2013) that lead to uncertainty about nutrient sources.

Better characterization of the regional hydrodynamics and nutrient circulation would support restoration efforts and may help to inform management decisions. For example, the Comprehensive Everglades Restoration Plan is being undertaken with plans to increase freshwater levels including greater surface runoff to Florida Bay and greater groundwater storage although it is unclear what role groundwater and runoff play in HABs in the Florida Bay estuary.

Being able to track nutrient circulation paths on a regional scale may identify nutrient sources that were previously obscured and not located in the Everglades, in turn confirming that increased freshwater input via the Everglades wetlands is an effective strategy for managing HABs in Florida Bay. In addition, comprehensive monitoring of algal blooms can help to track the progress of ongoing restoration efforts in an objective manner.

Acknowledgements

This research was conducted through the support of The National Aeronautics and Space Administration (NASA) Minority University Research and Education, WaterSCAPES, Program. Special thanks to Florida International University's Graduate

School Statistical Consulting Services, and the Southeast Environmental Research Center (SERC) for their contributions to this work.

References

Bauman, A.G., Burt, J., Feary, D., Marquis, E., Usseglio, P., 2010. Tropical harmful algal blooms: An emerging threat to coral reef communities? Mar. Pollut. Bull., doi:10.1016/j.marpolbul.2010.08.015.

Boyer, J., Kelbe, C., Ortner, P., Rudnick, D., 2009. Phytoplankton bloom status: Chlorophyll a biomass as an indicator of water quality condition in the southern estuaries of Florida, USA. Ecol. Indic. 9, s56-s67.

Boyer, J., Fourqurean, J., 1997. Spatial characterization of water quality in Florida Bay and Whitewater Bay by multi-variate analyses: Zones of similar influence. Estuaries 20 (4), 743-758.

Brand, L., 2002. The transport of terrestrial nutrients to south florida coastal waters. The Everglades, Florida Bay, and Coral Reefs of the Florida Keys: An Ecosystem Sourcebook, 361-413.

Briceño, H., Boyer, J., 2010. Climatic controls on phytoplankton biomass in a sub-tropical estuary, Florida Bay, USA. Estuar. Coast. 33, 541-553.

Bulter, M., Hunt, J., Herrnkind, W., Childress, M., Bertelsten, R., Sharp, W., Matthews, T., Field, J., Marshall, H., 1995. Cascading disturbances in Florida Bay, USA: cyanobacteria blooms, sponge mortality, and implications for juvenile spiny lobsters *Panulirus argus*. Mar. Ecol.-Prog. Ser. 129, 119-125.

Chen, M., Price, R., Yamashita, Y., Jaffe, R., 2010. Comparative study of dissolved organic matter from groundwater and surface water in the Florida Coastal Everglades using multi-dimensional spectrofluorometry combined with multivariate statistics. Appl. Geochem. 15, 872–880.

Childers, D., Jones, R., Trexler, J., Buzzelli, C., Dailey, S., Edwards, A., Gaiser, E., Jayachandaran, K., Kenne, A., Lee, D., Meeder, J., Pechmann, J., Renshaw, A., Richards, J., Rugge, M., Scinto, L., Sterling, P., Van Gelder, W., 2002. Quantifying the effects of low-level phosphorus additions on unenriched Everglades wetlands with in situ flumes and phosphorus dosing. The Everglades, Florida Bay, and Coral Reefs of the Florida Keys: An Ecosystem Sourcebook, 127-152.

Day, R.W., Quinn, G.P., 1989. Comparisons of treatments after an analysis of variance in ecology. Ecol. Monogr. 59, 433-463.

Gilbert, P., Heil, C., Madden, C., 2009. Florida Bay: A subtropical system increasingly influenced by multiple stressors. Contrib. Mar. Sci. 38, 1-4.

Gilbert, P., Heil, C., Rudnick, D., Madden, C., 2009. Florida Bay: Water quality status and trends, historic and emerging algal bloom problems. Contrib. Mar. Sci. 38, 5-17.

Guinder, V., Popovich, C., Molinero, J., Marcovecchio, J., 2013. Phytoplankton summer bloom dynamics in the Bahia Blanca Estuary in relation to changing environmental conditions. Cont. Shelf Res. 52, 150-158.

Heil, C., Revilla, M., Gilbert, P., Murasko, S., 2007. Nutrient quality drives differential phytoplankton community composition on the southwest Florida shelf. Limonol. Oceanogr. 52 (3), 1067-1078.

Jickells, T.D., Andrews, J., Parkes, D., Suratman, S., Aziz, A., Hee, Y., 2014. Nutrient transport through estuaries: The importance of the estuarine geography. Estuar. Coast. Shelf S. 150 (B), 215-219.

Jones, N.L., Patten, N., Krikke, D., Lowe, R., Waite, A., Ivey, G., 2014. Biophysical characteristics of a morphologically-complex macrotidal coastal system during a dry season. Estuar. Coast. Shelf S. 149, 96-108.

Kang, W., Trefry, J., 2012. Identifying increased inputs of terrestrial phosphorus to sediments of the southwestern Everglades and Florida Bay. Estuar. Coast. Shelf S. 129, 28-36.

Koch, M.S., Benz, R., Rudnick, D., 2001. Solid-phase phosphorus pools in highly organic carbonate sediments of north-eastern Florida Bay. Estuar. Coast. Shelf S. 52, 000-000.

Le, C., Chuanmin, H., English, D., Cannizzaro, J., Chen, Z., Kovach, C., 2013. Inherent and apparent optical properties of the complex estuarine waters of Tampa Bay: What controls light? Estuar. Coast. Shelf S. 117, 1-16.

Le, C., Chuanmin, H., English, D., Cannizzaro, J., Kovach, C., 2013. Climate-driven chlorophyll-*a* changes in a turbid estuary: Observations from satellites and implications for management. Remote Sens. Environ. 130, 11-24.

Lee, T., Williams, E., Johns, E., Wilson, D., Smith, N., 2002. Transport processes linking South Florida coastal ecosystems. The Everglades, Florida Bay, and Coral Reefs of the Florida Keys: An Ecosystem Sourcebook, 309-342.

Lee, T., Smith, N., 2002. Volume transport variability through the Florida Keys tidal channels. Cont. Shelf Res. 22, 1361-1377.

McCarthy, M.J., Gardner, W., Lavrentyev, P., Jochem, F., Williams, C., 2009. Water Column Nitrogen Cycling and Microbial Plankton in Florida Bay. Contrib. Mar. Sci. 38, 49-62.

Melesse, A.M., Jayachandran, K., Zhang, K., 2008. Modeling coastal eutrophication at Florida Bay using neural networks. J Coastal Res 24, 190–196

O'Neil, J., Davis, T., Burford, M., Gobler, C., 2012. The rise of harmful cyanobacterial blooms: The potential roles of eutrophication and climate change. Harmful Algae 14, 313-334.

Phlips, E.J., T. Lynch, T., S. Badylak, S., 1995. Chlorophyll a, tripton, color and light availability in a shallow tropical inner-shelf lagoon, Florida Bay, USA. Mar. Ecol.-Prog. Ser. 127, 223-234

Phlips, E., Badylak, S., Lynch, T., 1999. Blooms of the picoplanktonic cyanobacterium Synechoccus in Florida Bay, a subtropical inner-shelf lagoon. Limnol. Oceanogr. 44 (4), 1166-1175.

Price, R., Swart, P., Fourqurean, J., 2006. Coastal groundwater discharge – an additional source of phosphorus for the oligotrophic wetlands of the Everglades. Hydrobiologia 569 (1), 23-36.

Richardson, B., 2009. Physiological Characteristics and Competitive Strategies of Bloom-forming Cyanobacteria and Diatoms of Florida Bay. Contrib. Mar. Sci. 38, 19-36.

Richardson, L., Zimba, P., 2002. Spatial and temporal patterns of phytoplankton in Florida Bay: Utility of algal accessory pigments and remote sensing to assess bloom dynamics. The Everglades, Florida Bay, and Coral Reefs of the Florida Keys: An Ecosystem Sourcebook. 461-478.

Rudnick, D., Chen, Z., Childers, D., Boyer, J., Fontaine, T., 1999. Phosphorus and nitrogen inputs to Florida Bay: The importance of the everglades watershed. Estuaries 22 (2B), 389-416.

South Florida Natural Resources Center (SFNRC), Everglades National Park and National Park Service, Department of the Interior, 2012. Salinity and Hydrology of Florida Bay, Status and Trends 1990 – 2009. SFNRC Technical Series 2012 (1).

Spence, V., 2011. Estimating groundwater discharge in the oligohaline ecotone of the Everglades using temperature as a tracer and variable-density groundwater models. Graduate Theses and Dissertations. http://scholarcommons.usf.edu/etd/3361

Steinman, A., Havens, K., Carrick, H., VanZee, R., 2002. The past, present, and future hydrology and ecology of Lake Okeechobee and its watersheds. The Everglades, Florida Bay, and Coral Reefs of the Florida Keys: An Ecosystem Sourcebook, 19-37.

Sutula, M., Perez, B., Reyes, E., Childers, D., Davis, S., Day, J., Rudnick, D., Sklar, F., 2003. Factors affecting spatial and temporal variability in material exchange between the Southern Everglades wetlands and Florida Bay. Estuar. Coast. Shelf S. 57, 757-781.

Taylor, K.H., Purkis, S.J., 2012. Evidence for the southward migration of mud banks in Florida Bay. Mar. Geol. 311-314, 52-56.

Vargo, G.A., Hitchcock, G., Neely, M., 2009. Estimates of phytoplankton growth from a Lagrangian experiment in Western Florida Bay, USA. Contrib. Mar. Sci. 38, 63-71.

Wanless, H., Tagett, M., 1989. Origin, growth and evolution of carbonate mudbanks in Florida Bay. B. Mar. Sci., 44 (1), 445-489.

Zanardi-Lamardo, E., Moore, C., Zika, R., 2004. Seasonal variation in molecular mass and optical properties of chromophoric dissolved organic material in coastal waters of southwest Florida. Mar. Chem. 89, 37-54.

3 SUPERVISED CLASSIFICATION OF BENTHIC REFLECTANCE IN SHALLOW SUBTROPICAL WATERS USING A GENERALIZED PIXEL-BASED CLASSIFIER ACROSS A TIME SERIES

Blakey T, Melesse A, Hall M (2015) Supervised Classification of Benthic Reflectance in Shallow Subtropical Waters Using a Generalized Pixel-Based Classifier across a Time Series. Remote Sensing, 7, 5098-5116.

Abstract

We tested a supervised classification approach with Landsat 5 Thematic Mapper (TM) data for time-series mapping of seagrass in a subtropical lagoon. Seagrass meadows are an integral link between marine and inland ecosystems and are at risk from upstream processes such as runoff and erosion. Despite the prevalence of image-specific approaches, the classification accuracies we achieved show that pixel-based spectral classes may be generalized and applied to a time series of images that were not included in the classifier training. We employed *in-situ* data on seagrass abundance from 2007–2011 to train and validate a classification model. We created depth-invariant bands from TM bands 1, 2, and 3 to correct for variations in water column depth prior to building the classification model. *In-situ* data showed mean total seagrass cover remained relatively stable over the study area and period, with seagrass cover generally denser in the west than the east. Our approach achieved mapping accuracies (67% and 76% for two validation years) comparable with those attained using spectral libraries, but was simpler to implement. We produced a series of annual maps illustrating inter-annual variability in seagrass occurrence. Accuracies may be improved in future work by better addressing the spatial mismatch between pixel size of remotely sensed data

and footprint of field data and by employing atmospheric correction techniques that normalize reflectances across images.

Keywords: benthic reflectance; supervised classification; Landsat; Florida Bay; seagrass landscapes; long-term monitoring

3.1 Introduction

Seagrass meadows are an intricate link between inland and marine ecosystems. In subtropical and tropical estuaries and coastal lagoons, large contiguous seagrass meadows support a range of ecosystem services including nutrient cycling, nursery grounds for many fish and crustacean species, food for endangered large grazers, such as dugong and turtles, and coastal protection by sediment accretion and stabilization [1–3]. Seagrasses are productive carbon fixers [4,5], which places their economic value among the highest of the world's ecosystems [6]. Seagrasses are threatened by a variety of upstream processes, and the loss or reduction in the capacity of seagrasses to perform ecosystem services will influence the balance of adjoining ecosystems, such as coral reefs. Conservation of seagrasses requires management that addresses the spatially and temporally variable nature of hydrologic discharges at coasts.

Seagrass meadows grow at the nexus of terrestrial and marine environments and are impacted by highly dynamic anthropogenic and natural factors. Despite their environmental and economic significance, seagrass populations are threatened worldwide by coastal development and eutrophication and may be nearing a crisis with respect to global sustainability [7]. The land-water interaction along coasts is influenced by freshwater networks where hydrologic impacts to seagrass ecosystems include increases

in nutrients such as nitrogen and phosphorus occurring from industrial or agricultural sources [8], sediment discharge from watershed deforestation and mangrove clearing [8], and disruption of the natural salinity regime [2,9]. Without appropriate management, widespread loss of seagrass habitats is predicted to continue [10], especially given continued development of coastal lands.

Researchers and managers would benefit from maps showing temporal changes in the density and distribution of seagrass cover to help inform decisions for minimizing negative impacts to seagrass resources. Continued study of coastal landscape dynamics with accurate, quantitative measurements of areal extent and density of seagrasses is needed to better understand the mosaic of their distribution (degree of patchiness, gap dynamics, habitat edge type, and connectivity) in conjunction with the temporal and spatial variability of hydrologic inputs to coastal areas [7]. Characterizing these dynamics from a synoptic, repeatable perspective with remotely sensed data [11] can strongly augment more accurate point measures of change derived *in-situ* [12].

Long-term, global archives of satellite multispectral imagery are now readily accessible; yet, the data are not widely used for thematic mapping of benthic cover [13]. Intensive field and laboratory data collection campaigns have been undertaken to calibrate satellite-based retrospective benthos mapping and to validate products used for time series analysis, but the amount of research exploiting satellite archives could be increased if less costly benthic mapping methodologies were identified. The archive of the Landsat 5 Thematic Mapper (TM) sensor offers multispectral imagery at 30 m spatial resolution at 16-day intervals from 1984 to 2011 and currently is an underutilized global

resource for long-term data on coastal environments. The long and consistent record provides an opportunity for scientists to retrieve information from periods of time where no other forms of quantitative data are available, making the archive especially valuable in understanding seagrass habitats and coastal dynamics.

Approaches for mapping seagrasses in optically shallow water bodies have evolved from visual interpretation of aerial photography to semi-automated mapping from high resolution airborne or satellite image datasets in association with field-survey and hydro-optical data [14]. A relatively simple and widely used approach for creating seagrass maps is image-specific, pixel-based supervised classification where training pixels are selected to represent each of the classes being mapped and an algorithm matches the spectral properties of image pixels to the most similar, pre-defined, class. Whereas field data are required to ensure appropriate selection of training pixels, this method may be carried out without additional hydro-optical data from the field or lab.

Maps produced from Landsat data and pixel-based supervised classification have been demonstrated to appropriately represent the spatial characteristics of seagrass meadows. Seagrass cover was mapped in Moreton Bay, Australia, by Roelfsema *et al.* [15] with training pixels for five different seagrass cover classes extracted from a Landsat 5 image of the Bay. Results showed that >75% of the Bay was mapped with high categorical reliability. Wabnitz *et al.* [16] tested the feasibility of achieving large-scale seagrass mapping for the Wider Caribbean region with limited ground truth data, obtaining an average overall accuracy of 68% across sites for the three-class scheme. Pu *et al.* [17] mapped seagrass along the western coast of Florida using Landsat 5 data to calculate depth-invariant bands and achieved a 93% and 66% overall accuracy for their three-class

and five-class schemes, respectively. However, the applicability of the pixel-based classifier in producing a time series of benthic map products was not tested in these studies.

Time series maps of seagrass abundance have recently been produced from Landsat 5 data and pixel-based classification [18–20] using image-specific training areas so that each date in the series is associated with a unique classifier. The "quality" and relevance of classes derived from satellite data are variable across images [21] so that transferring pixel-based definitions of class spectra to other images has been considered impractical [11]. Constraining class definitions to the image in which training pixels are identified, however, limits the resulting multi-temporal analysis to dates where *in-situ* or other ground truth source is available for the selection of calibration data.

To be as objective as possible and increase the capacity for multi-temporal and multi-site comparison of classification results it is necessary to decouple field work and satellite sensor imaging [22] such as through the use of a spectral library. In the spectral library approach, remote sensing reflectance of individual pixels are compared with simulated spectra created using measured values of bottom reflectance and water inherent optical properties [23]. The spectral library method requires specialized equipment to capture the bottom reflectances and optical properties specific to the study site as well as a radiative transfer model to simulate the spectra of varying water columns over different substrates [22–27]. Although the spectral library method is objective and repeatable, the high degree of expertise and optical data required to define the library may be unattainable in the near term for many seagrass systems. Further, studies have indicated that image-based

classification provides similar or even higher accuracy benthic maps compared to the spectral library method [28, 29].

A study by Lyons *et al.* [30] demonstrated that image-based classification methods are applicable to periods without concurrent *in-situ* data so that long term seagrass maps over the entire Landsat record can be produced allowing management agencies to build a baseline assessment of their resources, understand past changes and help inform implementation and planning of management policy to address potential future changes. Instead of pixel-based methods, the object-based supervised classification applied by Lyons *et al.* [30] was guided by hierarchical rule sets, which achieved an overall classification accuracy of approximately 65%. The thresholds and membership functions in the rule sets were manually adjusted for each image. Although this research illustrated the utility of time-series seagrass maps produced without intensive data collection, the work also indicated a need for mapping methodologies that can improve upon transferability between image dates. Although object-oriented classification can greatly improve accuracy compared with traditional supervised classification, the difficulty in applying the rule-based system for seagrass habitats requires further study to test the appropriateness of object-based classification in the successful extraction of seagrass features [31].

The seagrass meadows mapped in this study are located in Florida Bay, a shallow semi-enclosed estuary in South Florida. The Florida Bay ecosystem has experienced large changes in water quality concurrent with massive die-offs of seagrasses [32]. In 1987 approximately 40 km^2 of *Thalassia testudinum* meadows experienced a major "die-off"

in Florida Bay, and that die-off has been followed by smaller (<1 km^2) patchy episodes of mortality on an annual basis [1].

Despite tremendous losses suffered in the past 30 years, South Florida still supports roughly 55%–65% of Florida's seagrass resources and the greatest population densities on the state's coastline [33]. The Florida Bay seagrass meadows are intricately linked to the reefs of the Florida Keys, a popular tourist destination with approximately 2.5 million visitors annually generating nearly $1.2 billion for the region [32]. Although the Florida Bay seagrass landscape is an invaluable cultural and economic resource, a consensus on the primary cause of seagrass losses there has never been ascertained [33]. Therefore, the study area is representative of coastal systems that require better understanding to characterize, monitor and analyze seagrass landscape dynamics to support resource management decisions.

The underlying motivation for this work was to promote the development of remote sensing techniques that can be easily and objectively applied to the span of Landsat 5 images, including periods for which no ground truth data are available, to encourage greater interpretation of satellite archives for resource management. More specifically, a pixel-based classifier trained using ground truthed pixels compiled from three recent images was applied to a series of older images to test the transferability of the image-based spectral characterizations of classes. This work focused on using widely accessible practices to complete the tasks of: (1) normalizing the various dates of satellite data to ensure comparability of the spectral profiles across dates; and (2) defining seagrass classes that are spectrally separable and ecologically relevant.

3.2. Data and Methods

3.2.1. Study Site

Florida Bay is a shallow, sub-tropical lagoon bordered to the north by the southern tip of the Florida Peninsula and to the south and east by the nearly contiguous islands of the Florida Keys (Figure 3.1). Tidal range throughout the bay is minimal, as physical formations limit exchange with the Gulf of Mexico and Atlantic Ocean, including a series of natural, carbonate mudbanks that divide the bay into numerous shallow basins further reducing water exchange within the system [34]. Winds in the study area are from the east from fall through spring, with the strength of wind forcing and the current response decreasing in spring [35]. Along the Southwest Florida Shelf immediately west of Florida Bay, the long-term mean flow is toward the southeast, with seasonal variation in wind forcing resulting in maximum outflows from Florida Bay through the Keys in winter and spring following cold front passages associated with winds toward the east. Minimum outflows occur in the fall when winds toward the west are frequent and inflow across the Keys to Florida Bay can persist for several days [36].

Seagrass communities within the study area are characterized by dense seagrass growth, whereas more eastern Florida Bay communities are dominated by sparse, patchy seagrass cover [39]. The study basins are particularly interesting for seagrass dynamics as a bay-wide investigation into decadal changes in seagrass (1984–1994) found turtle grass decline was not homogeneous throughout the Bay, with the largest reductions in shoot density and biomass occurring in central and western Florida Bay [41]. Statistical

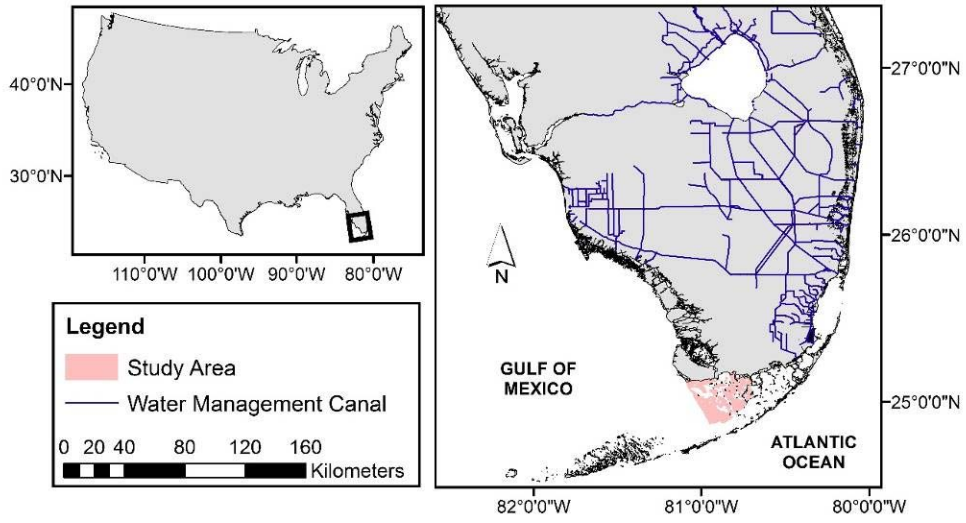

Figure 3.1 Map showing location of the study area in western Florida Bay, Florida, USA.

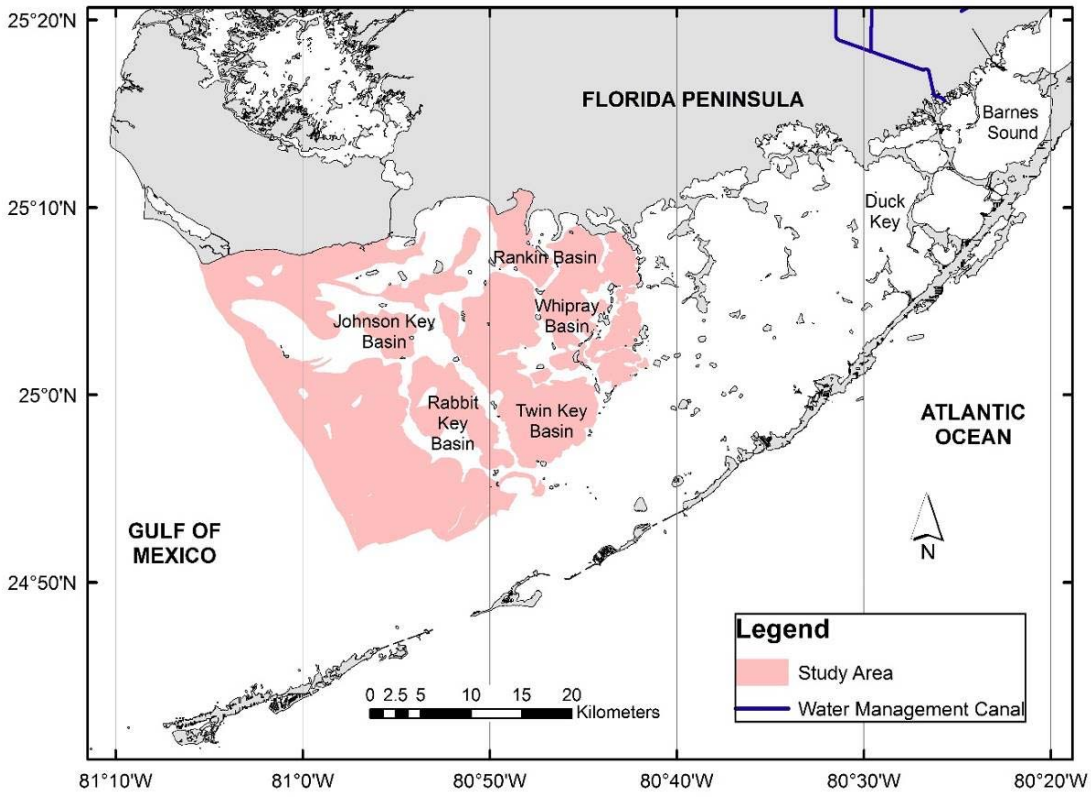

Figure 3.2 Map overview of Florida Bay and the study area. Field data on seagrass abundance were obtained for labeled basins.

analysis of the study area's *in-situ* seagrass cover data from 1995 to 2012 showed seasonal variation to be low and annual variation to be incremental, as would be expected, since tropical seagrass beds are typically stable over the temporal scale of years, even in the advent of severe storms [17].

3.2.2. Data Sets

3.2.2.1. In-Situ Data

The Florida Bay Fisheries Habitat Assessment Program (FHAP) was initiated during spring 1995 in response to continuing concerns over environmental changes and seagrass loss within the region. The goal of FHAP is to provide spatially explicit information on the distribution, abundance, species composition, and population dynamics of Florida Bay seagrasses [42]. Sampling for FHAP is conducted during the spring (May–June) at 10 basins representing a range of conditions and gradients in Florida Bay. Five of the FHAP surveyed basins, Johnson Key, Rabbit Key, Twin Key, Whipray, and Rankin, are located within the study area (Figure 3.2). The basins are partitioned into approximately 30 tessellated, hexagonal grid cells (ranging from 0.5 to 2.6 km^2 depending on basin size) for survey purposes, and at every cell seagrass cover is visually quantified within each of four (1995–2004) or eight randomly located 0.25 m^2 quadrats using the Braun Blanquet abundance scale [42]. The abundance scale is described in Table 3.1, where cover is defined as the fraction of the bottom that is obscured by seagrass when viewed by a diver from directly above [43]. Whereas seagrass cover data were available for individual seagrass species (*Thalassia testudinum*, *Halodule wrightii*, *Syringodium filiforme*, *Ruppia maritime* and *Halophila engelmanii*) from the beginning of the dataset, observations of total seagrass abundance were first recorded in the 2007 dataset. Total seagrass

abundance from the 2007–2011 campaigns were employed as ground-truth, reference data in this study.

Table 3.1 Definition of Braun Blanquet abundance scores used to characterize seagrass cover *in-situ*.

Score	Percent Cover
5	75 to 100
4	50 to 75
3	25 to 50
2	5 to 25
1	<5

We conducted a preliminary investigation of trends and variability in the FHAP dataset for total seagrass cover prior to employing the survey data for classification purposes. The investigation included a simple graphical analysis of the portion of sites associated with each abundance class and the mean, median and mode class by basin across all available years of data. For the dominant species, *Thalassia testudinum*, the graphical analysis was also conducted on the full extent of the species-specific FHAP dataset that included seasonal surveys (spring and fall) for the period from 1995 to 2003.

3.2.2.2. Satellite Data

Landsat 5 TM Level-1 data for the study area were obtained from the USGS. One scene, path 15/row 43, covering all study basins was selected for each of the five years (2007–2011) of concurrent FHAP data on total seagrass density. Images of this scene were also retrieved for nine years (1998–2006) for which no total seagrass data were available, to use for qualitative assessment of the classifier. Landsat images were selected to minimize cloud cover and temporal distance from the reference data that were collected

in May. The dates of the selected Landsat images with associated *in-situ* data were 21 April 2007, 7 April 2008, 26 April 2009, 13 April 2010, and 3 June 2011. The dates of selected Landsat images used in the qualitative analysis were 5 May 1998, 3 March 1999, 17 April 2000, 6 May 2001, 18 February 2002, 31 July 2003, 11 March 2004, 15 April 2005, and 4 May 2006. The acquisition time at the sensor was between 10:25 am and 10:45 am (Eastern Time) for all 14 images.

3.2.3. Satellite Data Pre-Processing

Given the relatively low spectral response that reaches remote sensors from underwater subjects [11] and the objective of utilizing the image-based classifier across images, pre-processing of satellite data to adequately correct for atmospheric and water column variation was an important step of this study. The underlying motivation of working towards a mapping methodology that is easily implemented with a minimum of specialized equipment and software influenced the decisions on pre-processing techniques. With the exception of cloud-masking, all pre-processing of the Landsat images, including radiometric calibration, atmospheric correction and water column correction, was completed using ENVI 5.1 image processing software.

The Fmask (Function of mask) algorithm [44] was used to remove cloud and cloud shadows, as well as land pixels, before atmospheric correction was carried out in ENVI. The Fmask algorithm uses Landsat Top-of-Atmosphere reflectance and Brightness Temperatures as inputs to detect clouds over land and water separately. Geometry-based cloud shadow detection is employed in generation of the shadow layer through use of a flood-fill transformation. The Fmask algorithm separates clouds from shallow or turbid water accurately and can also detect thin clouds and their shadows [44].

Radiometric calibration was carried out in ENVI to convert digital numbers to at-sensor spectral radiance using ENVI's built-in calibration coefficients for the TM sensor.

The Fast Line-of-Sight Atmospheric Analysis of Spectral Hypercubes (FLAASH) module included in ENVI was implemented to translate at-sensor radiance to at-water reflectance. The tropical atmosphere model and maritime aerosol model in FLAASH were selected for the study area. Assessment of the FLAASH atmospheric correction code under a similar parameterization of the module and using *in-situ* spectral samples was performed in a previous study in western Florida, which found spectra extracted from the atmospherically corrected Landsat data to show an approximately consistent tendency of spectral variation when compared with the *in-situ* samples [17]. Aerosol and water vapor retrieval options were not activated for the current study. The historical meteorological data corresponding with each of the Landsat scenes did not support changing the modeled atmospheric conditions across the various years.

Detection of seagrasses and other benthic environments is complicated by the fact that they are covered by a water column that attenuates the light reaching, interacting with, and being reflected from the benthos. As attenuation is a function of the depth of the overlying water column, a correction for water column depth was performed prior to classification. Because of the relative ease of implementation and proven effectiveness [45–47], Lyzenga's method for creating depth-invariant bands [48,49] was implemented.

Lyzenga's method assumes that light attenuation follows an exponential decay curve with increasing depth, which is often satisfied for tropical coastal waters [47]. Although the ratios of the water attenuation coefficients for the wavelength bands used are required as input for the water column depth correction, these parameters can be obtained from the

Landsat images as long as pixels representing a uniform substrate but variable depth can be identified, given differences in reflectance between different pixels of the same substrate are attributable entirely to differences in depth. Bare mud pixels varying from approximately 1 m to 4 m in depth were selected from the calibration images based on the Florida Bay Bottom Types map, bathymetric contours produced by the USGS, and visual interpretation of the imagery. Three ratios of attenuation, between wavelength bands 1 (0.45–0.52 μm) and 2 (0.52–0.60 μm), bands 1 and 3 (0.63–0.69 μm), and bands 2 and 3 were calculated. Comparison of the ratios derived for this study with the measured downwelling attenuation coefficient showed the derived ratios to be reasonable, lying between those measured *in-situ* immediately west of Florida Bay and in the Caribbean Sea (where a spectral shape typical for oligotrophic Case I waters was measured) [50]. All three depth-invariant bands produced based on the calculated ratios of attenuation were then used for the benthic classification.

3.2.4. Seagrass Classification

The Landsat scenes from the years 2009 to 2011 were used for calibration of the classifier (training pixel selection), and 2007 and 2008 were used for validation purposes. This segregation of the *in-situ* data represented the scenario where field data are collected to retrospectively map a time series of seagrass density and allows evaluation of the transferability of the pixel-based classifier to older images. Every pixel containing a field sampling station from the 2009 to 2011 calibration set that was not identified as cloud or land was employed in training the classifier. For the validation pixels, sampling site pixels identified as cloud or land or classified as turbid were omitted from accuracy assessment calculations.

As seagrass percent cover often varies at a spatial scale of <1 m [30], using a single pixel instead of a neighborhood average was deemed appropriate. The FHAP field data record the Braun Blanquet abundance class at four quadrats making up each survey site. The average abundance score for each field site was calculated as the mean of the quadrat scores and then used to group the field sites into four classes, as shown in Table 3.2. The sparse cover class was defined to represent areas that are predominantly bare sediment. Specification of low and dense classes was based on typical definitions for these classes from the literature [13–17]. Spectral evaluation of the four reference classes revealed that medium and dense training pixels were difficult to distinguish from one another, so they were merged to define a single medium-dense spectral class. Turbid water areas, evidenced by visual interpretation of the calibration scenes and preliminary unsupervised K-means classification, were sampled to define a fourth class.

Table 3.2 Summary of seagrass cover classes employed in this study, including the number of pixels used for training and validation. Pixels representing medium and dense seagrass cover were grouped for selection of training pixels.

Class	**Avg. Braun-Blanquet Score**	**Training Samples (Pixels)**			**Validation Samples (Pixels)**	
		2009	**2010**	**2011**	**2007**	**2008**
Dense	>4.5	82	104	98	15	10
Medium	2.5 to 4.5				74	76
Low	1.5 to 2.5	25	13	26	19	40
Sparse	<1.5	4	5	5	20	8

3.2.5. Error Matrix and Accuracy Assessment

Seagrass maps were produced based on the three depth-invariant bands for each year, and statistics on the spectral classes (from training pixels spanning years 2009 to 2011) using ENVI's Maximum Likelihood classifier with no probability threshold and a data scale factor of 1. The Maximum Likelihood classification method is based on the Bayes' theorem, with class mean vector and covariance matrix input to a discriminant function to assign pixels to the class with the highest likelihood [51]. The geo-referenced field data corresponding to the 2007 and 2008 images, which were not included in the calibration, were used as reference pixels to derive the error matrix and calculate the producer's, user's and overall accuracies of the classifier. The error matrix displays the proportion of all mapped pixels that are of map class i and reference class j (pij), where the diagonals of the matrix represent correctly classified areas and off-diagonals identify classification errors. Row margins (pi+) are the proportion of pixels classified as class i and column margins (p + j) estimate the proportion of area of class j. Table 3.3 [52,53] shows the producer's, user's and overall accuracies of our resulting classification.

Table 3.3 Seagrass cover classification error matrix and accuracy assessment measures for each validation scene.

			Reference Class					
			Dense	Medium	Low	Sparse	Total	** Users Accuracy
Map Class	**2007**	Med-Dense	9%	48%	5%	0%	63%	93%
		Low	2%	8%	6%	4%	20%	31%
		Sparse	0%	2%	4%	12%	17%	68%
		Total	12%	58%	4%	16%	*** Overall	
		* Producers Accuracy	80%	84%	42%	75%	Accuracy = 76%	
	2008	Med-Dense	7%	51%	8%	0%	66%	88%
		Low	0%	4%	4%	1%	8%	45%
		Sparse	0%	2%	18%	5%	25%	21%
		Total	7%	57%	30%	6%	Overall Accuracy	
		Producers Accuracy	100%	89%	13%	88%	= 67%	

***** Producer's accuracy, a measure of the error of omission for each class, is the proportion of correctly mapped pixels for a given class in the reference data. ****** User's accuracy, a c measure of the error of commission, is the proportion of pixels incorrectly identified as belonging to a given class. ******* Overall accuracy measures agreement at the map level, as opposed to the category level, where overall accuracy is the sum of the error matrix diagonals. For more detail on accuracy measures, the reader is directed to Liu *et al.* [52] and Olofsson *et al.* [53].

To further examine the validity of the study methodology, Landsat 5 images from 1998 to 2006 were classified. Only the interior basins that are less affected by waves were included in this mapping exercise. Although no *in-situ* survey data on total seagrass cover were available for the 1998–2006 maps, the extended temporal span enables a qualitative assessment of the applicability of the methodology to time series data through evaluation of the longer term changes depicted by the map products.

3.3. Results and Discussion

The classified maps produced in this study showed general agreement with the trends indicated by the point data from the *in-situ* surveys. Assessment of the changes in seagrass cover suggests that interior basins were classified more accurately than the portions of the study area adjacent to the Gulf of Mexico.

3.3.1. In-Situ Data Description and Distribution

Evaluation of the *in-situ* dataset of seagrass cover collected by the FHAP indicated there were temporal trends in seagrass distribution that varied with space throughout the study area. Although the seagrass dataset also included fall cover surveys for years from 1995 to 2003 (whereas spring surveys were conducted over the program's entire duration until 2012), no pattern of seasonal variability was discerned within any of the study area survey basins.

Total seagrass cover from 2007 to 2012 showed mean cover remaining relatively stable from year to year within each basin over the five most recent years. Mean total seagrass cover increased toward the west within the surveyed study area basins, as shown in the plots of *in-situ* survey data in Figure 3.3. The median and mode of total seagrass cover also generally increased to the west. The *in-situ* points suggested annual variability in seagrass abundance illustrated by changes in the location of the transition from low to medium-dense cover each year.

Observation of species-specific seagrass abundance from early in the FHAP survey (before total seagrass cover was recorded) showed greater inter-annual variability over the period from 1995 to the early 2000's than in more recent years. Since 1995, *Thalassia*

testudinum showed an increasing trend in the northern FHAP basins included in the study area and a more stable or possibly decreasing cover trend to the south.

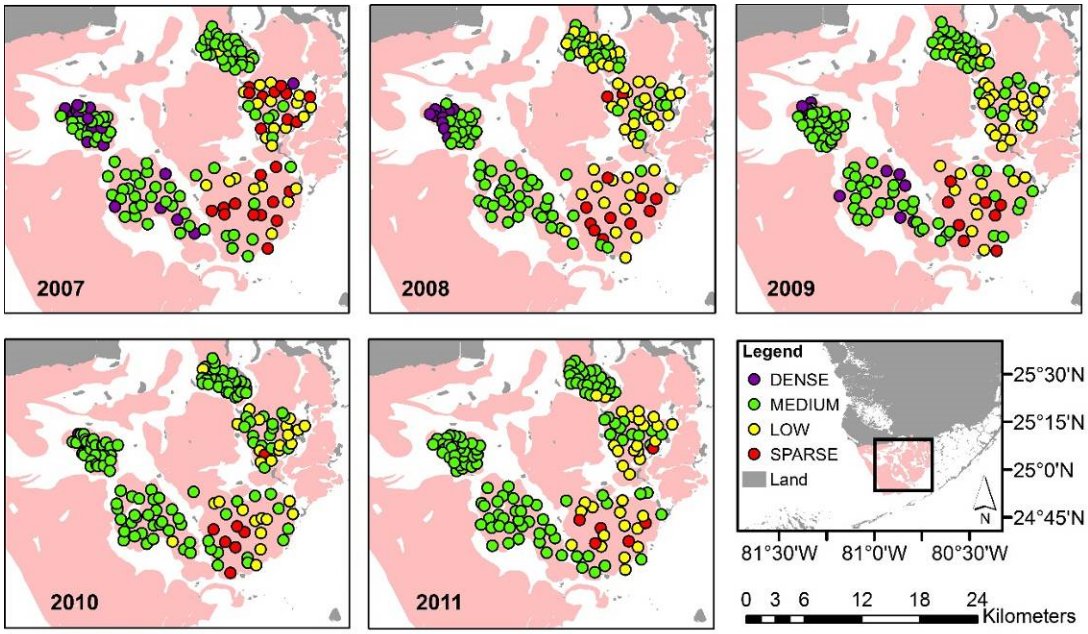

Figure 3.3. Map summary of *in-situ* data showing the distribution of cover classes across survey sites.

3.3.2. Image Classification

The overall accuracy for each validation year of 67% in 2007 and 76% in 2008 was within the range of accuracies achieved from other studies employing supervised classification of Landsat data to map seagrass [16,17,30]. Substantial differences in the classification accuracy by cover class are apparent, with the Low cover class performing the worst and all other cover classes exceeding 75% producer's accuracy in either validation year (Table 3.3). Because seagrasses have been observed to be patchier at lower standing crop [12], the poor producer's accuracy of the low cover class may be caused by high intra-pixel variation for pixels exhibiting areas of low cover.

From visual interpretation, the arrangement of cover classes in the map products for the validation years appear to match the patterns represented in the *in-situ* data (Figure 3.4). The portions of the study area providing the most interesting indicators of classification accuracy are the two easternmost basins, which included a more heterogeneous mix of cover classes in the ground truth data. Although these heterogeneous areas perform worse in terms of matching the field data class to the class assigned to the corresponding pixel, misclassified pixels tend to be located along the transitions between larger groups of different cover classes or in areas where the reference class is only present in small patches within a more dominant cover class according to the map product. These observations suggest that some of the classification error may result from the difference in the spatial scale of the *in-situ* observation and satellite pixel.

The discrepancy between the spatial domain represented by a single Landsat pixel (30 m by 30 m) and *in-situ* reference site (0.5 m by 0.5 m) remained a substantial source of uncertainty for both classifier calibration and accuracy assessment. For example, very few field survey sites were classified as having dense cover each year and no dense field sites were observed in calibration year 2011. Therefore, it may be unrealistic for the much larger Landsat pixels to have dense cover throughout even though some pixels were classified as dense based on the field sample contained by those pixels. In other words, the field sample may not accurately represent the more expansive Landsat pixel so that actual classification accuracy may be higher than those reported in Table 3.3.

Another evaluation of the classification accuracy was to determine whether the trends and variability expressed through the map products were reasonable. The interior regions

did not show much change in seagrass cover, but the easternmost basins indicated seagrass loss between 2007 and 2008 and an apparent westward retreat of the transition zone from dense to sparse cover (see also Figure 3.5). The location and timing of the change in seagrass indicated by the 2007 and 2008 maps may be attributed to an algal bloom in the eastern portions of Florida Bay. The algal bloom began in fall of 2005 within the vicinity of Barnes Sound and extended along eastern Florida Bay to Duck Key by November 2005 [54]. The northeastern algal bloom reoccurred seasonally in 2006 and 2007, extending to north-central portions of the Bay in 2007 and subsiding by May 2008 [54]. It is reasonable to surmise that seagrass cover was reduced in areas adjacent to the persistent algal bloom.

The portions of the study area immediately adjacent to the Gulf of Mexico show a westward expansion of dense seagrass in the 2007 and 2008 map products, as well as a reduction in turbid water area, from 2007 to 2008. In these western portions of the bay, which are more influenced by tides and waves than are the interior portions of the study area, the classifier may be categorizing turbid water as low and sparse seagrass. Although it is difficult to determine without corresponding field data whether the Gulf-adjacent areas are misclassified, the classifier may be inappropriate for these portions of the bay.

Figure 3.5 presents the results of applying the classifier to the interior portions of the study area over an extended time series back to 1998. The inter-annual variability illustrated by the map products shown in Figure 3.5 is consistent with the observed trends in the dominant *Thalassia testudinum*'s FHAP survey data from the 1998 to 2006. An increasing trend in *T. testudinum*'s cover class data is indicated in Johnson Key and Rankin basins over the 1998 to 2008 period while an increasing trend persisted in Rabbit

Key Basin from 1998 to the mid-2000s. The *Thalassia* cover data show a steady or somewhat decreasing trend in Twin Key Basin, though no trend is apparent in Whipray Basin over the 1998–2008 period.

A more statistically thorough investigation into the FHAP survey data, conducted by Landry in 2005 [55] on the data available up to that point (1995–2004) also corroborates the inter-annual variability indicated by the Figure 3.5 map products. For example, Landry found that for Rankin Basin, *Halodule* densities, which were generally denser in north and eastern portions of the basin, dominated until 2002 when *Thalassia*, which was denser in the south part of the basin, surpassed *Halodule*. Additionally, Landry found *Thalassia* to be generally denser around the perimeter and western area of Twin Key basin, that *Thalassia* is much denser in the eastern portions of Rabbit Key basin than in western portions, and that Rabbit Key *Thalassia* densities rebound and then level off over the 1998 to 2004 period.

Although Figure 3.5 shows that turbidity is still an issue in multiple years even in the interior basins, the proximity of areas classified as turbid and medium-dense in 1999 suggests that the remainder of the map product (*i.e.*, area not classified as turbid) is valid for the purposes of landscape scale monitoring of the benthic environment.

One caution with our methodology is that the water column optical properties must be similar for all pixels within a study area and across the various scenes evaluated. We minimized variation in water column components across scenes in this study by using data from the same season each year. In addition, turbidity was minimized since the study scenes occurred toward the end of the dry season.

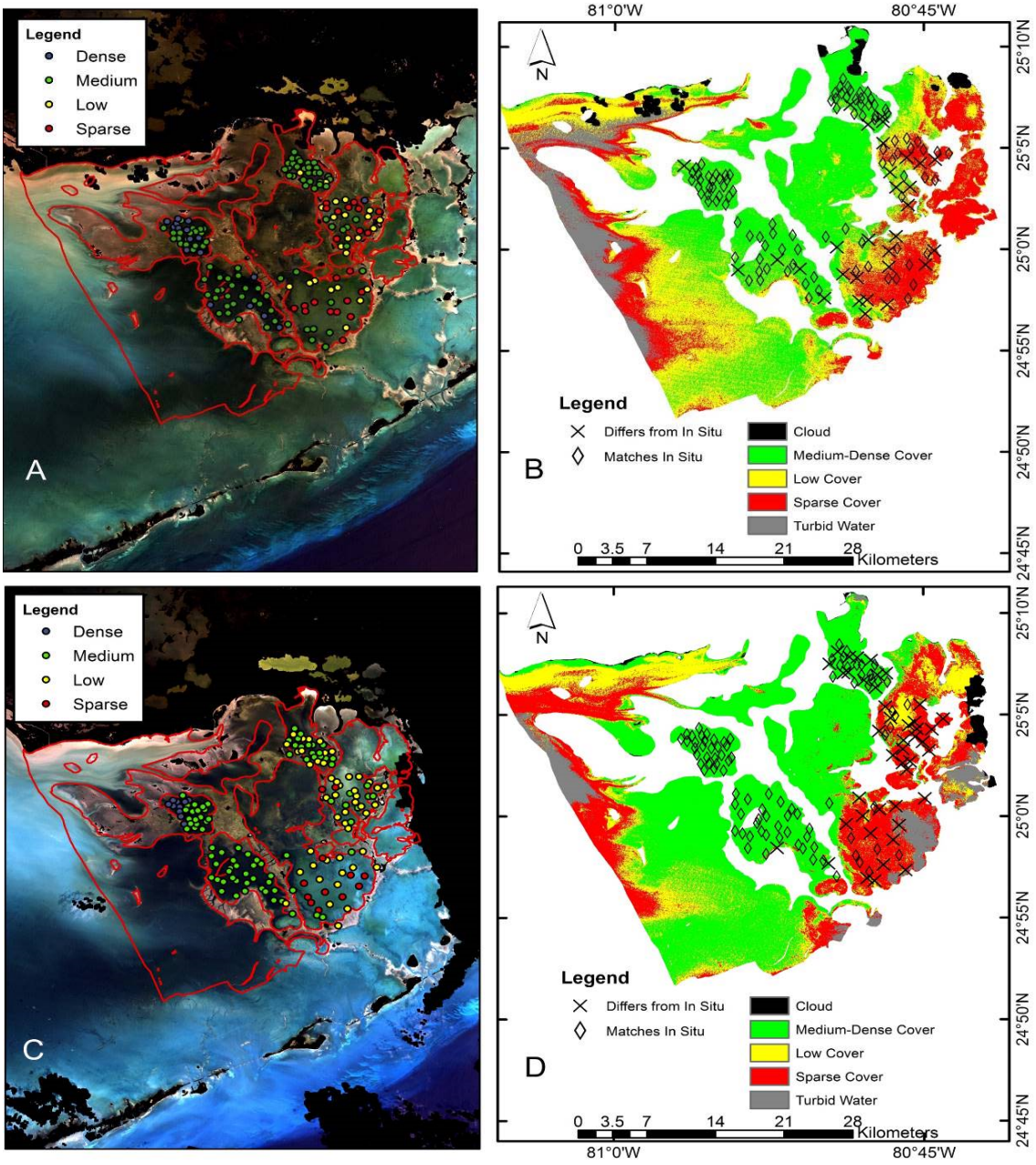

Figure 3.4. (A) 2007 true color composite of the study area showing *in-situ* data; (B) 2007 seagrass cover mapping product showing coherence with *in-situ* data; (C) 2008 true color composite of study area showing *in-situ* data; (D) 2008 seagrass cover mapping product showing coherence with *in-situ* data.

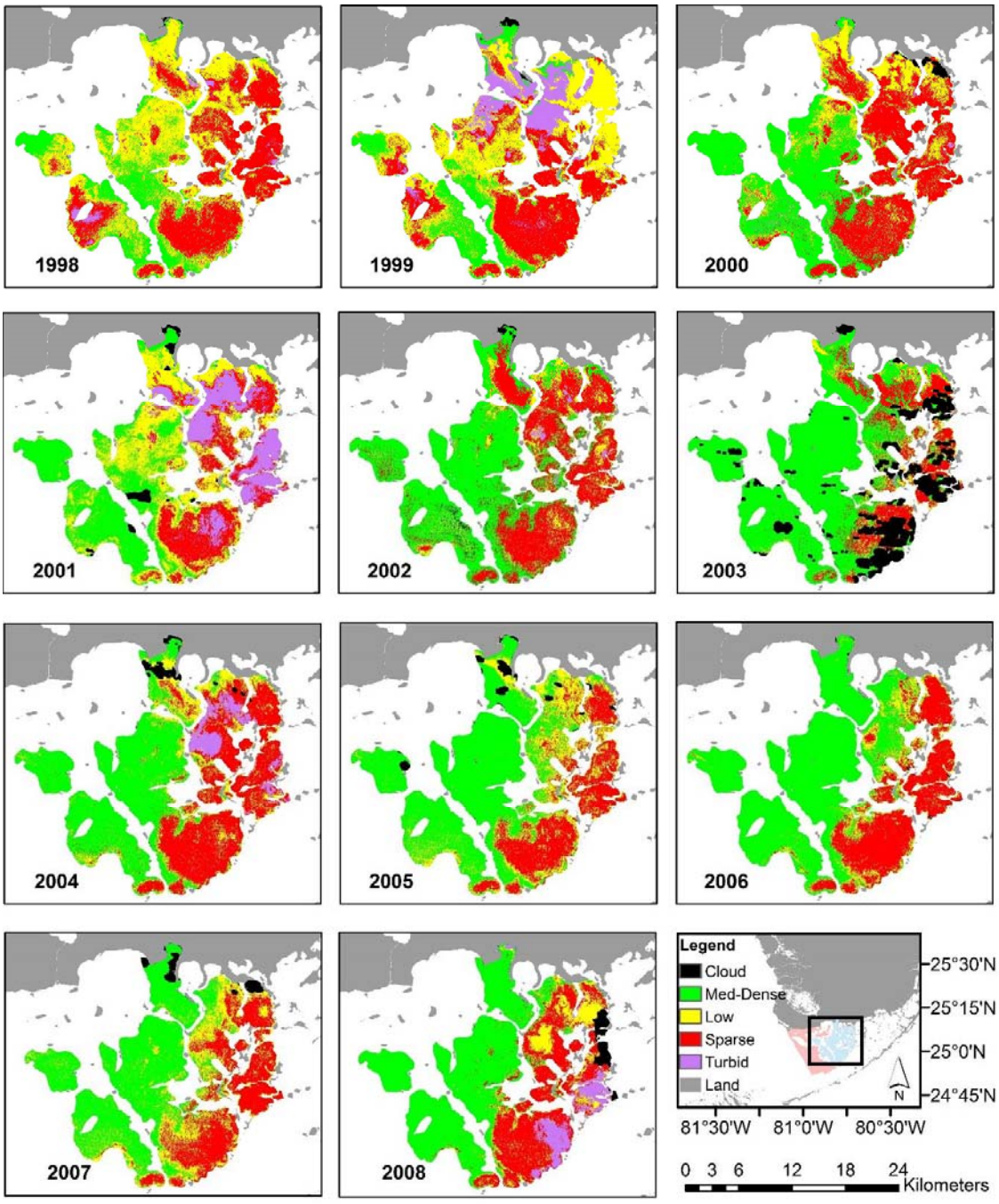

Figure 3.5 Seagrass cover mapping products for 1998 to 2008.

3.4. Conclusions

This study demonstrated that a pixel-based classifier trained on data compiled using Landsat 5 images from three consecutive years was extendible to time-series images from an earlier period for the same study area. Although spectral library methods may be preferred in terms of transferability across images, the classification accuracies achieved in this study (76% and 67% overall accuracy, but 75% to 100% accuracy for three of four classes in the two validation images) showed that meaningful information could be obtained through simpler techniques.

Although there are limitations to the methodology employed in this study, the importance of understanding valuable and dynamic coastal systems warrants the use of methodologies that allow greater interpretation of available synoptic data. Estimating the status of valuable coastal marine habitats provides better evidence for environmental changes and aids in the description of the processes that are behind the changes [28]. For example, the patchy mortality characteristic of seagrass die-off is very different from the gradual thinning and loss of seagrasses due to decreased water clarity [41]. Despite these benefits, the potential for using remote sensing to monitor environmental factors influencing seagrass loss has, thus far, been little explored [8]. Our assessment suggests that pixel-based classifiers of benthic habitats developed for specific images can be generalized and extended to images from other years, expediting the time series mapping that is required to adequately inform coastal resource management.

As reflectances from benthic environments and the water column are integrated in remotely sensed images of shallow, relatively clear coastal waters, maps of benthic properties which can be assumed stable over some period of time are also helpful in

interpreting satellite data for information on water column properties. For example, if the benthic cover can be assumed fixed over a season or longer variations in reflectance may be attributed to changes in water column properties. Remote sensing products that accurately detect transient water column properties, particularly chlorophyll-*a* which is indicative of algal blooms, can then be used to improve the environmental conditions affecting coastal ecosystems.

Because a common radiometric scale is assumed across all images in a time series mapped with a single classifier, atmospheric correction is an important consideration for the studied methodology. Atmospheric correction procedures derived specifically for normalizing surface reflectance values across images, although likely to improve the transferability of pixel-based classifiers, were not employed in this study and should be evaluated in future work.

The accessibility of our method, in terms of equipment, software and expertise required, promotes the use of the Landsat archive for multi-temporal analyses of coastal dynamics. Future field data collection efforts for application to benthic habitat mapping are recommended to consider the remote sensor's spatial resolution during survey design. The ability to identify the benthic characteristics for an entire pixel from field data would improve the precision of both classifier training and accuracy assessment, potentially increasing the utility of the resulting map products to researchers and managers.

Acknowledgments

This study was funded by the NASA WaterSCAPES Project and the Florida Education Fund's McKnight Fellowship program. The authors would like to thank the Florida Fish

and Wildlife Conservation Commission, which collected and provided the *in-situ* data for this study.

Author Contributions

Tara Blakey was the primary analyst and author for this work. Assefa Melesse was the corresponding author and contributed as a supervisor to the research and writing of the paper. Margaret Hall contributed to the research and writing as an expert on the in situ dataset.

Conflicts of Interest

The authors declare no conflicts of interest.

References

1. Koch, M.S.; Schopmeye, S.; Holmer, M.; Madden, C.; Kyn-Hansen, C. *Thalassia testudinum* response to the interactive stressors hypersalinity, sulfide and hypoxia. *Aquat. Bot.* 2007, *87*, 104–110.

2. Madden, C.J.; Rudnick, D.T.; McDonald, A.A.; Cunniff, K.M.; Fourqurean, J.W. Ecological indicators for assessing and communicating seagrass status and trends in Florida Bay. *Ecol. Indic.* 2009, *9*, S68–S82.

3. Yaakub, S.M.; Chen, E.; Bouma, T.; Erftemeijer, P.; Todd, P. Chronic light reduction reduces overall resilience to additional shading stress in the seagrass *Halophila ovalis*. *Mar. Pollut. Bull.* 2013, *83*, 467–474.

4. Fourqurean, J.W.; Duarte, C.; Kennedy, H.; Marba, N.; Holmer, M.; Mateo, M.; Apostolaki, E.; Kendrick, G.; Krause-Jensen, D.; McGlathery, K.; *et al*. Seagrass ecosystems as a globally significant carbon stock. *Nat. Geosci.* 2012, *5*, 505–509.

5. Fourqurean, J.W.; Kendrick, G.A.; Collins, L.S.; Chambers, R.M.; Vanderklift, M.A.
Carbon, nitrogen and phosphorous storage in subtropical seagrass meadows: Examples from Florida Bay and Shark Bay. *Mar. Freshw. Res.* 2012, *63*, 967–983.

6. Collier, C.J.; Waycott, M.; Ospina, A. Responses of four Indo-West Pacific seagrass species to shading. *Mar. Pollut. Bull.* 2012, *65*, 342–354.

7. Hill, V.J.; Zimmerman, R.; Bissett, W.; Dierssen, H.; Kohler, D. Evaluating light availability, seagrass biomass, and productivity using hyperspectral airborne remote sensing in Saint Joseph's Bay, Florida. *Estuaries Coasts* 2014, *37*, 1467–1489.

8. Ferweda, J.; de Leeuw, J.; Atzberger, C.; Vekerdy, Z. Satellite-based monitoring of tropical seagrass vegetation: Current techniques and future developments. *Hydrobiologia* 2007, *591*, 59–71.

9. Thorhaug, A.; Richardson, A.; Berlyn, G. Spectral reflectance of *Thalassia testudinum* (Hydrocharitaceae) seagrass: Low salinity effects. *Am. J. Bot.* 2006, *93*, 110–117.

10. Yaakub, S.M.; McKenzie, L.; Erftemeijer, P.; Bouma, T.; Todd, P. Courage under fire: Seagrass persistence adjacent to a highly urbanized city-state. *Mar. Pollut. Bull.* 2014, *83*, 417–424.

11. Dekker, A.; Brando, V.; Anstee, J.; Fyfe, S.; Malthus, T.; Karpouzli, E. Remote sensing of seagrass ecosystems: Use of spaceborne and airborne sensors. In *Seagrass:*

Biology, Ecology, and Conservation; Springer: Dordrecht, The Netherlands, 2006; Chapter 15, pp. 347–359.

12. Mumby, P.J.; Green, E.P.; Edwards, A.J.; Clark, C.D. Measurement of seagrass standing crop using satellite and digital airborne remote sensing. *Mar. Ecol. Prog. Ser.* 1997, *159*, 51–60.

13. Lyons, M.B.; Phinn, S.R.; Roelfsema, C.M. Long term land cover and seagrass mapping using Landsat and object-based image analysis from 1972 to 2010 in the coastal environment of South East Queensland, Australia. *ISPRS J. Photogramm. Remote Sens.* 2012, *71*, 34–46.

14. Phinn, S.; Roelfsema, C.; Dekker, A.; Brando, V.; Anstee, J. Mapping seagrass species, cover and biomass in shallow waters: An assessment of satellite mutli-spectral and airborne hyperspectral imaging systems in Moreton Bay (Australia). *Remote Sens. Environ.* 2008, *112*, 3413–3425.

15. Roelfsema, C.M.; Phinn, S.R.; Udy, N.; Maxwell, P. An integrated field and remote sensing approach for mapping seagrass cover, Moreton Bay, Australia. *Spat. Sci.* 2009, *54*, 45–62.

16. Wabnitz, C.C.; Andrefouet, S.; Torres-Pulliza, D.; Muller-Karger, F.E.; Kramer, P.A. Regional scale seagrass habitat mapping in the Wider Caribbean region using Landsat sensors: Applications to conservation and ecology. *Remote Sens. Environ.* 2008, *112*, 3455–3467.

17. Pu, R.; Bell, S.; Meyer, C.; Baggett, L.; Zhao, Y. Mapping and assessing seagrass along the western coast of Florida using Landsat TM and EO-1 ALI/Hyperion imagery. *Estuar. Coast. Shelf Sci.* 2012, *115*, 234–245.

18. Kim, K.; Choi, J.; Ryu, J.; Jeong, H.J.; Lee, K.; Park, M.G.; Kim, K.Y. Observation of typhoon-induced seagrass die-off using remote sensing. *Estuar. Coast. Shelf Sci.* 2015, *154*, 111–121.

19. Pu, R.; Bell, S.; Meyer, C. Mapping and assessing seagrass bed changes in Central Florida's west coast using multitemporal Landsat TM imagery. *Estuar. Coast. Shelf Sci.* 2014, *149*, 68–79.

20. Roelfsema, C.; Kovacs, E.; Saunders, M.I.; Phinn, S.; Lyons, M.; Maxwell, P. Challenges of remote sensing for quantifying changes in large complex seagrass environments. *Estuar. Coast. Shelf Sci.* 2013, *133*, 161–171.

21. Kutser, T.; Miller, I.; Jupp, D. Mapping coral reef benthic substrates using hyperspectral space-borne images and spectral libraries. *Estuar. Coast. Shelf Sci.* 2006, *70*, 449–460.

22. Dekker, A.G.; Brando, V.E.; Anstee, J.M. Retrospective change detection in a shallow coastal tidal Australian lake. *Remote Sens. Environ.* 2005, *97*, 415–433.

23. Louchard, E.M.; Reid, P.; Stephens, F.; Davis, C.; Leathers, R.; Downes, V. Optical remote sensing of benthic habitats and bathymetry in coastal environments at Lee Stocking Island, Bahamas: A comparative spectral classification approach. *Limnol. Oceanogr.* 2003, *48*, 511–521.

24. Wolf, P.; Robler, S.; Schneider, T.; Melzer, A. Collecting *in situ* remote sensing reflectances of submersed macrophytes to build up a spectral for lake monitoring. *Eur. J. Remote Sens.* 2013, *46*, 401–416.

25. Dierssen, H.M.; Zimmerman, R.C.; Drake, L.A.; Burdige, D. Benthic ecology from space: Optics and net primary production in seagrass and benthic algae across the Great Bahama Bank. *Mar. Ecol. Prog. Ser.* 2010, *411*, 1–15.

26. Kutser, T.; Vahtmae, E.; Metsamaa, L. Spectral library of macroalgae and benthic substrates in Estonian coastal waters. *Proc. Est. Acad. Sci. Biol. Ecol.* 2006, *55*, 329–340.

27. Dierssen, H.; Zimmerman, R.C.; Leathers, R.A.; Downes, T.V.; Davis, C.O. Ocean color remote sensing of seagrass and bathymetry in the Bahamas Banks by high-resolution airborne imagery. *Limnol. Oceanogr.* 2003, *48*, 444–455.

28. Vahtmae, E.; Kutser, T. Classifying the Baltic Sea shallow water habitats using image-based and spectral library methods. *Remote Sens.* 2013, *5*, 2451–2474.

29. Zomer, R.J.; Trabucco, A.; Ustin, S. Building spectral libraries for wetlands land cover classification and hyperspectral remote sensing. *J. Environ. Manag.* 2009, *90*, 2170–2177.

30. Lyons, M.B.; Roelfsema, C.M.; Phinn, S.R. Towards understanding temporal and spatial dynamics of seagrass landscapes using time-series remote sensing. *Estuar. Coast. Shelf Sci.* 2012, *120*, 42–53.

31. Hossain, M.S.; Bujang, J.S.; Zakaria, M.H.; Hashim, M. The application of remote sensing to seagrass ecosystems: An overview and future prospects. *Int. J. Remote Sens.* 2015, *36*, 61–114.

32. Barnes, B.B.; Hu, C.; Holekamp, K.; Blonski, S.; Spiering, B.; Palandro, D.; Lapointe, B. Use of Landsat data to track historical water quality changes in Keys marine environments. *Remote Sens. Environ.* 2014, *140*, 485–496.

33. McPherson, M.L.; Hill, V.J.; Zimmerman, R.C.; Dierssen, H.M. The optical properties of Greater Florida Bay: Implications for seagrass abundance. *Estuar. Coasts* 2011, *34*, 1150–1160.

34. Nagel, J.L.; Kemp, W.M.; Cornwell, J.C.; Owens, M.S.; Hinkle, D.; Madden, C.J. Seasonal and regional variations in net ecosystem production in Thalassia testudinum communities throughout Florida Bay. *Contrib. Mar. Sci.* 2009, *38*, 91–108.

35. Lee, T.; Williams, E.; Johns, E.; Wilson, D.; Smith, N.P. Transport processes linking south Florida coastal systems. In *The Evergades, Florida Bay and Coral Reefs of the Florida Keys: An Ecosystem Sourcebook*; CRC Press: Boca Raton, FL, USA, 2002; pp. 309–341.

36. Lee, T.; Smith, N. Volume transport variability through the Florida Keys tidal channels. *Cont. Shelf Res.* 2002, *22*, 1361–1377.

37. Taylor, K.H.; Purkis, S.J. Evidence for the southward migration of mud banks in Florida Bay. *Mar. Geol.* 2012, *311*, 52–56.

38. Boyer, J.N.; Fourqurean, J.W.; Jones, R.D. Spatial characterization of water quality in Florida Bay and Whitewater Bay by multivariate analyses: Zones of similar influence. *Estuaries* 1997, *4*, 743–758.

39. Zieman, J.C.; Fourqurean, J.W.; Iverson, R.L. Distribution, abundance and productivity of seagrasses and macroalgae in Florida Bay. *Bull. Mar. Sci.* 1989, *441*, 292–311.

40. Phlips, E.J.; Lynch, T.C.; Badylak, S. Chlorophyll a, tripton, color, and light availability in a shallow tropical inner-shelf lagoon, Florida Bay, USA. *Mar. Ecol. Prog. Ser.* 1995, *127*, 223–234.

41. Hall, M.O.; Durako, M.J.; Fourqurean, J.W.; Zieman, J.C. Decadal changes in seagrass distribution and abundance in Florida Bay. *Estuaries* 1999, *22*, 445–459.

42. Hall, M.; Madley, K.; Durako, M.; Zieman, J.; Robblee, M. Florida Bay. *Seagrass Status and Trends in the Northern Gulf of Mexico: 1940–2002*; Scientific Investigations Report 2006-5287; U.S. Geologic Survey: Reston, VA, USA, 2007; pp. 242–252.

43. Fourqurean, J.W.; Durako, M.; Hall, M.; Hefty, L. Seagrass distribution in South Florida: A multi-agency coordinated monitoring program. In *The Evergades, Florida Bay and Coral Reefs of the Florida Keys: An Ecosystem Sourcebook*; CRC Press: Boca Raton, FL, USA, 2002; pp. 497–522.

44. Zhu, Z.; Woodcock, C.E. Object-based cloud and shadow detection in Landsat imagery. *Remote Sens. Environ.* 2012, *118*, 83–94.

45. Zoffoli, M.L.; Frouin, R.; Kampel, M. Water column correction for coral reef studies by remote sensing. *Sensors* 2014, *14*, 16881–16931.

46. Amran, M.A. Estimation of seagrass coverage by depth invariant indices on quickbird imagery. *Biotropia* 2010, *17*, 42–50.

47. Mumby, P.J.; Clark, C.D.; Green, E.P.; Edwards, A.J. Benefits of water column correction and contextual editing for mapping coral reefs. *Int. J. Remote Sens.* 1998, *19*, 203–210.

48. Lyzenga, D.R. Passive remote sensing techniques for mapping water depth and bottom features. *Appl. Opt.* 1978, *17*, 379–383.

49. Lyzenga, D.R. Remote sensing of bottom reflectance and water attenuation parameters in shallow water using aircraft and Landsat data. *Int. J. Remote Sens.* 1981, *2*, 71–82.

50. Zhao, J.; Barnes, B.; Melo, N.; English, D.; Lapointe, B.; Muller-Karger, F.; Schaeffer, B.; Hu, C. Assessment of satellite-derived diffuse attenuation coefficients and euphotic depths in south Florida coastal waters. *Remote Sens. Environ.* 2013, *131*, 38–50.

51. Ahmad, A.; Quegan, S. Analysis of Maximum Likelihood classification on multispectral data. *Appl. Math. Sci.* 2012, *6*, 6425–6436.

52. Liu, C.; Frazier, P.; Kumar, L. Comparative assessment of the measures of thematic classification accuracy. *Remote Sens. Environ.* 2007, *107*, 606–616.

53. Olofsson, P.; Foody, G.M.; Herold, M.; Stehman, S.V.; Woodcock, C.E.; Wulder, M.A.
Good practice for estimating area and assessing the accuracy of land change. *Remote Sens. Environ.* 2014, *148*, 42–57.

54. Restoration Coordination and Verification (RECOVER). *2009 System Status Report. Comprehensive Everglades Restoration Plan*; Restoration Coordination and Verification Program, c/o United States Army Corps of Engineers: Jacksonville, FL, USA; South Florida Water Management District: West Palm Beach, FL, USA, 2010.

55. Landry, J.B. Changes in the distribution and density of Florida Bay Macrophytes: 1995–2004. Master's Thesis, University of North Carolina Wilmington, Wilmington, NC, USA, 2005.

4 IMPROVING SATELLITE-BASED CHLOROPHYLL *A* ESTIMATING ALGORITHMS IN SHALLOW, COASTAL WATERS USING BENTHIC CLASS-SPECIFIC ALGORITHMS

Blakey T, Melesse A, Sukop M, Tachiev G, Whitman D, Miralles-Wilhelm F (2015)

Abstract

In this study, the ability to improve Sea-Viewing Wide Field-of-View Sensor (SeaWIFS) chl-*a* retrieval from optically shallow coastal waters by applying algorithms specific to the pixels' benthic class was evaluated. The form of the Ocean Color (OC) algorithm was assumed for this study. The operational atmospheric correction producing Level 2 SeaWiFS data was retained since the focus of this study was on establishing the benefit from the alternative specification of the bio-optical algorithm. Benthic class was determined through satellite image-based classification methods. Accuracy of the chl-*a* algorithms evaluated was determined through comparison with coincident *in situ* measurements of chl-*a*. The regionally-tuned models that were allowed to vary by benthic class produced more accurate estimates of chl-*a* than the single, unified regionally-tuned model. Mean absolute percent difference was approximately 70% for the regionally-tuned, benthic class-specific algorithms. Evaluation of the residuals indicated the potential for further improvement to chl-*a* estimation through finer characterization of benthic environments. Atmospheric correction procedures specialized to coastal environments are indicated as areas for future improvement as these procedures would improve both classification and algorithm tuning.

Key words: Chl-*a*, optically shallow, bottom reflectance, SeaWiFS, ocean color remote sensing

4.1 Introduction

As an index for phytoplankton, remotely-sensed chlorophyll *a* (chl-*a*) has been recognized as useful for establishing a baseline for water quality conditions and for assessing current status even in optically-complex nearshore (Schaeffer 2012, Le 2013a) and inland (Palmer 2015) environments. The Sea-Viewing Wide Field-of-View Sensor (SeaWIFS) sensor (1997-2010) provides a valuable archive of synoptic data with one day revisit and bands tuned for retrieval of chl-*a*. However, the Ocean Chlorophyll (OC) algorithm, the chl-*a* algorithm currently operational for SeaWiFS, is known to overestimate chl-*a* in nearshore waters (Blondeau-Patissier 2014, Werdell 2009). The OC algorithm uses empirical correlations derived from global *in situ* data sets and, therefore, cannot account for systematic differences in the bio-optical relationship that may temporarily or permanently exist in certain geographic zones (Werdell 2007).

Compared to satellite-derived chl-*a* for oceanic waters, nearshore environments pose challenges from colored dissolved organic matter (CDOM), suspended sediments, bottom reflectance and atmospheric conditions which, like chl-*a*, absorb blue light preferentially. While semi-analytical approaches that can distinguish between the optically significant constituents in the water column exist, these algorithms require accurate remote sensing reflectance (R_{rs}), and may fail in the presence of negative R_{rs} so that they sacrifice daily spatial coverage in comparison to empirical algorithms (Werdell 2007).

Few, if any, studies have evaluated improvements to the accuracy of SeaWiFS chl-*a* retrievals in optically shallow water where bottom reflectance is substantial. Le *et al*. (2013a) developed a Red-Green-Chlorophyll-Index for SeaWiFS retrieval from

estuarine waters achieving uncertainties comparable to those from the OC algorithm in open ocean waters, but pixels contaminated by bottom reflectance were excluded. Using R_{rs} falling outside the transparency window (i.e., $R_{rs}412$ and $R_{rs}670$), Cannizzaro *et al*. (2006) improved chl-*a* algorithm accuracy for optically-shallow water with substantial bottom reflectance. Although the algorithm developed by Cannizzaro used wavelengths available from SeaWiFS, that work utilized shipboard and mooring-collected reflectances and did not explicitly test the applicability to satellite-based ocean color data.

In the present study, the ability to improve satellite chl-*a* retrieval from optically shallow coastal waters by applying algorithms specific to the pixels' benthic class was evaluated. Because of the global use of the OC algorithm, and because band-ratio algorithms have been shown to have the potential to derive chl-*a* in estuarine waters (Le 2013b), the form of the OC algorithm was assumed for this study. The operational atmospheric correction producing Level 2 SeaWiFS data was retained since the focus of this study was on establishing the benefit from the alternative specification of the bio-optical algorithm. Accuracy of the algorithms evaluated was determined through comparison with coincident *in situ* measurements of chl-*a*. The regionally-tuned models that were allowed to vary by benthic class produced more accurate estimates of chl-*a* than the single regionally-tuned model. Evaluation of the residuals indicated the potential for further improvement to chl-*a* estimation through better characterization of benthic environments.

4.2 Data and Methods

4.2.1 *In Situ* Data

A network of water quality monitoring stations, the South Florida Water Quality Management Network, was established in Florida Bay by the Southeast Environmental Research Center at Florida International University. Field measurement of chl-*a* was conducted at water quality stations distributed across Florida Bay with data from six stations included in this study (Figure 4.1). Water column measurements and samples were collected every other month from July 1989 to December 1990 and monthly from March 1991 to September 2008 (Briceño and Boyer, 2010). The data are available from the Center's website at serc.fiu.edu/wqmnetwork. Details on sampling methodology and laboratory analysis for chl-*a* were described by Boyer and Fourqurean (1997) and Briceño and Boyer (2010).

Figure 4.1 Location of study area sample stations in Florida Bay, Florida, USA

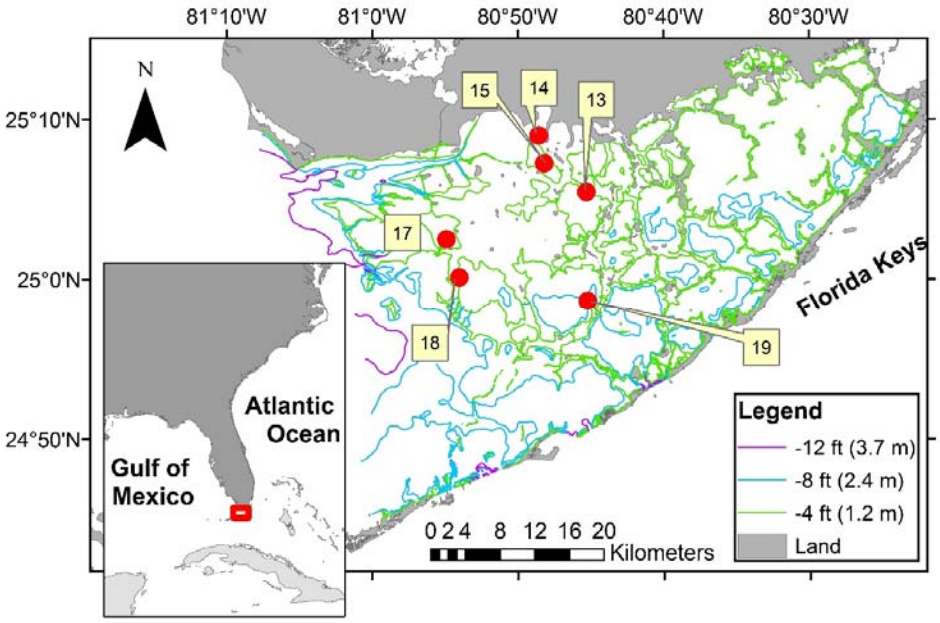

4.2.2 Satellite Data

SeaWiFS Level 2 data spanning 10 years from 1998 to 2008, as shown in Table 4.1, were downloaded from the NASA Goddard Space Flight Center's website (http://oceandata.sci.gsfc.nasa.gov/SeaWiFS/L2/). Single pixels containing *in situ* samples on the same day as the satellite overpass were considered as matchups to the *in situ* measurement. Matchups were screened to exclude data where the viewing and zenith angles exceed 60° and 75°, respectively, accounting for limitations on the atmospheric correction algorithms at extreme viewing and solar geometries (Werdell 2006). Pixels flagged for land, cloud, stray light, sun glint, high top-of-atmosphere, low $R_{rs}555$ and atmospheric correction failure were also excluded as in Bailey and Werdell (2006).

Table 4.1 Summary of matchup data showing per season counts and average in situ chl-*a* annually

Year	Spring	Summer	Fall	Winter	Total	Mean chl-*a* (mg m^{-3})
1998				1	1	0.6
1999	6	2			8	0.5
2000	2	3	3	1	9	1.3
2001			2	3	5	0.4
2002		4	7		11	1.6
2003	1		5		6	2.7
2004	5	2	1	3	11	0.3
2005	3	3	3	7	16	1.1
2006	1	9		11	21	1.7
2007	6	4	3		13	1.1
2008	2				2	0.7
Total	**26**	**27**	**24**	**26**	**103**	**1.2**

4.2.3 Seagrass Class Data

A supervised classification of the benthic habitat from the study area that was previously calibrated and validated (Blakey et al., 2015) was employed in the present

study. A brief summary of the classification methodology is presented. Landsat images from 2009-2011 were used to train the classifier while data from 2007 and 2008 were used for validation. Pixels were classified as 1) medium-dense seagrass, 2) low seagrass, 3) sparse seagrass, or 4) turbid determined by three depth-invariant bands employing data from the visible wavelengths.

Sparse and low classes were combined in the present study so that a 2-class scheme was used to distinguish between all study area benthic habitats. The benthos were classified each year from spring and early summer images when phytoplankton concentrations are generally low. The classifications produced from the spring/early summer data were assumed constant throughout the calendar year (from the January before the classified image to the December following the classified image). New maps, describing the mode of a 1 km radius around each 30 m grid cell, were created to account for SeaWiFS spatial resolution of 1.1 km at nadir.

4.2.4 Bio-optical Algorithm

The empirical OC algorithm estimates were evaluated against the *in situ* measurements. The current version of the operational algorithm, OC4v6, relates chl-*a* to a log-transformed ratio (X) of remote sensing reflectances (R_{rs}) (O'Reilly 1998):

$$chla = 10^{(a0+a1*X+a2*X^2+a3*X^3+a4*X^4)} \quad (1)$$

$$X = \log_{10}(\lambda_b/\lambda_g) \quad (2)$$

For the OC4v6 algorithm, λ_b is the greatest of $R_{rs}443$, $R_{rs}490$, and $R_{rs}510$, and λ_g is $R_{rs}555$. The best fit polynomial was derived using the globally-distributed NASA Bio-optical Marine Algorithm Data set (O'Reilly 2000) with coefficients a1 = 0.3272, a2 = -2.9940, a3 = -1.2259 and a4 = -0.5683.

4.2.5 Statistical Analyses

Regionally-tuned algorithms, including models 1) that use alternative band ratios and 2) with coefficients tuned to benthic cover class, were tested for potential improvement of the chl-*a* estimates. All tested algorithms were derived through linear regression against the *in situ* data set conducted in SPSS version 21.

Two alternative band ratios, X_{br} and X_{rg}, were evaluated as substitutes for X in optically-shallow nearshore water. Band ratio X_{br} retains the maximum of $R_{rs}443$, $R_{rs}490$, and $R_{rs}510$ in the numerator and employs λ_r ($R_{rs}670$) as the reference wavelength while ratio X_{rg} avoids the blue wavelengths entirely:

$$X_{br} = \log_{10} (\lambda_b/\lambda_r) \quad (3)$$

$$X_{rg} = \log_{10} (\lambda_r/\lambda_g) \quad (4)$$

The *in situ* data set was segmented by benthic cover class with unique coefficients derived for pixels associated with 1) medium-dense seagrass and 2) sparse-low seagrass cover. The satellite image-based seagrass classification products described previously were used to segment the dataset.

Statistics used to assess the accuracy of the various algorithms included the adjusted R^2 and the mean absolute percent difference (APD).

4.3 Results

Beyond the quadratic, statistical agreement (i.e., adjusted R^2) between *in situ* and modeled chl-*a* generally did not improve with increasingly higher order polynomial formulations for any of the band ratios tested. Therefore, a quadratic formulation was adopted for all regressions.

4.3.1 Models without Seagrass Distinction

The operational band ratio, employing the maximum of $R_{rs}443$, $R_{rs}490$, and $R_{rs}510$ and $R_{rs}555$, performed better than X_{br} and X_{rg} for the study area as shown in Table 4.2. The regression that used X produced positive coefficients for the linear and quadratic terms. The positive coefficient for the linear term indicated that concentrations of chl-*a* increased as the ratio of blue to green reflectance decreased. The inverse relationship between X and chl-*a* is consistent with the absorption properties of chl-*a* as X was negative for every data point. Figure 4.2 plots the estimated versus the *in situ* $\log_{10}$chl-*a* for the OC4v6 and regionally-tuned models. From Figure 4.2 it is evident that the positive bias produced through the OC4v6 algorithm is less of an issue for the regionally-tuned model. It was expected that the regionally-tuned model would overestimate chl-*a* overlying medium-dense seagrass because of the increased blue absorption of the seagrass. However, the chl-*a* associated with sparse-low seagrass was overestimated to a higher degree than chl-*a* associated with medium-dense seagrass as a result of the positive coefficient for the quadratic term.

Table 4.2 Coefficients and goodness of fit for regionally tuned chl-*a* retrieval models including those based on alternative band ratios

Ratio	a0	a1	a2	Adjusted R^2
X	-0.161	2.382	10.777	0.191
X_{br}	0.003	0.646	0.394	-0.013
X_{rg}	3.704	-3.036	0.553	0.140

Figure 4.2 In situ versus A) OC4v6 chl-*a* product and B) unified regionally-tuned model chl-*a*

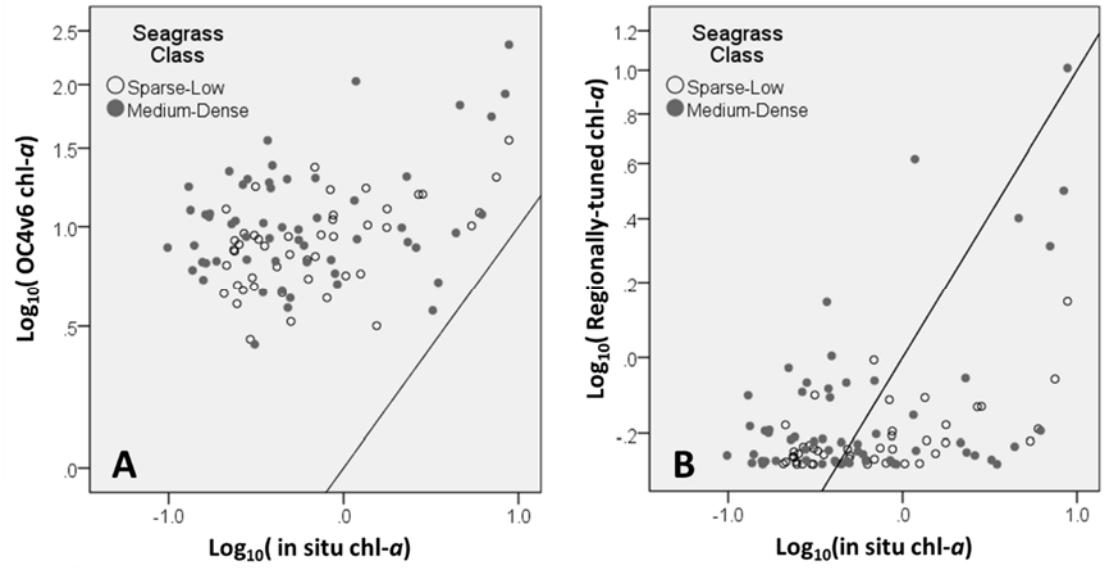

4.3.2 Benthic Class-Specific Models

The signs and order-of-magnitude of the coefficient for the algorithms tuned to benthic class-specific data (Table 4.3) were the same as those for the unified, regionally-tuned model. Segmenting the data by benthic class did improve the accuracy of the resulting chl-*a* estimates in terms of the adjusted R^2 and in representing the range of chl-*a* observed in situ (Table 4.4). While these class-specific regional algorithms offer improvements over the single regional model and the OC algorithm, further improvement to predictive power may be desired before chl-*a* estimates are utilized for coastal monitoring. Assessment of the residuals by season, location and over time suggest that further enhancement of the algorithms is possible.

Table 4.3 Coefficients and goodness of fit for benthic class-specific chl-*a* retrieval models

Class-Specific Model	a0	a1	a2	Adjusted R^2
Sparse-Low	-0.075	5.095	25.241	0.332
Medium-Dense	0.146	5.557	16.282	0.234

Table 4.4 Dynamic range of in situ chl-*a* compared to ranges of chl-*a* retrieved through models

Seagrass Class	In Situ	OC4v6	Regionally-tuned	Class-Specific
Sparse-Low	0.3-8.4	2.8-36.1	0.5-1.4	0.5-6.2
Medium-Dense	0.1-8.4	2.6-231.1	0.5-10.3	0.5-10.4

As the seagrass classification for an entire year was derived from spring or early summer reflectances, the seasonal accuracy of the class-specific chl-*a* algorithms was of particular interest because systematic biases in winter and fall could be representative of intra-annual changes in seagrass density that were not captured in the annual classification. The mean absolute percent difference for each season, presented in Table 4.5, show summer retrievals to be the most accurate for the regionally-tuned, benthic class-specific models. Figure 4.3 shows the residuals of the class-specific algorithms with markers differentiated by season. From inspection of Figure 4.3 the algorithm for sparse-low seagrass does not appear to produce seasonal biases. The medium-dense seagrass algorithm, however, appears to overestimate chl-*a* in fall and underestimate chl-*a* in spring and winter. These biases are presumed not to result from mis-classifications of the seagrass in those seasons as the biases are only suggested for the medium-dense

algorithm and are also suggested for spring estimates. Because the medium-dense seagrass generally occurred in western portions of the study area, seasonal variations in water column constitution or aerosols could account for the seasonal bias in chl-*a* estimates.

Table 4.5 Mean absolute percent difference by season for the operational SeaWiFS and benthic-class specific models

	Spring	Summer	Fall	Winter	All
OC4v6	1908%	2590%	1214%	2917%	2180%
Sparse-Low	42%	80%	80%	62%	64%
Medium-Dense	85%	87%	38%	131%	87%

Figure 4.3 Residuals from A) Sparse-low and B) Medium-dense models with markers distinguished by season

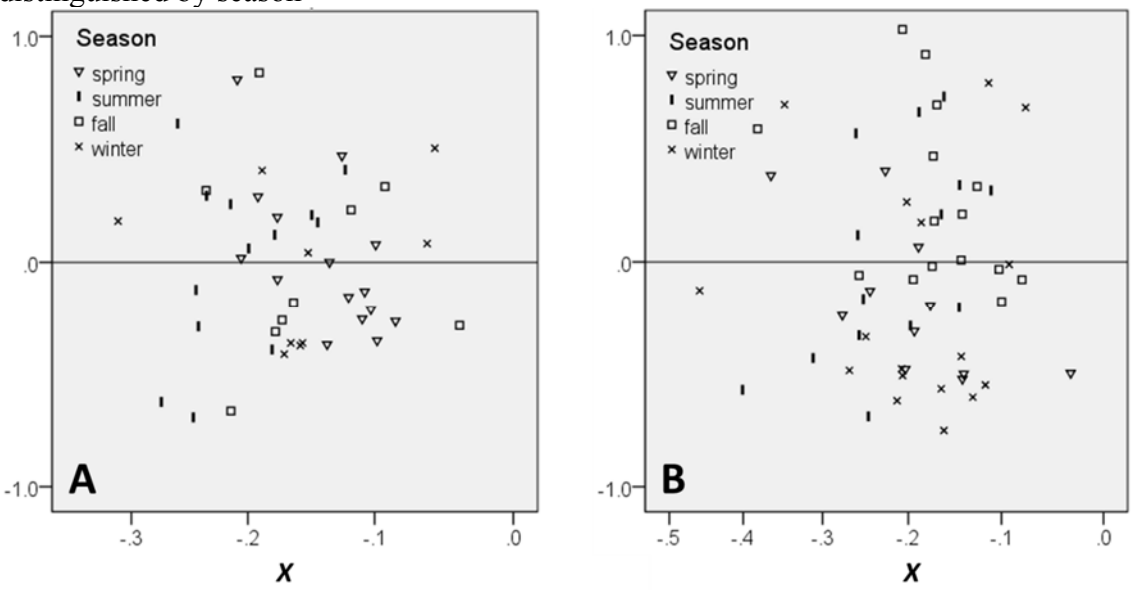

Assessment of the time-series of the residuals for the class-specific algorithms also suggested biases in the medium-dense algorithm. As shown in Figure 4.4, estimates of chl-*a* overlying medium-dense seagrass from stations 15, 17 and 18 are increasingly

overestimated with time. As these stations were in basins associated with increasing seagrass density, the trend of increasing negative bias may be related to increased blue absorption from higher seagrass density. Similarly, all estimates of chl-*a* overlying medium-dense seagrass at station 13, where seagrass was typically sparse-low, were underestimated. The negative bias at station 13 may be related to relatively low seagrass density, and lesser blue absorption, compared to the average for the medium-dense class.

Figure 4.4 Residuals from A) Sparse-low and B) Medium-dense models with markers distinguished by station

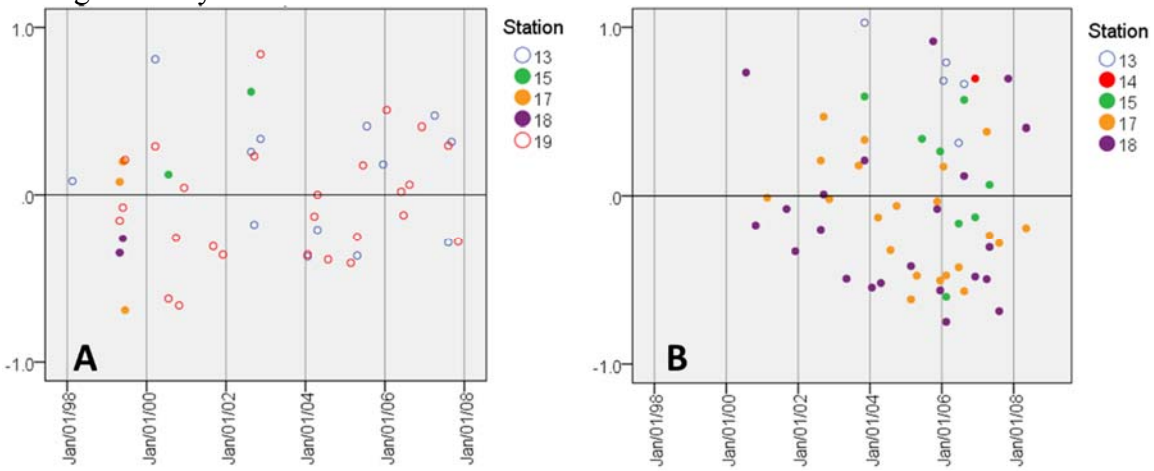

These results suggest that increasing the number of seagrass classes would improve the chl-*a* estimates for the study area. By creating more divisions in the benthic classification, variations in *X* are more likely to be attributed to differences in chl-*a* as opposed to bottom reflectance.

4.4 Discussion

Benthic-class specific chl-*a* retrieval algorithms that use the same blue-green band ratio employed for the operational OC4v6 algorithm were found to greatly reduce the absolute error of retrievals compared to OC4v6 and also improve performance relative to the unified regionally-tuned model. All regionally-tuned models performed significantly better than OC4v6 in capturing the dynamic range of chl-*a* where the minimum chl-*a* estimated through OC4v6 was substantially higher than annual mean *in situ* chl-*a* for ten of the 11 years of data. While mean APD for the benthic class-specific models was approximately 70%, these results are encouraging given the performance of the operational algorithm in the optically-shallow conditions and the oligo- to mesotrophic nature of the study area.

Because of the *in vivo* absorption peak near 676 nm, spectral bands near 676 nm have been widely used for the retrieval of chl-*a* in coastal waters (Blondeau-Patissier 2014). The success of these algorithms is attributed to avoidance of the blue wavelengths which minimizes the impact from CDOM interference in the blue wavelengths and from atmospheric correction errors that affect blue wavelengths more strongly than green and red wavelengths (Le 2012). While the blue to red ratio X_{br} was not evidenced as useful for retrieving chl-*a* concentrations in the present study, the red to green ratio X_{rg} achieved R^2 values similar to those for the traditional blue to green ratio. Because λ_b and λ_r both measure reflectances associated with chl-*a* absorption, differences in phytoplankton may be cancelled out in X_{br} (increases in phytoplankton cause increased absorption in both λ_b and λ_r), accounting for the poor retrieval performance. The X_{rg}, however, compares red absorption to a green reference and warrants further study given the known issues with

satellite-retrieved blue bands. With increased attenuation from water in the red wavelengths, X_{rg} in optically shallow water may be influenced by variations in water column depth and variable modulation of the bottom reflectance. In this case, utilizing bands that have been corrected for variable water column depth can improve the performance of X_{rg} in chl-*a* retrieval.

Regardless of the band ratio and functional forms employed, type-specific chl-*a* retrieval algorithms present an opportunity for greater applicability of global satellite data to nearshore areas. For example, water type-specific algorithms were shown to improve the error of multi-spectral satellite retrievals of chl-*a* over a unified model tuned for all water types without classification (Sun 2014) in turbid estuaries. As benthic and water types can be identified through satellite remote sensing, type-specific algorithms offer reduction in uncertainty without sacrificing coverage.

The present study assumed negligible intra-annual variability of the seagrass class and made use of seasonally low phytoplankton to identify annual benthic class. The applicability of these assumptions to other study areas requires further study. In some study areas, the phenology of submerged aquatic vegetation may require more frequent variation of bottom reflectance although seasonal factoring may suffice in those situations.

While better characterization of the benthos showed potential to improve chl-*a* retrieval, the capacity for this finer level of discrimination was not tested.

The desire for finer benthic classification and the use of the blue wavelengths in the present study highlight the need for coastal atmospheric correction regimes. The atmospheric correction procedure in the nearshore is complicated by the potential for

absorbing aerosols, such as smoke, dust, NO_2 and CO_2, and straylight contamination from nearby bright land and clouds (Muow 2015). Similar to the capability of regionally-tuned models to better represent chl-*a* in nearshore areas, atmospheric correction procedures tuned to nearshore coastal areas would result in more accurate coastal R_{rs}. Reducing the satellite R_{rs} uncertainty would benefit chl-*a* retrieval directly and allow for better identification of benthic class or water types.

4.5 Conclusions

The present study demonstrated that improvements in chl-*a* retrieving algorithm performance were achievable through benthic class-specific tuning of retrieval algorithms. SeaWiFS satellite R_{rs} and satellite-derived bottom classifications were utilized for evaluation of potential reduction in satellite uncertainty. Addressing multi-spectral ocean color satellite uncertainty is important as these datasets allow for the derivation of ecological baselines which can be used to detect changes in coastal system dynamics as well as be used in hindsight to assess prevailing bloom conditions and to identify the biological and physical parameters that triggered or terminated an algal event (Blondeau-Patissier 2014).

While the uncertainty in estimated chl-*a* for benthic class-specific algorithms remains substantial, type-specific models may be useful for a detecting the presence of chl-*a* concentrations above a certain threshold (Carvalho 2010) if not for estimating actual chl-*a* concentrations.

Algorithms can be optimized once benthic class and/or water types can be adequately characterized in terms of definition of classes as well as spatial and temporal variability. Therefore, the most pressing opportunity to further improve satellite-based

chl-*a* retrieval in nearshore areas is atmospheric correction procedures specialized to coastal environments as these procedures would improve both classification and algorithm tuning.

References

Bailey, S.W., Werdell, P.J. (2006). A multi-sensor approach for the on-orbit validation of ocean color satellite data products. Remote Sensing of the Environment, 102, 12-23.

Blakey, T., Melesse, A., Hall, M. (2015). Supervised classification of benthic reflectance in shallow subtropical waters using a generalized pixel-based classifier across a time series. Remote Sensing, 7, 5098-5116.

Blondeau-Patissier, D., Gower, J.F.R., Dekker, A.G., Phinn, S.R. (2014). A review of ocean color remote sensing methods and statistical techniques for the detection, mapping and analysis of phytoplankton blooms in coastal and open oceans. Progress in Oceanography, 123, 123-144.

Boyer, J., Fourqurean, J. (1997). Spatial characterization of water quality in Florida Bay and Whitewater Bay by multi-variate analyses: zones of similar influence. Estuaries, 20, 743-758.

Briceño, H., Boyer, J. (2010). Climatic controls on phytoplankton biomass in a sub-tropical estuary, Florida Bay, USA. Estuaries and Coasts, 33, 541-553.

Cannizzaro, J.P., Carder, K.L. (2006). Estimating chlorophyll *a* concentrations from remote sensing reflectance in optically shallow waters. Remote sensing of the Environment, 101, 13-24.

Cannizzaro, J.P., Hu, C., Carder, K.L., Kelble, C.R., Melo, N., Johns, E.M., Vargo, G.A., Heil, C.A. (2013). On the accuracy of SeaWiFS Ocean Color data products on the West Florida Shelf. Journal of Coastal Research, 29, 1257-1272.

Carvalho, G.A., Minnet, P.J., Fleming, L.E., Banzon, V.F., Baringer, W. (2010). Satellite remote sensing of harmful algal blooms: A new multi-algorithm method for detecting the Florida Red Tide (*Karenia brevis*). Harmful Algae, 9, 440-448.

Gordon, H., Wang, M. (1994). Retrieval of water-leaving radiance and aerosol optical thickness over the oceans with SeaWiFS: A preliminary algorithm. Applied Optics, 33, 443-452.

Le, C., Hu, C., English, D., Cannizzaro, J., Chen, Z., Feng, L., Boler, R., Kovach, C. (2012). Towards a long-term chlorophyll-a data record in a turbid estuary using MODIS observations. Progress in Oceanography, 109, 90-103.

Le, C., Hu, C., Cannizzaro, J., English, D., Muller-Karger, F., Lee, Z. (2013). Evaluation of chlorophyll-a remote sensing algorithms for an optically complex estuary. Remote sensing of the Environment, 129, 75-89.

Le, C., Hu, C., English, D., Cannizzaro, J., Kovach, C. (2013). Climate-driven chlorophyll-a changes in a turbid estuary: Observations from satellites and implications for management. Remote sensing of the Environment, 130, 11-24.

Muow, C.B., Greb, S., Aurin, D., DiGiacomo, P.M., Lee, Z., Twardowski, M., Binding, C., Hu, C., Ma, R., Moore, T., Moses, W., Craig, S.E. (2015). Aquatic radiometry remote sensing of coastal and inland waters: Challenges and recommendations for future satellite missions. Remote sensing of the Environment, 160, 15-30.

O'Reilly, J.E., Maritorena, S., Mitchell, G., Siegel, D., Carder, K.L., Garver, S.A., Kahru, M., McClain, C. (1998). Ocean color chlorophyll algoritms for SeaWiFS. Journal of Geophysical Research, 103, 24,937 – 24, 953.

O'Reilly, J.E., Maritorena, S., O'Brien, M.C., Siegel, D.A., Toole, D., Menzies, D., Smith, R.C., Mueller, J.L., Mitchell, B.G., Kahru, M., Chavez, F.P., Strutton, P., Cota, G.F., Hooker, S.B., McClain, C.R., Carder, K.L., Muller-Karger, F., Harding, L., Magnuson, A., Phinney, D., Moore, G.F., Aiken, J., Arrigo, K.R., Letelier, R., Culver, M. (2000). SeaWiFS postlaunch calibration and validation analyses, part 3, NASA Technical memorandum 2000-206892, Vol. 11, ed. Hooker, S. B., and Firestone, E. R, 49 pp. Greenbelt, MD: NASA Goddard Space Flight Center.

Palmer, S.C.J., Hunter, P.D., Lankester, T., Hubbard, S., Spyrakos, E., Tyler, A.N., Présig, M., Horváth, H., Lamb, A., Balzter, H., Tóth, V. (2015). Validation of Envisat MERIS algorithms for chlorophyll retrieval in a large, turbid and optically-complex shallow lake. Remote sensing of the Environment, 157, 158-169.

Schaeffer, B.A., Hagy, J.D., Conmy, R.N., Lehrter, J.C., Stumpf, R.P. (2012). An approach to developing numeric water quality criteria for coastal waters using the SeaWiFS satellite data record. Environmental Science and Technology, 46, 916-922.

Sun, D., Hu, C., Qui, Z., Cannizzaro, J.P., Barnes, B.B. (2014). Influence of red band-based water classification approach on chlorophyll algorithms for optically complex estuaries. Remote sensing of the Environment, 155, 289-302.

Werdell, J.P., Franz, B.A., Bailey, S.W., Harding, L.W., Feldman, G.C. (2007). Approach for the long-term spatial and temporal evaluation of ocean color satellite data products in a coastal environment. Proc. Of SPIE Vol. 6680 66800G-1

Werdell, J.P., Bailey, S.W., Franz, B.A., Harding, L.W., Feldman, G.C., McClain, C.R. (2009). Regional and seasonal variability of chlorophyll-a in Chesapeake Bay as observed by SeaWiFS and MODIS-aqua. Remote Sensing of the Environment, 113, 1319-1330.

5 CONCLUSIONS AND RECOMMENDATIONS

Chlorophyll *a* (chl-*a*) concentrations represent a link between inland system dynamics and the health of marine ecosystems as they are indicative of phytoplankton blooms and eutrophication of the downstream, marine environment. Effective management of freshwater inputs to coastal systems is a high priority because services provided by coastal ecosystems such as estuarine habitat, sediment accretion and stabilization, nutrient retention and mitigation of climate change through carbon sequestration (Koch 2007; Yaakub 2013) should prove to be increasingly valuable as sea levels rise. One of the NASA's latest reports on future ocean color mission requirements (IOCCG Report 13, page 14) stated that phytoplankton blooms' timing, frequency, composition and intensity are expected to change with climate in ways that may be hard to predict, making reliable and accurate detection of algal blooms an objective for future missions (Blondeau-Patissier 2014).

Long-term global archives of multi-spectral imagery are now readily accessible; however, the full temporal extent in terms of length and frequency of acquisition of these archives is not widely utilized (Lyons 2013). Unraveling the history of Earth system interactions recorded in satellite data provides a base for long-term ecosystem monitoring programs and informs forecasting models, both of which are critical for expanding the knowledge base that is available to deal with pressing challenges such as climate change.

Understanding the seasonality and drivers of global deep water chl-*a* concentrations is one such achievement that took advantage of remote sensing records to link processes in topographically-adjacent regions but also to link physical processes

(temperature and nutrient upwelling) to chemical processes (ocean primary production). Methods for quantifying chl-*a* from remote sensing in coastal waters however, have been more elusive as these waters are influenced by terrestrial inputs such as colored dissolved organic matter (CDOM) and suspended particles which may be falsely interpreted as chl-*a* since all of these constituents absorb blue light strongly (Le 2012). Because actual, water column chl-*a* concentrations are also influenced by various terrestrial inputs, such as nutrients, chl-*a* is an integrative component of coastal systems with the potential to reveal much about the contributing environments including upstream as well as global processes.

Accurate estimates of coastal chl-*a* pose a challenge to the research community and an obstacle to water quality managers. Traditional empirical (i.e. OC4) and semi-analytical algorithms developed for open ocean waters rely on blue-green wavelengths. In optically-shallow coastal water, besides constituents other than phytoplankton that often dominate the optical properties in the blue-green wavelengths (Le 2012), bottom contamination will also cause large changes in the measured reflectance (Barnes 2014). The blue-green ocean color band ratios, therefore, are known to significantly overestimate chl-*a* where nominal uncertainty can be > 100% in coastal waters (Blondeau-Patissier 2014).

This aim of this work was to improve upon the accuracy of chl-*a* estimating algorithms derived from spaceborne data on subtropical Florida Bay, Florida so that the multi-decadal record of satellite data can be applied to characterizing and monitoring the coupled Earth processes there. Improvements made to chl-*a* algorithms can provide information that directly supports water managers in reducing negative impacts to coastal ecosystems as well as inform future flight mission design for ocean color sensors.

Successful estimation methods needed to distinguish between water column constituents and the bottom reflectance that are vertically integrated in the spectral signatures of optically shallow water. Four research objectives comprised the scope of this work:

- **Research Objective 1** – Understand the spatial and temporal dynamics of chl-*a* concentrations in the study area, including links to inland activities, as observed from in situ data records.
- **Research Objective 2** – Understand the spatial and temporal dynamics of submerged aquatic vegetation (SAV) observed in the study area, including correlations with chl-*a* concentrations, as observed from in situ data records.
- **Research Objective 3** – Classify and map seagrass and SAV from space-borne images of the study area through the use of spectral data and information gained from completion of Objectives 1 and 2.
- **Research Objective 4** – Improve on available algorithms for deriving chl-*a* concentration indicators from space-borne imagery in coastal, optically shallow water, such as those found in the study area.

5.1 Conclusions

Identification of seasonality and trends apparent in the *in situ* chl-*a* dataset guided the focus of this work by indicating the time of year and location of algal bloom occurrence. Areas in the western portions of the Bay were selected for further study as eastern portions were not associated with elevated chl-*a* at any time of the year. In western study areas, chl-*a* concentrations at the end of the dry season were typically low and did not vary across years so these months were deemed appropriate for establishing the seagrass

classes each year even though the retrieved bottom reflectance is modulated by the overlying water column.

Evaluation of the seagrass survey data illustrated the stability of bottom reflectances in terms of intra- and inter- annual variability. Because no seasonality was evidenced in the data, annual classification of the seagrass bottom reflectance was employed in the chl-*a* algorithm tested for Objective 4. Inter-annual trends observed in the seagrass cover data were useful for validating the benthic classification maps produced through completion of Objective 3.

Acceptable accuracies, especially in terms of overall, basin-wide trends, were achieved in the supervised classification of benthic habitats from Landsat images of the interior portions of the study area. The overall accuracy of the classifier, based on available field data, was 67% and 76% for the two validation years. The westernmost portions of the bay that are open to the Gulf-of-Mexico were shown to be influenced by turbidity with a higher potential for misclassifying the benthic habitat compared to more interior portions of the study area. Therefore, where identification of the benthic class was a key aspect of the work performed under Objective 4, the westernmost portions were excluded from further study.

Finally, although improvement to the accuracy of satellite retrieved chl-*a* was demonstrated, the accuracy of the improved chl-*a* estimated remained low. Algorithms tuned to the sparse-low seagrass bottom ($r^2 = 0.234$, mean APD = 71%) performed better than those associated with medium-dense seagrass ($r^2 = 0.332$, mean APD = 66%). The positive bias produced by the traditional OC4 algorithm was removed through the

regionally-tuned algorithms but the residuals of the medium-dense seagrass affiliated chl-*a* did suggest a seasonality in the bias of the improved estimates.

This work showed that the fine spatial and temporal resolution available through satellite remote sensing is required to adequately understand the dynamics of coastal chl-*a*. Because coastal dynamics are the result of the complex interactions between local hydrology, weather and anthropogenic inputs, nutrient sources and circulation pathways are easily obscured. The coverage and frequency currently only offered from remote sensing products can illustrate small scale differences which may be indicative of diffuse or subtle processes that cannot be captured through *in situ* sampling efforts.

In contrast, discontinuous field data were shown to be useful for developing satellite-based chl-*a* retrieval algorithms. For example, evaluation of the *in situ* datasets allowed for identification of appropriate times of year for classifying benthic habitats and the assumption of annually invariable bottom reflectance. Without these findings, bottom reflectance and water column constituents would need to be derived simultaneously which may not be feasible for multispectral data sources. In the end, developing chl-*a* algorithms with assumptions based on an ecosystem characterization established from field data proved a viable strategy for improving chl-*a* retrieval accuracy.

A novel achievement of this work was the use of bottom type-specific algorithms to improve the accuracy of satellite based chl-*a*. Because the bottom type was retrospectively classified from satellite imagery, this methodology can be applied to any optically shallow nearshore area. The finding that a generalized, image-based classifier is transferrable in time enhances the applicability of the tested methodology.

5.2 Recommendations

Testing the transferability of image-based optical signatures in space to other study areas is an important next step for this methodology. A well-defined spectral library of pixel-based classes would improve assessment of global chl-a dynamics, which is especially important given global climate change. The accessibility of the studied methodology, in terms of equipment, software and expertise required, and the lack of research into the SeaWiFS archive for multi-temporal analyses of coastal dynamics support continued development of the novel methodology.

A limitation of the methodology tested in this study is that the assumptions employed may not be applicable in other study areas. The identification of bottom types was dependent on seasonally invariable water columns so that satellite-retrieved optical signatures were valid for identifying the seagrass class. Unless water column contribution can be predicted or considered negligible, the variation in reflectance cannot be attributed to differences in benthic habitat. Similarly, if bottom reflectance is highly variable, it will be difficult to identify variability in chl-*a*.

If coastal water and bottom types can be adequately categorized, then chl-*a* can be retrieved globally through the tested methodology and a single set of chl-*a* algorithms, allowing for objective analysis of global trends. The results of the chl-*a* algorithm validation suggest that, for seagrass, a bottom type classification with more than two classes is appropriate. Working towards a global set of coastal water types requires research into how to optimally define classes to minimize confusion when distinguishing between types from space-borne reflectance.

A common radiometric scale is assumed across time-series highlighting the need for coastal atmospheric correction procedures. Atmospheric correction procedures derived specifically for normalizing surface reflectances across images are likely to improve the transferability of pixel-based classifiers as well as the performance of empirical chl-*a* algorithms. Therefore, while greater differentiation of bottom types is expected to improve the accuracy of the tested methodology, coastal atmospheric correction is considered a higher priority topic for further study.

In situ collection of water-leaving radiance is recommended for Florida Bay as a next step towards developing chl-*a* algorithms for optically shallow nearshore areas. Field campaigns to investigate the differences between "ground-truthed" water-leaving radiance and satellite-retrieved reflectance may be key to advancing coastal atmospheric correction. Additionally, *in situ* optical signatures may help to identify inherent groupings for bottom types.

References

Barnes, B., Hu, C., Holekamp, K., Blonski, S., Spiering, B., Palandro, D., Lapointe, B. (2014). Use of Landsat data to track historical water quality changes in Florida Keys marine environments. Remote Sensing of the Environment, 140, 485-496.

Blondeau-Patissier, D., Gower, J., Dekker, A., Phinn, S., Brando, V. (2014). A Review of ocean color remote sensing methods and statistical techniques for the detection, mapping and analysis of phytoplankton blooms in coastal and open oceans. Progress in Oceanography, 123, 123-144.

Boyer, J., Fourqurean, J. (1997). Spatial characterization of water quality in Florida Bay and Whitewater Bay by multi-variate analyses: Zones of similar influence. Estuaries, 20, 743-758.

Rudnick, D., Chen, Z., Childers, D., Boyer, J., Fontaine, T. (1999). Phosphorus and nitrogen inputs to Florida Bay: The importance of the everglades watershed. Estuaries, 22, 389-416.

Gilbert, P., Heil, C., Madden, C. (2009). Florida Bay: A subtropical system increasingly influenced by multiple stressors. Contributions in Marine Science, 38, 1-4.

Gilbert, P., Heil, C., Rudnick, D., Madden, C., (2009). Florida Bay: Water quality status and trends, historic and emerging algal bloom problems. Contributions in Marine Science, 38, 5-17.

Koch, M., Schopmeyer, S., Holmer, M., Madden, C., Kyhn-Hansen, C. (2007). Thalassia testudinum response to the interactive stressors hypersalinity, sulfide and hypoxia. Aquatic Botany, 87, 104-110.

Le, C., Chuanmin, H., English, D., Cannizzaro, J., Chen, Z., Kovach, C. (2013). Inherent and apparent optical properties of the complex estuarine waters of Tampa Bay: What controls light? Estuarine Coastal Shelf Science, 117, 1-16.

Le, C., Chuanmin, H., English, D., Cannizzaro, J., Kovach, C. (2013). Climate-driven chlorophyll-*a* changes in a turbid estuary: Observations from satellites and implications for management. Remote Sensing of the Environment, 130, 11-24.

Lyons, M., Roelfsema, C., Phinn, S. (2013). Towards understanding temporal and spatial dynamics of seagrass landscapes using time-series remote sensing. Estuarine Coastal and Shelf Science, 120, 42-53.

Yaakub, S., Chen, E., Bouma, T., Erftemeijer, P., Todd, P. (2013). Chronic light reduction reduces overall resilience to additional shading stress in the seagrass Halophila ovalis. Marine Pollution Bulletin, 83, 467-474.

APPENDICES

Appendix A By Station ANOVA for Monthly Log-transformed Chl-a

Station	ZSI	ANOVA F	ANOVA p-value	Equal Variance
1	FBE	1.001	0.447	Y
2	FBE	0.318	0.981	Y
3	FBE	1.008	0.441	Y
4	FBE	1.017	0.432	Y
5	FBE	1.159	0.317	Y
6	FBE	1.395	0.177	Y
7	NB	3.237	**0.000**	Y
8	NB	0.932	0.511	Y
10	NB	1.608	0.099	Y
11	NB	2.925	**0.001**	Y
9	FBEC	1.264	0.247	Y
23	FBEC	1.434	0.159	Y
24	FBEC	1.06	0.395	Y
12	FBC	1.359	0.195	N
13	FBC	2.812	**0.002**	N
14	FBC	4.680	**0.000**	Y
15	FBC	4.322	**0.000**	N
19	FBS	5.050	**0.000**	Y
20	FBS	1.848	**0.048**	Y
21	FBS	1.075	0.383	Y
22	FBS	1.128	0.341	N
16	FBW	2.219	**0.015**	Y
17	FBW	1.989	**0.031**	Y
18	FBW	3.912	**0.002**	N
25	FBW	1.656	0.086	Y
26	FBW	1.614	0.098	Y
27	FBW	2.828	**0.002**	Y
28	FBW	2.522	**0.006**	N

Appendix B Monthly Comparison of Log-transformed Chl-a by Station

Station 7: Tukey HSD

(I) MON		Mean Difference (I-J)	Std. Error	Sig.	95% Confidence Interval	
					Lower Bound	Upper Bound
1.0	2.0	-.06603	.11215	1.000	-.4369	.3049
	3.0	-.07295	.11058	1.000	-.4387	.2928
	4.0	-.07903	.11058	1.000	-.4447	.2867
	5.0	.11699	.11058	.996	-.2487	.4827
	6.0	.14399	.11058	.978	-.2217	.5097
	7.0	.19427	.10916	.827	-.1667	.5553
	8.0	.23410	.11215	.632	-.1368	.6050
	9.0	.29799	.10916	.220	-.0630	.6590
	10.0	.32390	.11389	.170	-.0527	.7006
	11.0	.12177	.11058	.994	-.2439	.4875
	12.0	.12732	.11215	.993	-.2436	.4982
2.0	1.0	.06603	.11215	1.000	-.3049	.4369
	3.0	-.00692	.11058	1.000	-.3726	.3588
	4.0	-.01300	.11058	1.000	-.3787	.3527
	5.0	.18302	.11058	.886	-.1827	.5487
	6.0	.21002	.11058	.758	-.1557	.5757
	7.0	.26030	.10916	.421	-.1007	.6213
	8.0	.30013	.11215	.246	-.0708	.6710
	9.0	.36402*	.10916	.046	.0030	.7250
	10.0	.38993*	.11389	.035	.0133	.7666
	11.0	.18780	.11058	.867	-.1779	.5535
	12.0	.19335	.11215	.855	-.1775	.5642
3.0	1.0	.07295	.11058	1.000	-.2928	.4387
	2.0	.00692	.11058	1.000	-.3588	.3726
	4.0	-.00608	.10899	1.000	-.3665	.3544
	5.0	.18994	.10899	.846	-.1705	.5504
	6.0	.21695	.10899	.699	-.1435	.5774
	7.0	.26722	.10754	.356	-.0884	.6229
	8.0	.30705	.11058	.198	-.0587	.6728
	9.0	.37095*	.10754	.033	.0153	.7266
	10.0	.39686*	.11234	.025	.0253	.7684
	11.0	.19472	.10899	.823	-.1657	.5552
	12.0	.20027	.11058	.810	-.1654	.5660

Station 7: Tukey HSD

(I) MON		Mean Difference (I-J)	Std. Error	Sig.	95% Confidence Interval	
					Lower Bound	Upper Bound
4.0	1.0	.07903	.11058	1.000	-.2867	.4447
	2.0	.01300	.11058	1.000	-.3527	.3787
	3.0	.00608	.10899	1.000	-.3544	.3665
	5.0	.19602	.10899	.817	-.1644	.5565
	6.0	.22302	.10899	.661	-.1374	.5835
	7.0	.27330	.10754	.321	-.0824	.6290
	8.0	.31313	.11058	.175	-.0526	.6788
	9.0	.37702*	.10754	.027	.0214	.7327
	10.0	.40294*	.11234	.021	.0314	.7745
	11.0	.20080	.10899	.792	-.1596	.5612
	12.0	.20635	.11058	.779	-.1594	.5721
5.0	1.0	-.11699	.11058	.996	-.4827	.2487
	2.0	-.18302	.11058	.886	-.5487	.1827
	3.0	-.18994	.10899	.846	-.5504	.1705
	4.0	-.19602	.10899	.817	-.5565	.1644
	6.0	.02700	.10899	1.000	-.3334	.3875
	7.0	.07728	.10754	1.000	-.2784	.4330
	8.0	.11711	.11058	.996	-.2486	.4828
	9.0	.18100	.10754	.874	-.1747	.5367
	10.0	.20692	.11234	.793	-.1646	.5785
	11.0	.00478	.10899	1.000	-.3557	.3652
	12.0	.01033	.11058	1.000	-.3554	.3760
6.0	1.0	-.14399	.11058	.978	-.5097	.2217
	2.0	-.21002	.11058	.758	-.5757	.1557
	3.0	-.21695	.10899	.699	-.5774	.1435
	4.0	-.22302	.10899	.661	-.5835	.1374
	5.0	-.02700	.10899	1.000	-.3875	.3334
	7.0	.05028	.10754	1.000	-.3054	.4060
	8.0	.09011	.11058	1.000	-.2756	.4558
	9.0	.15400	.10754	.956	-.2017	.5097
	10.0	.17991	.11234	.907	-.1916	.5515
	11.0	-.02222	.10899	1.000	-.3827	.3382
	12.0	-.01667	.11058	1.000	-.3824	.3490

Station 7: Tukey HSD

(I) MON		Mean Difference (I-J)	Std. Error	Sig.	95% Confidence Interval	
					Lower Bound	Upper Bound
7.0	1.0	-.19427	.10916	.827	-.5553	.1667
	2.0	-.26030	.10916	.421	-.6213	.1007
	3.0	-.26722	.10754	.356	-.6229	.0884
	4.0	-.27330	.10754	.321	-.6290	.0824
	5.0	-.07728	.10754	1.000	-.4330	.2784
	6.0	-.05028	.10754	1.000	-.4060	.3054
	8.0	.03983	.10916	1.000	-.3212	.4008
	9.0	.10372	.10608	.998	-.2471	.4546
	10.0	.12963	.11094	.991	-.2373	.4965
	11.0	-.07250	.10754	1.000	-.4282	.2832
	12.0	-.06695	.10916	1.000	-.4280	.2941
8.0	1.0	-.23410	.11215	.632	-.6050	.1368
	2.0	-.30013	.11215	.246	-.6710	.0708
	3.0	-.30705	.11058	.198	-.6728	.0587
	4.0	-.31313	.11058	.175	-.6788	.0526
	5.0	-.11711	.11058	.996	-.4828	.2486
	6.0	-.09011	.11058	1.000	-.4558	.2756
	7.0	-.03983	.10916	1.000	-.4008	.3212
	9.0	.06389	.10916	1.000	-.2971	.4249
	10.0	.08981	.11389	1.000	-.2868	.4665
	11.0	-.11233	.11058	.997	-.4780	.2534
	12.0	-.10678	.11215	.998	-.4777	.2641
9.0	1.0	-.29799	.10916	.220	-.6590	.0630
	2.0	-.36402*	.10916	.046	-.7250	-.0030
	3.0	-.37095*	.10754	.033	-.7266	-.0153
	4.0	-.37702*	.10754	.027	-.7327	-.0214
	5.0	-.18100	.10754	.874	-.5367	.1747
	6.0	-.15400	.10754	.956	-.5097	.2017
	7.0	-.10372	.10608	.998	-.4546	.2471
	8.0	-.06389	.10916	1.000	-.4249	.2971
	10.0	.02591	.11094	1.000	-.3410	.3928
	11.0	-.17622	.10754	.893	-.5319	.1794
	12.0	-.17067	.10916	.920	-.5317	.1903

Station 7: Tukey HSD

(I) MON		Mean Difference (I-J)	Std. Error	Sig.	95% Confidence Interval	
					Lower Bound	Upper Bound
10.0	1.0	-.32390	.11389	.170	-.7006	.0527
	2.0	-.38993*	.11389	.035	-.7666	-.0133
	3.0	-.39686*	.11234	.025	-.7684	-.0253
	4.0	-.40294*	.11234	.021	-.7745	-.0314
	5.0	-.20692	.11234	.793	-.5785	.1646
	6.0	-.17991	.11234	.907	-.5515	.1916
	7.0	-.12963	.11094	.991	-.4965	.2373
	8.0	-.08981	.11389	1.000	-.4665	.2868
	9.0	-.02591	.11094	1.000	-.3928	.3410
	11.0	-.20214	.11234	.817	-.5737	.1694
	12.0	-.19659	.11389	.854	-.5732	.1801
11.0	1.0	-.12177	.11058	.994	-.4875	.2439
	2.0	-.18780	.11058	.867	-.5535	.1779
	3.0	-.19472	.10899	.823	-.5552	.1657
	4.0	-.20080	.10899	.792	-.5612	.1596
	5.0	-.00478	.10899	1.000	-.3652	.3557
	6.0	.02222	.10899	1.000	-.3382	.3827
	7.0	.07250	.10754	1.000	-.2832	.4282
	8.0	.11233	.11058	.997	-.2534	.4780
	9.0	.17622	.10754	.893	-.1794	.5319
	10.0	.20214	.11234	.817	-.1694	.5737
	12.0	.00555	.11058	1.000	-.3602	.3713
12.0	1.0	-.12732	.11215	.993	-.4982	.2436
	2.0	-.19335	.11215	.855	-.5642	.1775
	3.0	-.20027	.11058	.810	-.5660	.1654
	4.0	-.20635	.11058	.779	-.5721	.1594
	5.0	-.01033	.11058	1.000	-.3760	.3554
	6.0	.01667	.11058	1.000	-.3490	.3824
	7.0	.06695	.10916	1.000	-.2941	.4280
	8.0	.10678	.11215	.998	-.2641	.4777
	9.0	.17067	.10916	.920	-.1903	.5317
	10.0	.19659	.11389	.854	-.1801	.5732
	11.0	-.00555	.11058	1.000	-.3713	.3602

*. The mean difference is significant at the 0.05 level.

Station 11: Tukey HSD

(I) MON		Mean Difference (I-J)	Std. Error	Sig.	95% Confidence Interval	
					Lower Bound	Upper Bound
1.0	2.0	-.07916	.09308	.999	-.3870	.2287
	3.0	.03023	.09177	1.000	-.2733	.3338
	4.0	-.01665	.09177	1.000	-.3202	.2869
	5.0	.04470	.09177	1.000	-.2588	.3482
	6.0	-.03932	.09177	1.000	-.3429	.2642
	7.0	-.04441	.09059	1.000	-.3440	.2552
	8.0	-.10394	.09308	.994	-.4118	.2039
	9.0	-.20945	.09177	.493	-.5130	.0941
	10.0	-.31936*	.09452	.040	-.6320	-.0067
	11.0	-.21045	.09059	.464	-.5101	.0892
	12.0	-.16192	.09452	.860	-.4745	.1507
2.0	1.0	.07916	.09308	.999	-.2287	.3870
	3.0	.10939	.09177	.989	-.1941	.4129
	4.0	.06251	.09177	1.000	-.2410	.3660
	5.0	.12386	.09177	.971	-.1797	.4274
	6.0	.03983	.09177	1.000	-.2637	.3434
	7.0	.03475	.09059	1.000	-.2649	.3344
	8.0	-.02478	.09308	1.000	-.3326	.2831
	9.0	-.13029	.09177	.958	-.4338	.1732
	10.0	-.24020	.09452	.321	-.5528	.0724
	11.0	-.13129	.09059	.952	-.4309	.1683
	12.0	-.08276	.09452	.999	-.3954	.2299
3.0	1.0	-.03023	.09177	1.000	-.3338	.2733
	2.0	-.10939	.09177	.989	-.4129	.1941
	4.0	-.04688	.09045	1.000	-.3460	.2523
	5.0	.01448	.09045	1.000	-.2847	.3136
	6.0	-.06955	.09045	1.000	-.3687	.2296
	7.0	-.07463	.08925	1.000	-.3698	.2206
	8.0	-.13417	.09177	.949	-.4377	.1694
	9.0	-.23967	.09045	.260	-.5388	.0595
	10.0	-.34959*	.09324	.012	-.6580	-.0412
	11.0	-.24068	.08925	.236	-.5359	.0545
	12.0	-.19215	.09324	.651	-.5005	.1162

Station 11: Tukey HSD

(I) MON		Mean Difference (I-J)	Std. Error	Sig.	95% Confidence Interval	
					Lower Bound	Upper Bound
4.0	1.0	.01665	.09177	1.000	-.2869	.3202
	2.0	-.06251	.09177	1.000	-.3660	.2410
	3.0	.04688	.09045	1.000	-.2523	.3460
	5.0	.06135	.09045	1.000	-.2378	.3605
	6.0	-.02268	.09045	1.000	-.3218	.2765
	7.0	-.02776	.08925	1.000	-.3230	.2674
	8.0	-.08729	.09177	.998	-.3908	.2162
	9.0	-.19280	.09045	.601	-.4920	.1064
	10.0	-.30271	.09324	.060	-.6111	.0057
	11.0	-.19380	.08925	.572	-.4890	.1014
	12.0	-.14527	.09324	.922	-.4536	.1631
5.0	1.0	-.04470	.09177	1.000	-.3482	.2588
	2.0	-.12386	.09177	.971	-.4274	.1797
	3.0	-.01448	.09045	1.000	-.3136	.2847
	4.0	-.06135	.09045	1.000	-.3605	.2378
	6.0	-.08403	.09045	.999	-.3832	.2151
	7.0	-.08911	.08925	.998	-.3843	.2061
	8.0	-.14864	.09177	.900	-.4522	.1549
	9.0	-.25415	.09045	.184	-.5533	.0450
	10.0	-.36406*	.09324	.007	-.6724	-.0557
	11.0	-.25515	.08925	.164	-.5504	.0401
	12.0	-.20662	.09324	.540	-.5150	.1017
6.0	1.0	.03932	.09177	1.000	-.2642	.3429
	2.0	-.03983	.09177	1.000	-.3434	.2637
	3.0	.06955	.09045	1.000	-.2296	.3687
	4.0	.02268	.09045	1.000	-.2765	.3218
	5.0	.08403	.09045	.999	-.2151	.3832
	7.0	-.00508	.08925	1.000	-.3003	.2901
	8.0	-.06462	.09177	1.000	-.3681	.2389
	9.0	-.17012	.09045	.770	-.4693	.1290
	10.0	-.28004	.09324	.115	-.5884	.0283
	11.0	-.17112	.08925	.747	-.4663	.1241
	12.0	-.12260	.09324	.976	-.4310	.1858

Station 11: Tukey HSD

(I) MON		Mean Difference (I-J)	Std. Error	Sig.	95% Confidence Interval	
					Lower Bound	Upper Bound
7.0	1.0	.04441	.09059	1.000	-.2552	.3440
	2.0	-.03475	.09059	1.000	-.3344	.2649
	3.0	.07463	.08925	1.000	-.2206	.3698
	4.0	.02776	.08925	1.000	-.2674	.3230
	5.0	.08911	.08925	.998	-.2061	.3843
	6.0	.00508	.08925	1.000	-.2901	.3003
	8.0	-.05953	.09059	1.000	-.3592	.2401
	9.0	-.16504	.08925	.789	-.4602	.1302
	10.0	-.27496	.09207	.120	-.5795	.0296
	11.0	-.16604	.08804	.767	-.4572	.1251
	12.0	-.11752	.09207	.981	-.4220	.1870
8.0	1.0	.10394	.09308	.994	-.2039	.4118
	2.0	.02478	.09308	1.000	-.2831	.3326
	3.0	.13417	.09177	.949	-.1694	.4377
	4.0	.08729	.09177	.998	-.2162	.3908
	5.0	.14864	.09177	.900	-.1549	.4522
	6.0	.06462	.09177	1.000	-.2389	.3681
	7.0	.05953	.09059	1.000	-.2401	.3592
	9.0	-.10551	.09177	.992	-.4090	.1980
	10.0	-.21542	.09452	.495	-.5280	.0972
	11.0	-.10651	.09059	.990	-.4061	.1931
	12.0	-.05798	.09452	1.000	-.3706	.2546
9.0	1.0	.20945	.09177	.493	-.0941	.5130
	2.0	.13029	.09177	.958	-.1732	.4338
	3.0	.23967	.09045	.260	-.0595	.5388
	4.0	.19280	.09045	.601	-.1064	.4920
	5.0	.25415	.09045	.184	-.0450	.5533
	6.0	.17012	.09045	.770	-.1290	.4693
	7.0	.16504	.08925	.789	-.1302	.4602
	8.0	.10551	.09177	.992	-.1980	.4090
	10.0	-.10991	.09324	.990	-.4183	.1985
	11.0	-.00100	.08925	1.000	-.2962	.2942
	12.0	.04753	.09324	1.000	-.2608	.3559

Station 11: Tukey HSD

(I) MON		Mean Difference (I-J)	Std. Error	Sig.	95% Confidence Interval	
					Lower Bound	Upper Bound
10.0	1.0	.31936*	.09452	.040	.0067	.6320
	2.0	.24020	.09452	.321	-.0724	.5528
	3.0	.34959*	.09324	.012	.0412	.6580
	4.0	.30271	.09324	.060	-.0057	.6111
	5.0	.36406*	.09324	.007	.0557	.6724
	6.0	.28004	.09324	.115	-.0283	.5884
	7.0	.27496	.09207	.120	-.0296	.5795
	8.0	.21542	.09452	.495	-.0972	.5280
	9.0	.10991	.09324	.990	-.1985	.4183
	11.0	.10891	.09207	.990	-.1956	.4134
	12.0	.15744	.09594	.892	-.1599	.4748
11.0	1.0	.21045	.09059	.464	-.0892	.5101
	2.0	.13129	.09059	.952	-.1683	.4309
	3.0	.24068	.08925	.236	-.0545	.5359
	4.0	.19380	.08925	.572	-.1014	.4890
	5.0	.25515	.08925	.164	-.0401	.5504
	6.0	.17112	.08925	.747	-.1241	.4663
	7.0	.16604	.08804	.767	-.1251	.4572
	8.0	.10651	.09059	.990	-.1931	.4061
	9.0	.00100	.08925	1.000	-.2942	.2962
	10.0	-.10891	.09207	.990	-.4134	.1956
	12.0	.04853	.09207	1.000	-.2560	.3531
12.0	1.0	.16192	.09452	.860	-.1507	.4745
	2.0	.08276	.09452	.999	-.2299	.3954
	3.0	.19215	.09324	.651	-.1162	.5005
	4.0	.14527	.09324	.922	-.1631	.4536
	5.0	.20662	.09324	.540	-.1017	.5150
	6.0	.12260	.09324	.976	-.1858	.4310
	7.0	.11752	.09207	.981	-.1870	.4220
	8.0	.05798	.09452	1.000	-.2546	.3706
	9.0	-.04753	.09324	1.000	-.3559	.2608
	10.0	-.15744	.09594	.892	-.4748	.1599
	11.0	-.04853	.09207	1.000	-.3531	.2560

*. The mean difference is significant at the 0.05 level.

Station 13: Dunnett T3

(I) MON		Mean Difference (I-J)	Std. Error	Sig.	95% Confidence Interval	
					Lower Bound	Upper Bound
1.0	2.0	.04261	.19315	1.000	-.6676	.7528
	3.0	.14055	.16811	1.000	-.4861	.7672
	4.0	.31509	.15366	.875	-.2733	.9035
	5.0	.21679	.16023	1.000	-.3879	.8214
	6.0	.22805	.15991	.999	-.3758	.8319
	7.0	.10554	.15639	1.000	-.4891	.7002
	8.0	-.02565	.16763	1.000	-.6509	.5996
	9.0	-.07085	.17050	1.000	-.7046	.5629
	10.0	-.27104	.17922	.998	-.9343	.3922
	11.0	-.08371	.16786	1.000	-.7091	.5417
	12.0	-.01133	.17941	1.000	-.6741	.6515
2.0	1.0	-.04261	.19315	1.000	-.7528	.6676
	3.0	.09794	.15987	1.000	-.4954	.6913
	4.0	.27248	.14460	.943	-.2786	.8236
	5.0	.17418	.15155	1.000	-.3950	.7433
	6.0	.18544	.15121	1.000	-.3828	.7537
	7.0	.06293	.14749	1.000	-.4951	.6209
	8.0	-.06826	.15936	1.000	-.6601	.5235
	9.0	-.11346	.16238	1.000	-.7146	.4877
	10.0	-.31365	.17151	.966	-.9469	.3196
	11.0	-.12632	.15960	1.000	-.7183	.4657
	12.0	-.05394	.17171	1.000	-.6867	.5788
3.0	1.0	-.14055	.16811	1.000	-.7672	.4861
	2.0	-.09794	.15987	1.000	-.6913	.4954
	4.0	.17454	.10893	.994	-.2285	.5775
	5.0	.07625	.11801	1.000	-.3565	.5090
	6.0	.08750	.11757	1.000	-.3437	.5187
	7.0	-.03500	.11274	1.000	-.4494	.3794
	8.0	-.16620	.12788	1.000	-.6338	.3014
	9.0	-.21140	.13162	.995	-.6928	.2700
	10.0	-.41159	.14273	.311	-.9391	.1159
	11.0	-.22426	.12818	.983	-.6919	.2434
	12.0	-.15188	.14298	1.000	-.6782	.3744

Station 13: Dunnett T3

(I) MON		Mean Difference (I-J)	Std. Error	Sig.	95% Confidence Interval	
					Lower Bound	Upper Bound
4.0	1.0	-.31509	.15366	.875	-.9035	.2733
	2.0	-.27248	.14460	.943	-.8236	.2786
	3.0	-.17454	.10893	.994	-.5775	.2285
	5.0	-.09830	.09631	1.000	-.4514	.2548
	6.0	-.08704	.09578	1.000	-.4381	.2640
	7.0	-.20955	.08978	.711	-.5358	.1167
	8.0	-.34074	.10818	.181	-.7407	.0593
	9.0	-.38594	.11258	.099	-.8036	.0317
	10.0	-.58613*	.12539	.006	-1.0615	-.1107
	11.0	-.39880	.10853	.051	-.7985	.0009
	12.0	-.32642	.12567	.510	-.7997	.1469
5.0	1.0	-.21679	.16023	1.000	-.8214	.3879
	2.0	-.17418	.15155	1.000	-.7433	.3950
	3.0	-.07625	.11801	1.000	-.5090	.3565
	4.0	.09830	.09631	1.000	-.2548	.4514
	6.0	.01125	.10599	1.000	-.3763	.3988
	7.0	-.11125	.10060	1.000	-.4783	.2558
	8.0	-.24245	.11732	.883	-.6725	.1876
	9.0	-.28764	.12139	.681	-.7334	.1582
	10.0	-.48783	.13335	.060	-.9857	.0100
	11.0	-.30050	.11764	.535	-.7304	.1294
	12.0	-.22812	.13361	.985	-.7244	.2681
6.0	1.0	-.22805	.15991	.999	-.8319	.3758
	2.0	-.18544	.15121	1.000	-.7537	.3828
	3.0	-.08750	.11757	1.000	-.5187	.3437
	4.0	.08704	.09578	1.000	-.2640	.4381
	5.0	-.01125	.10599	1.000	-.3988	.3763
	7.0	-.12251	.10009	1.000	-.4876	.2426
	8.0	-.25370	.11688	.823	-.6823	.1749
	9.0	-.29890	.12096	.602	-.7433	.1455
	10.0	-.49909*	.13297	.048	-.9958	-.0024
	11.0	-.31176	.11720	.454	-.7402	.1167
	12.0	-.23938	.13323	.971	-.7345	.2557

Station 13: Dunnett T3

(I) MON		Mean Difference (I-J)	Std. Error	Sig.	95% Confidence Interval	
					Lower Bound	Upper Bound
7.0	1.0	-.10554	.15639	1.000	-.7002	.4891
	2.0	-.06293	.14749	1.000	-.6209	.4951
	3.0	.03500	.11274	1.000	-.3794	.4494
	4.0	.20955	.08978	.711	-.1167	.5358
	5.0	.11125	.10060	1.000	-.2558	.4783
	6.0	.12251	.10009	1.000	-.2426	.4876
	8.0	-.13119	.11202	1.000	-.5427	.2803
	9.0	-.17639	.11628	.998	-.6048	.2520
	10.0	-.37658	.12872	.298	-.8605	.1073
	11.0	-.18925	.11236	.990	-.6006	.2221
	12.0	-.11687	.12899	1.000	-.5989	.3652
8.0	1.0	.02565	.16763	1.000	-.5996	.6509
	2.0	.06826	.15936	1.000	-.5235	.6601
	3.0	.16620	.12788	1.000	-.3014	.6338
	4.0	.34074	.10818	.181	-.0593	.7407
	5.0	.24245	.11732	.883	-.1876	.6725
	6.0	.25370	.11688	.823	-.1749	.6823
	7.0	.13119	.11202	1.000	-.2803	.5427
	9.0	-.04520	.13100	1.000	-.5243	.4339
	10.0	-.24539	.14216	.984	-.7710	.2802
	11.0	-.05806	.12754	1.000	-.5233	.4072
	12.0	.01432	.14241	1.000	-.5101	.5387
9.0	1.0	.07085	.17050	1.000	-.5629	.7046
	2.0	.11346	.16238	1.000	-.4877	.7146
	3.0	.21140	.13162	.995	-.2700	.6928
	4.0	.38594	.11258	.099	-.0317	.8036
	5.0	.28764	.12139	.681	-.1582	.7334
	6.0	.29890	.12096	.602	-.1455	.7433
	7.0	.17639	.11628	.998	-.2520	.6048
	8.0	.04520	.13100	1.000	-.4339	.5243
	10.0	-.20019	.14554	1.000	-.7371	.3367
	11.0	-.01286	.13130	1.000	-.4921	.4663
	12.0	.05952	.14578	1.000	-.4763	.5953

Station 13: Dunnett T3

(I) MON		Mean Difference (I-J)	Std. Error	Sig.	95% Confidence Interval	
					Lower Bound	Upper Bound
10.0	1.0	.27104	.17922	.998	-.3922	.9343
	2.0	.31365	.17151	.966	-.3196	.9469
	3.0	.41159	.14273	.311	-.1159	.9391
	4.0	.58613*	.12539	.006	.1107	1.0615
	5.0	.48783	.13335	.060	-.0100	.9857
	6.0	.49909*	.13297	.048	.0024	.9958
	7.0	.37658	.12872	.298	-.1073	.8605
	8.0	.24539	.14216	.984	-.2802	.7710
	9.0	.20019	.14554	1.000	-.3367	.7371
	11.0	.18733	.14243	1.000	-.3384	.7130
	12.0	.25971	.15588	.990	-.3149	.8343
11.0	1.0	.08371	.16786	1.000	-.5417	.7091
	2.0	.12632	.15960	1.000	-.4657	.7183
	3.0	.22426	.12818	.983	-.2434	.6919
	4.0	.39880	.10853	.051	-.0009	.7985
	5.0	.30050	.11764	.535	-.1294	.7304
	6.0	.31176	.11720	.454	-.1167	.7402
	7.0	.18925	.11236	.990	-.2221	.6006
	8.0	.05806	.12754	1.000	-.4072	.5233
	9.0	.01286	.13130	1.000	-.4663	.4921
	10.0	-.18733	.14243	1.000	-.7130	.3384
	12.0	.07238	.14268	1.000	-.4521	.5969
12.0	1.0	.01133	.17941	1.000	-.6515	.6741
	2.0	.05394	.17171	1.000	-.5788	.6867
	3.0	.15188	.14298	1.000	-.3744	.6782
	4.0	.32642	.12567	.510	-.1469	.7997
	5.0	.22812	.13361	.985	-.2681	.7244
	6.0	.23938	.13323	.971	-.2557	.7345
	7.0	.11687	.12899	1.000	-.3652	.5989
	8.0	-.01432	.14241	1.000	-.5387	.5101
	9.0	-.05952	.14578	1.000	-.5953	.4763
	10.0	-.25971	.15588	.990	-.8343	.3149
	11.0	-.07238	.14268	1.000	-.5969	.4521

*. The mean difference is significant at the 0.05 level.

Station 14: Tukey HSD

(I) MON		Mean Difference (I-J)	Std. Error	Sig.	95% Confidence Interval	
					Lower Bound	Upper Bound
1.0	2.0	.11002	.14630	1.000	-.3739	.5939
	3.0	.17817	.14630	.987	-.3057	.6621
	4.0	.33643	.14425	.457	-.1407	.8136
	5.0	.28660	.14425	.702	-.1905	.7637
	6.0	.11640	.14425	1.000	-.3607	.5935
	7.0	.13703	.14240	.998	-.3340	.6080
	8.0	-.22661	.14630	.925	-.7105	.2573
	9.0	-.10640	.14425	1.000	-.5835	.3707
	10.0	-.36180	.14857	.388	-.8532	.1296
	11.0	-.22113	.14240	.923	-.6921	.2499
	12.0	-.16404	.14857	.994	-.6554	.3274
2.0	1.0	-.11002	.14630	1.000	-.5939	.3739
	3.0	.06815	.14630	1.000	-.4157	.5521
	4.0	.22642	.14425	.918	-.2507	.7035
	5.0	.17658	.14425	.986	-.3005	.6537
	6.0	.00638	.14425	1.000	-.4708	.4835
	7.0	.02701	.14240	1.000	-.4440	.4980
	8.0	-.33662	.14630	.479	-.8205	.1473
	9.0	-.21642	.14425	.939	-.6936	.2607
	10.0	-.47182	.14857	.073	-.9632	.0196
	11.0	-.33115	.14240	.462	-.8021	.1398
	12.0	-.27405	.14857	.791	-.7655	.2174
3.0	1.0	-.17817	.14630	.987	-.6621	.3057
	2.0	-.06815	.14630	1.000	-.5521	.4157
	4.0	.15826	.14425	.995	-.3189	.6354
	5.0	.10843	.14425	1.000	-.3687	.5856
	6.0	-.06177	.14425	1.000	-.5389	.4154
	7.0	-.04114	.14240	1.000	-.5121	.4299
	8.0	-.40478	.14630	.203	-.8887	.0791
	9.0	-.28457	.14425	.711	-.7617	.1926
	10.0	-.53997*	.14857	.018	-1.0314	-.0486
	11.0	-.39930	.14240	.186	-.8703	.0717
	12.0	-.34221	.14857	.478	-.8336	.1492

Station 14: Tukey HSD

(I) MON		Mean Difference (I-J)	Std. Error	Sig.	95% Confidence Interval	
					Lower Bound	Upper Bound
4.0	1.0	-.33643	.14425	.457	-.8136	.1407
	2.0	-.22642	.14425	.918	-.7035	.2507
	3.0	-.15826	.14425	.995	-.6354	.3189
	5.0	-.04983	.14218	1.000	-.5201	.4204
	6.0	-.22004	.14218	.925	-.6903	.2502
	7.0	-.19941	.14029	.958	-.6634	.2646
	8.0	-.56304*	.14425	.007	-1.0402	-.0859
	9.0	-.44284	.14218	.086	-.9131	.0274
	10.0	-.69823*	.14655	.000	-1.1830	-.2135
	11.0	-.55757*	.14029	.005	-1.0216	-.0935
	12.0	-.50047*	.14655	.036	-.9852	-.0157
5.0	1.0	-.28660	.14425	.702	-.7637	.1905
	2.0	-.17658	.14425	.986	-.6537	.3005
	3.0	-.10843	.14425	1.000	-.5856	.3687
	4.0	.04983	.14218	1.000	-.4204	.5201
	6.0	-.17020	.14218	.989	-.6405	.3001
	7.0	-.14957	.14029	.996	-.6136	.3145
	8.0	-.51321*	.14425	.023	-.9903	-.0361
	9.0	-.39300	.14218	.204	-.8633	.0773
	10.0	-.64840*	.14655	.001	-1.1331	-.1637
	11.0	-.50773*	.14029	.019	-.9718	-.0437
	12.0	-.45064	.14655	.096	-.9354	.0341
6.0	1.0	-.11640	.14425	1.000	-.5935	.3607
	2.0	-.00638	.14425	1.000	-.4835	.4708
	3.0	.06177	.14425	1.000	-.4154	.5389
	4.0	.22004	.14218	.925	-.2502	.6903
	5.0	.17020	.14218	.989	-.3001	.6405
	7.0	.02063	.14029	1.000	-.4434	.4847
	8.0	-.34300	.14425	.426	-.8201	.1341
	9.0	-.22280	.14218	.919	-.6931	.2475
	10.0	-.47820	.14655	.057	-.9629	.0065
	11.0	-.33753	.14029	.407	-.8016	.1265
	12.0	-.28043	.14655	.749	-.7652	.2043

Station 14: Tukey HSD

(I) MON		Mean Difference (I-J)	Std. Error	Sig.	95% Confidence Interval	
					Lower Bound	Upper Bound
7.0	1.0	-.13703	.14240	.998	-.6080	.3340
	2.0	-.02701	.14240	1.000	-.4980	.4440
	3.0	.04114	.14240	1.000	-.4299	.5121
	4.0	.19941	.14029	.958	-.2646	.6634
	5.0	.14957	.14029	.996	-.3145	.6136
	6.0	-.02063	.14029	1.000	-.4847	.4434
	8.0	-.36363	.14240	.314	-.8346	.1074
	9.0	-.24343	.14029	.850	-.7075	.2206
	10.0	-.49883*	.14473	.033	-.9775	-.0201
	11.0	-.35816	.13838	.294	-.8159	.0996
	12.0	-.30106	.14473	.637	-.7798	.1776
8.0	1.0	.22661	.14630	.925	-.2573	.7105
	2.0	.33662	.14630	.479	-.1473	.8205
	3.0	.40478	.14630	.203	-.0791	.8887
	4.0	.56304*	.14425	.007	.0859	1.0402
	5.0	.51321*	.14425	.023	.0361	.9903
	6.0	.34300	.14425	.426	-.1341	.8201
	7.0	.36363	.14240	.314	-.1074	.8346
	9.0	.12020	.14425	1.000	-.3569	.5973
	10.0	-.13519	.14857	.999	-.6266	.3562
	11.0	.00547	.14240	1.000	-.4655	.4765
	12.0	.06257	.14857	1.000	-.4288	.5540
9.0	1.0	.10640	.14425	1.000	-.3707	.5835
	2.0	.21642	.14425	.939	-.2607	.6936
	3.0	.28457	.14425	.711	-.1926	.7617
	4.0	.44284	.14218	.086	-.0274	.9131
	5.0	.39300	.14218	.204	-.0773	.8633
	6.0	.22280	.14218	.919	-.2475	.6931
	7.0	.24343	.14029	.850	-.2206	.7075
	8.0	-.12020	.14425	1.000	-.5973	.3569
	10.0	-.25540	.14655	.846	-.7401	.2293
	11.0	-.11473	.14029	1.000	-.5788	.3493
	12.0	-.05763	.14655	1.000	-.5424	.4271

Station 14: Tukey HSD

(I) MON		Mean Difference (I-J)	Std. Error	Sig.	95% Confidence Interval	
					Lower Bound	Upper Bound
10.0	1.0	.36180	.14857	.388	-.1296	.8532
	2.0	.47182	.14857	.073	-.0196	.9632
	3.0	.53997*	.14857	.018	.0486	1.0314
	4.0	.69823*	.14655	.000	.2135	1.1830
	5.0	.64840*	.14655	.001	.1637	1.1331
	6.0	.47820	.14655	.057	-.0065	.9629
	7.0	.49883*	.14473	.033	.0201	.9775
	8.0	.13519	.14857	.999	-.3562	.6266
	9.0	.25540	.14655	.846	-.2293	.7401
	11.0	.14067	.14473	.998	-.3380	.6194
	12.0	.19777	.15080	.977	-.3010	.6966
11.0	1.0	.22113	.14240	.923	-.2499	.6921
	2.0	.33115	.14240	.462	-.1398	.8021
	3.0	.39930	.14240	.186	-.0717	.8703
	4.0	.55757*	.14029	.005	.0935	1.0216
	5.0	.50773*	.14029	.019	.0437	.9718
	6.0	.33753	.14029	.407	-.1265	.8016
	7.0	.35816	.13838	.294	-.0996	.8159
	8.0	-.00547	.14240	1.000	-.4765	.4655
	9.0	.11473	.14029	1.000	-.3493	.5788
	10.0	-.14067	.14473	.998	-.6194	.3380
	12.0	.05710	.14473	1.000	-.4216	.5358
12.0	1.0	.16404	.14857	.994	-.3274	.6554
	2.0	.27405	.14857	.791	-.2174	.7655
	3.0	.34221	.14857	.478	-.1492	.8336
	4.0	.50047*	.14655	.036	.0157	.9852
	5.0	.45064	.14655	.096	-.0341	.9354
	6.0	.28043	.14655	.749	-.2043	.7652
	7.0	.30106	.14473	.637	-.1776	.7798
	8.0	-.06257	.14857	1.000	-.5540	.4288
	9.0	.05763	.14655	1.000	-.4271	.5424
	10.0	-.19777	.15080	.977	-.6966	.3010
	11.0	-.05710	.14473	1.000	-.5358	.4216

*. The mean difference is significant at the 0.05 level.

Station 15: Dunnett T3

(I) MON		Mean Difference (I-J)	Std. Error	Sig.	95% Confidence Interval	
					Lower Bound	Upper Bound
1.0	2.0	.18996	.16105	1.000	-.3987	.7786
	3.0	.24560	.12308	.916	-.2053	.6965
	4.0	.37269	.12762	.281	-.0930	.8384
	5.0	.32803	.12780	.526	-.1389	.7949
	6.0	.22818	.12434	.967	-.2273	.6836
	7.0	.01897	.14784	1.000	-.5170	.5549
	8.0	.01685	.13715	1.000	-.4825	.5161
	9.0	-.05226	.12715	1.000	-.5170	.4124
	10.0	-.28779	.14255	.906	-.8093	.2337
	11.0	-.16943	.15695	1.000	-.7407	.4018
	12.0	-.05811	.14577	1.000	-.5902	.4740
2.0	1.0	-.18996	.16105	1.000	-.7786	.3987
	3.0	.05564	.14561	1.000	-.4848	.5961
	4.0	.18274	.14947	1.000	-.3689	.7343
	5.0	.13807	.14963	1.000	-.4144	.6905
	6.0	.03822	.14668	1.000	-.5056	.5820
	7.0	-.17098	.16707	1.000	-.7784	.4364
	8.0	-.17311	.15768	1.000	-.7507	.4045
	9.0	-.24222	.14907	.993	-.7930	.3085
	10.0	-.47775	.16241	.272	-1.0728	.1173
	11.0	-.35939	.17518	.894	-.9959	.2771
	12.0	-.24807	.16524	.999	-.8518	.3557
3.0	1.0	-.24560	.12308	.916	-.6965	.2053
	2.0	-.05564	.14561	1.000	-.5961	.4848
	4.0	.12709	.10749	1.000	-.2628	.5170
	5.0	.08243	.10771	1.000	-.3093	.4741
	6.0	-.01742	.10357	1.000	-.3937	.3589
	7.0	-.22663	.13086	.985	-.7047	.2514
	8.0	-.22875	.11864	.942	-.6624	.2049
	9.0	-.29786	.10693	.362	-.6866	.0909
	10.0	-.53339*	.12485	.011	-.9953	-.0715
	11.0	-.41503	.14107	.276	-.9350	.1049
	12.0	-.30371	.12852	.686	-.7781	.1707

Station 15: Dunnett T3

(I) MON		Mean Difference (I-J)	Std. Error	Sig.	95% Confidence Interval	
					Lower Bound	Upper Bound
4.0	1.0	-.37269	.12762	.281	-.8384	.0930
	2.0	-.18274	.14947	1.000	-.7343	.3689
	3.0	-.12709	.10749	1.000	-.5170	.2628
	5.0	-.04466	.11287	1.000	-.4546	.3653
	6.0	-.14451	.10893	1.000	-.5402	.2512
	7.0	-.35372	.13514	.485	-.8454	.1380
	8.0	-.35585	.12335	.300	-.8051	.0934
	9.0	-.42496*	.11213	.033	-.8322	-.0177
	10.0	-.66048*	.12934	.001	-1.1364	-.1846
	11.0	-.54212*	.14505	.042	-1.0740	-.0102
	12.0	-.43080	.13288	.143	-.9187	.0571
5.0	1.0	-.32803	.12780	.526	-.7949	.1389
	2.0	-.13807	.14963	1.000	-.6905	.4144
	3.0	-.08243	.10771	1.000	-.4741	.3093
	4.0	.04466	.11287	1.000	-.3653	.4546
	6.0	-.09985	.10915	1.000	-.4973	.2976
	7.0	-.30906	.13531	.748	-.8018	.1837
	8.0	-.31118	.12354	.563	-.7618	.1394
	9.0	-.38029	.11234	.096	-.7892	.0286
	10.0	-.61582*	.12952	.003	-1.0928	-.1388
	11.0	-.49746	.14521	.092	-1.0303	.0353
	12.0	-.38614	.13305	.296	-.8752	.1029
6.0	1.0	-.22818	.12434	.967	-.6836	.2273
	2.0	-.03822	.14668	1.000	-.5820	.5056
	3.0	.01742	.10357	1.000	-.3589	.3937
	4.0	.14451	.10893	1.000	-.2512	.5402
	5.0	.09985	.10915	1.000	-.2976	.4973
	7.0	-.20921	.13205	.996	-.6914	.2729
	8.0	-.21133	.11995	.981	-.6498	.2271
	9.0	-.28044	.10838	.508	-.6750	.1141
	10.0	-.51597*	.12610	.018	-.9821	-.0498
	11.0	-.39761	.14217	.362	-.9211	.1259
	12.0	-.28629	.12973	.798	-.7648	.1922

Station 15: Dunnett T3

(I) MON		Mean Difference (I-J)	Std. Error	Sig.	95% Confidence Interval	
					Lower Bound	Upper Bound
7.0	1.0	-.01897	.14784	1.000	-.5549	.5170
	2.0	.17098	.16707	1.000	-.4364	.7784
	3.0	.22663	.13086	.985	-.2514	.7047
	4.0	.35372	.13514	.485	-.1380	.8454
	5.0	.30906	.13531	.748	-.1837	.8018
	6.0	.20921	.13205	.996	-.2729	.6914
	8.0	-.00213	.14417	1.000	-.5251	.5208
	9.0	-.07124	.13469	1.000	-.5619	.4195
	10.0	-.30676	.14932	.892	-.8503	.2368
	11.0	-.18840	.16312	1.000	-.7793	.4025
	12.0	-.07708	.15240	1.000	-.6307	.4766
8.0	1.0	-.01685	.13715	1.000	-.5161	.4825
	2.0	.17311	.15768	1.000	-.4045	.7507
	3.0	.22875	.11864	.942	-.2049	.6624
	4.0	.35585	.12335	.300	-.0934	.8051
	5.0	.31118	.12354	.563	-.1394	.7618
	6.0	.21133	.11995	.981	-.2271	.6498
	7.0	.00213	.14417	1.000	-.5208	.5251
	9.0	-.06911	.12286	1.000	-.5174	.3791
	10.0	-.30464	.13874	.808	-.8127	.2035
	11.0	-.18628	.15350	1.000	-.7458	.3733
	12.0	-.07495	.14205	1.000	-.5941	.4442
9.0	1.0	.05226	.12715	1.000	-.4124	.5170
	2.0	.24222	.14907	.993	-.3085	.7930
	3.0	.29786	.10693	.362	-.0909	.6866
	4.0	.42496*	.11213	.033	.0177	.8322
	5.0	.38029	.11234	.096	-.0286	.7892
	6.0	.28044	.10838	.508	-.1141	.6750
	7.0	.07124	.13469	1.000	-.4195	.5619
	8.0	.06911	.12286	1.000	-.3791	.5174
	10.0	-.23553	.12887	.967	-.7105	.2394
	11.0	-.11717	.14463	1.000	-.6482	.4139
	12.0	-.00584	.13243	1.000	-.4928	.4812

Station 15: Dunnett T3

(I) MON		Mean Difference (I-J)	Std. Error	Sig.	95% Confidence Interval	
					Lower Bound	Upper Bound
10.0	1.0	.28779	.14255	.906	-.2337	.8093
	2.0	.47775	.16241	.272	-.1173	1.0728
	3.0	.53339*	.12485	.011	.0715	.9953
	4.0	.66048*	.12934	.001	.1846	1.1364
	5.0	.61582*	.12952	.003	.1388	1.0928
	6.0	.51597*	.12610	.018	.0498	.9821
	7.0	.30676	.14932	.892	-.2368	.8503
	8.0	.30464	.13874	.808	-.2035	.8127
	9.0	.23553	.12887	.967	-.2394	.7105
	11.0	.11836	.15835	1.000	-.4596	.6963
	12.0	.22968	.14728	.997	-.3102	.7696
11.0	1.0	.16943	.15695	1.000	-.4018	.7407
	2.0	.35939	.17518	.894	-.2771	.9959
	3.0	.41503	.14107	.276	-.1049	.9350
	4.0	.54212*	.14505	.042	.0102	1.0740
	5.0	.49746	.14521	.092	-.0353	1.0303
	6.0	.39761	.14217	.362	-.1259	.9211
	7.0	.18840	.16312	1.000	-.4025	.7793
	8.0	.18628	.15350	1.000	-.3733	.7458
	9.0	.11717	.14463	1.000	-.4139	.6482
	10.0	-.11836	.15835	1.000	-.6963	.4596
	12.0	.11132	.16125	1.000	-.4759	.6985
12.0	1.0	.05811	.14577	1.000	-.4740	.5902
	2.0	.24807	.16524	.999	-.3557	.8518
	3.0	.30371	.12852	.686	-.1707	.7781
	4.0	.43080	.13288	.143	-.0571	.9187
	5.0	.38614	.13305	.296	-.1029	.8752
	6.0	.28629	.12973	.798	-.1922	.7648
	7.0	.07708	.15240	1.000	-.4766	.6307
	8.0	.07495	.14205	1.000	-.4442	.5941
	9.0	.00584	.13243	1.000	-.4812	.4928
	10.0	-.22968	.14728	.997	-.7696	.3102
	11.0	-.11132	.16125	1.000	-.6985	.4759

*. The mean difference is significant at the 0.05 level.

Station 16: Tukey HSD

(I) MON		Mean Difference (I-J)	Std. Error	Sig.	95% Confidence Interval	
					Lower Bound	Upper Bound
1.0	2.0	.02677	.09902	1.000	-.3007	.3542
	3.0	-.06050	.09763	1.000	-.3833	.2623
	4.0	-.04283	.09637	1.000	-.3615	.2759
	5.0	-.04565	.09763	1.000	-.3685	.2772
	6.0	.12824	.09763	.977	-.1946	.4511
	7.0	.14560	.09523	.931	-.1693	.4605
	8.0	.08702	.09763	.999	-.2358	.4099
	9.0	-.03808	.09763	1.000	-.3609	.2848
	10.0	-.17188	.10226	.875	-.5100	.1663
	11.0	-.16437	.09637	.864	-.4831	.1543
	12.0	-.07279	.09902	1.000	-.4002	.2546
2.0	1.0	-.02677	.09902	1.000	-.3542	.3007
	3.0	-.08727	.09763	.999	-.4101	.2356
	4.0	-.06960	.09637	1.000	-.3883	.2491
	5.0	-.07242	.09763	1.000	-.3953	.2504
	6.0	.10147	.09763	.997	-.2214	.4243
	7.0	.11883	.09523	.984	-.1961	.4337
	8.0	.06025	.09763	1.000	-.2626	.3831
	9.0	-.06485	.09763	1.000	-.3877	.2580
	10.0	-.19865	.10226	.731	-.5368	.1395
	11.0	-.19114	.09637	.704	-.5098	.1276
	12.0	-.09956	.09902	.997	-.4270	.2279
3.0	1.0	.06050	.09763	1.000	-.2623	.3833
	2.0	.08727	.09763	.999	-.2356	.4101
	4.0	.01768	.09495	1.000	-.2963	.3317
	5.0	.01486	.09623	1.000	-.3033	.3331
	6.0	.18874	.09623	.719	-.1295	.5069
	7.0	.20611	.09379	.553	-.1040	.5163
	8.0	.14752	.09623	.930	-.1707	.4657
	9.0	.02242	.09623	1.000	-.2958	.3406
	10.0	-.11138	.10092	.994	-.4451	.2224
	11.0	-.10387	.09495	.995	-.4179	.2101
	12.0	-.01229	.09763	1.000	-.3351	.3106

Station 16: Tukey HSD

(I) MON		Mean Difference (I-J)	Std. Error	Sig.	95% Confidence Interval	
					Lower Bound	Upper Bound
4.0	1.0	.04283	.09637	1.000	-.2759	.3615
	2.0	.06960	.09637	1.000	-.2491	.3883
	3.0	-.01768	.09495	1.000	-.3317	.2963
	5.0	-.00282	.09495	1.000	-.3168	.3112
	6.0	.17106	.09495	.815	-.1429	.4851
	7.0	.18843	.09248	.667	-.1174	.4943
	8.0	.12985	.09495	.968	-.1841	.4438
	9.0	.00475	.09495	1.000	-.3092	.3187
	10.0	-.12905	.09971	.979	-.4588	.2007
	11.0	-.12155	.09366	.979	-.4313	.1882
	12.0	-.02996	.09637	1.000	-.3487	.2887
5.0	1.0	.04565	.09763	1.000	-.2772	.3685
	2.0	.07242	.09763	1.000	-.2504	.3953
	3.0	-.01486	.09623	1.000	-.3331	.3033
	4.0	.00282	.09495	1.000	-.3112	.3168
	6.0	.17388	.09623	.812	-.1443	.4921
	7.0	.19125	.09379	.666	-.1189	.5014
	8.0	.13267	.09623	.966	-.1855	.4509
	9.0	.00757	.09623	1.000	-.3106	.3258
	10.0	-.12623	.10092	.984	-.4600	.2075
	11.0	-.11873	.09495	.984	-.4327	.1953
	12.0	-.02714	.09763	1.000	-.3500	.2957
6.0	1.0	-.12824	.09763	.977	-.4511	.1946
	2.0	-.10147	.09763	.997	-.4243	.2214
	3.0	-.18874	.09623	.719	-.5069	.1295
	4.0	-.17106	.09495	.815	-.4851	.1429
	5.0	-.17388	.09623	.812	-.4921	.1443
	7.0	.01737	.09379	1.000	-.2928	.3275
	8.0	-.04121	.09623	1.000	-.3594	.2770
	9.0	-.16632	.09623	.853	-.4845	.1519
	10.0	-.30011	.10092	.124	-.6338	.0336
	11.0	-.29261	.09495	.094	-.6066	.0214
	12.0	-.20102	.09763	.652	-.5239	.1218

Station 16: Tukey HSD

(I) MON		Mean Difference (I-J)	Std. Error	Sig.	95% Confidence Interval	
					Lower Bound	Upper Bound
7.0	1.0	-.14560	.09523	.931	-.4605	.1693
	2.0	-.11883	.09523	.984	-.4337	.1961
	3.0	-.20611	.09379	.553	-.5163	.1040
	4.0	-.18843	.09248	.667	-.4943	.1174
	5.0	-.19125	.09379	.666	-.5014	.1189
	6.0	-.01737	.09379	1.000	-.3275	.2928
	8.0	-.05858	.09379	1.000	-.3687	.2516
	9.0	-.18368	.09379	.721	-.4938	.1265
	10.0	-.31748	.09860	.064	-.6435	.0086
	11.0	-.30998*	.09248	.044	-.6158	-.0042
	12.0	-.21839	.09523	.485	-.5333	.0965
8.0	1.0	-.08702	.09763	.999	-.4099	.2358
	2.0	-.06025	.09763	1.000	-.3831	.2626
	3.0	-.14752	.09623	.930	-.4657	.1707
	4.0	-.12985	.09495	.968	-.4438	.1841
	5.0	-.13267	.09623	.966	-.4509	.1855
	6.0	.04121	.09623	1.000	-.2770	.3594
	7.0	.05858	.09379	1.000	-.2516	.3687
	9.0	-.12510	.09623	.978	-.4433	.1931
	10.0	-.25890	.10092	.307	-.5926	.0748
	11.0	-.25140	.09495	.261	-.5654	.0626
	12.0	-.15981	.09763	.893	-.4827	.1630
9.0	1.0	.03808	.09763	1.000	-.2848	.3609
	2.0	.06485	.09763	1.000	-.2580	.3877
	3.0	-.02242	.09623	1.000	-.3406	.2958
	4.0	-.00475	.09495	1.000	-.3187	.3092
	5.0	-.00757	.09623	1.000	-.3258	.3106
	6.0	.16632	.09623	.853	-.1519	.4845
	7.0	.18368	.09379	.721	-.1265	.4938
	8.0	.12510	.09623	.978	-.1931	.4433
	10.0	-.13380	.10092	.975	-.4675	.1999
	11.0	-.12629	.09495	.974	-.4403	.1877
	12.0	-.03471	.09763	1.000	-.3576	.2881

Station 16: Tukey HSD

(I) MON		Mean Difference (I-J)	Std. Error	Sig.	95% Confidence Interval	
					Lower Bound	Upper Bound
10.0	1.0	.17188	.10226	.875	-.1663	.5100
	2.0	.19865	.10226	.731	-.1395	.5368
	3.0	.11138	.10092	.994	-.2224	.4451
	4.0	.12905	.09971	.979	-.2007	.4588
	5.0	.12623	.10092	.984	-.2075	.4600
	6.0	.30011	.10092	.124	-.0336	.6338
	7.0	.31748	.09860	.064	-.0086	.6435
	8.0	.25890	.10092	.307	-.0748	.5926
	9.0	.13380	.10092	.975	-.1999	.4675
	11.0	.00750	.09971	1.000	-.3222	.3372
	12.0	.09909	.10226	.998	-.2391	.4373
11.0	1.0	.16437	.09637	.864	-.1543	.4831
	2.0	.19114	.09637	.704	-.1276	.5098
	3.0	.10387	.09495	.995	-.2101	.4179
	4.0	.12155	.09366	.979	-.1882	.4313
	5.0	.11873	.09495	.984	-.1953	.4327
	6.0	.29261	.09495	.094	-.0214	.6066
	7.0	.30998*	.09248	.044	.0042	.6158
	8.0	.25140	.09495	.261	-.0626	.5654
	9.0	.12629	.09495	.974	-.1877	.4403
	10.0	-.00750	.09971	1.000	-.3372	.3222
	12.0	.09159	.09637	.998	-.2271	.4103
12.0	1.0	.07279	.09902	1.000	-.2546	.4002
	2.0	.09956	.09902	.997	-.2279	.4270
	3.0	.01229	.09763	1.000	-.3106	.3351
	4.0	.02996	.09637	1.000	-.2887	.3487
	5.0	.02714	.09763	1.000	-.2957	.3500
	6.0	.20102	.09763	.652	-.1218	.5239
	7.0	.21839	.09523	.485	-.0965	.5333
	8.0	.15981	.09763	.893	-.1630	.4827
	9.0	.03471	.09763	1.000	-.2881	.3576
	10.0	-.09909	.10226	.998	-.4373	.2391
	11.0	-.09159	.09637	.998	-.4103	.2271

*. The mean difference is significant at the 0.05 level.

Station 17: Tukey HSD

(I) MON		Mean Difference (I-J)	Std. Error	Sig.	95% Confidence Interval	
					Lower Bound	Upper Bound
1.0	2.0	.16061	.13206	.987	-.2757	.5970
	3.0	.12606	.13040	.998	-.3048	.5569
	4.0	.13917	.13040	.996	-.2917	.5700
	5.0	.13126	.13206	.998	-.3051	.5676
	6.0	.03780	.13206	1.000	-.3986	.4741
	7.0	-.02612	.12888	1.000	-.4520	.3997
	8.0	.06909	.13206	1.000	-.3673	.5054
	9.0	.08598	.13206	1.000	-.3504	.5223
	10.0	-.26455	.13811	.748	-.7209	.1918
	11.0	-.18721	.13040	.955	-.6181	.2436
	12.0	.13206	.13388	.998	-.3103	.5744
2.0	1.0	-.16061	.13206	.987	-.5970	.2757
	3.0	-.03455	.13040	1.000	-.4654	.3963
	4.0	-.02145	.13040	1.000	-.4523	.4094
	5.0	-.02935	.13206	1.000	-.4657	.4070
	6.0	-.12282	.13206	.999	-.5592	.3135
	7.0	-.18673	.12888	.952	-.6126	.2391
	8.0	-.09152	.13206	1.000	-.5279	.3448
	9.0	-.07463	.13206	1.000	-.5110	.3617
	10.0	-.42516	.13811	.094	-.8815	.0312
	11.0	-.34783	.13040	.250	-.7787	.0830
	12.0	-.02855	.13388	1.000	-.4709	.4138
3.0	1.0	-.12606	.13040	.998	-.5569	.3048
	2.0	.03455	.13040	1.000	-.3963	.4654
	4.0	.01310	.12872	1.000	-.4122	.4384
	5.0	.00520	.13040	1.000	-.4257	.4361
	6.0	-.08827	.13040	1.000	-.5191	.3426
	7.0	-.15218	.12718	.989	-.5724	.2680
	8.0	-.05697	.13040	1.000	-.4878	.3739
	9.0	-.04008	.13040	1.000	-.4709	.3908
	10.0	-.39061	.13653	.163	-.8417	.0605
	11.0	-.31328	.12872	.388	-.7386	.1120
	12.0	.00600	.13224	1.000	-.4310	.4430

Station 17: Tukey HSD

(I) MON		Mean Difference (I-J)	Std. Error	Sig.	95% Confidence Interval	
					Lower Bound	Upper Bound
4.0	1.0	-.13917	.13040	.996	-.5700	.2917
	2.0	.02145	.13040	1.000	-.4094	.4523
	3.0	-.01310	.12872	1.000	-.4384	.4122
	5.0	-.00790	.13040	1.000	-.4388	.4230
	6.0	-.10137	.13040	1.000	-.5322	.3295
	7.0	-.16528	.12718	.978	-.5855	.2549
	8.0	-.07007	.13040	1.000	-.5009	.3608
	9.0	-.05318	.13040	1.000	-.4840	.3777
	10.0	-.40371	.13653	.129	-.8548	.0474
	11.0	-.32638	.12872	.324	-.7517	.0989
	12.0	-.00710	.13224	1.000	-.4441	.4299
5.0	1.0	-.13126	.13206	.998	-.5676	.3051
	2.0	.02935	.13206	1.000	-.4070	.4657
	3.0	-.00520	.13040	1.000	-.4361	.4257
	4.0	.00790	.13040	1.000	-.4230	.4388
	6.0	-.09347	.13206	1.000	-.5298	.3429
	7.0	-.15738	.12888	.987	-.5832	.2685
	8.0	-.06217	.13206	1.000	-.4985	.3742
	9.0	-.04528	.13206	1.000	-.4816	.3911
	10.0	-.39581	.13811	.161	-.8522	.0605
	11.0	-.31848	.13040	.383	-.7493	.1124
	12.0	.00080	.13388	1.000	-.4416	.4432
6.0	1.0	-.03780	.13206	1.000	-.4741	.3986
	2.0	.12282	.13206	.999	-.3135	.5592
	3.0	.08827	.13040	1.000	-.3426	.5191
	4.0	.10137	.13040	1.000	-.3295	.5322
	5.0	.09347	.13206	1.000	-.3429	.5298
	7.0	-.06392	.12888	1.000	-.4898	.3619
	8.0	.03130	.13206	1.000	-.4051	.4676
	9.0	.04819	.13206	1.000	-.3882	.4845
	10.0	-.30234	.13811	.559	-.7587	.1540
	11.0	-.22501	.13040	.855	-.6559	.2059
	12.0	.09427	.13388	1.000	-.3481	.5366

Station 17: Tukey HSD

(I) MON		Mean Difference (I-J)	Std. Error	Sig.	95% Confidence Interval	
					Lower Bound	Upper Bound
7.0	1.0	.02612	.12888	1.000	-.3997	.4520
	2.0	.18673	.12888	.952	-.2391	.6126
	3.0	.15218	.12718	.989	-.2680	.5724
	4.0	.16528	.12718	.978	-.2549	.5855
	5.0	.15738	.12888	.987	-.2685	.5832
	6.0	.06392	.12888	1.000	-.3619	.4898
	8.0	.09521	.12888	1.000	-.3306	.5210
	9.0	.11210	.12888	.999	-.3137	.5379
	10.0	-.23843	.13507	.835	-.6847	.2079
	11.0	-.16109	.12718	.982	-.5813	.2591
	12.0	.15818	.13074	.988	-.2738	.5902
8.0	1.0	-.06909	.13206	1.000	-.5054	.3673
	2.0	.09152	.13206	1.000	-.3448	.5279
	3.0	.05697	.13040	1.000	-.3739	.4878
	4.0	.07007	.13040	1.000	-.3608	.5009
	5.0	.06217	.13206	1.000	-.3742	.4985
	6.0	-.03130	.13206	1.000	-.4676	.4051
	7.0	-.09521	.12888	1.000	-.5210	.3306
	9.0	.01689	.13206	1.000	-.4195	.4532
	10.0	-.33364	.13811	.400	-.7900	.1227
	11.0	-.25631	.13040	.716	-.6872	.1746
	12.0	.06297	.13388	1.000	-.3794	.5053
9.0	1.0	-.08598	.13206	1.000	-.5223	.3504
	2.0	.07463	.13206	1.000	-.3617	.5110
	3.0	.04008	.13040	1.000	-.3908	.4709
	4.0	.05318	.13040	1.000	-.3777	.4840
	5.0	.04528	.13206	1.000	-.3911	.4816
	6.0	-.04819	.13206	1.000	-.4845	.3882
	7.0	-.11210	.12888	.999	-.5379	.3137
	8.0	-.01689	.13206	1.000	-.4532	.4195
	10.0	-.35053	.13811	.322	-.8069	.1058
	11.0	-.27320	.13040	.627	-.7041	.1577
	12.0	.04608	.13388	1.000	-.3963	.4885

Station 17: Tukey HSD

(I) MON		Mean Difference (I-J)	Std. Error	Sig.	95% Confidence Interval	
					Lower Bound	Upper Bound
10.0	1.0	.26455	.13811	.748	-.1918	.7209
	2.0	.42516	.13811	.094	-.0312	.8815
	3.0	.39061	.13653	.163	-.0605	.8417
	4.0	.40371	.13653	.129	-.0474	.8548
	5.0	.39581	.13811	.161	-.0605	.8522
	6.0	.30234	.13811	.559	-.1540	.7587
	7.0	.23843	.13507	.835	-.2079	.6847
	8.0	.33364	.13811	.400	-.1227	.7900
	9.0	.35053	.13811	.322	-.1058	.8069
	11.0	.07733	.13653	1.000	-.3738	.5284
	12.0	.39661	.13986	.173	-.0655	.8587
11.0	1.0	.18721	.13040	.955	-.2436	.6181
	2.0	.34783	.13040	.250	-.0830	.7787
	3.0	.31328	.12872	.388	-.1120	.7386
	4.0	.32638	.12872	.324	-.0989	.7517
	5.0	.31848	.13040	.383	-.1124	.7493
	6.0	.22501	.13040	.855	-.2059	.6559
	7.0	.16109	.12718	.982	-.2591	.5813
	8.0	.25631	.13040	.716	-.1746	.6872
	9.0	.27320	.13040	.627	-.1577	.7041
	10.0	-.07733	.13653	1.000	-.5284	.3738
	12.0	.31928	.13224	.401	-.1177	.7562
12.0	1.0	-.13206	.13388	.998	-.5744	.3103
	2.0	.02855	.13388	1.000	-.4138	.4709
	3.0	-.00600	.13224	1.000	-.4430	.4310
	4.0	.00710	.13224	1.000	-.4299	.4441
	5.0	-.00080	.13388	1.000	-.4432	.4416
	6.0	-.09427	.13388	1.000	-.5366	.3481
	7.0	-.15818	.13074	.988	-.5902	.2738
	8.0	-.06297	.13388	1.000	-.5053	.3794
	9.0	-.04608	.13388	1.000	-.4885	.3963
	10.0	-.39661	.13986	.173	-.8587	.0655
	11.0	-.31928	.13224	.401	-.7562	.1177

*. The mean difference is significant at the 0.05 level.

Station 18: Dunnett T3

(I) MON		Mean Difference (I-J)	Std. Error	Sig.	95% Confidence Interval	
					Lower Bound	Upper Bound
1.0	2.0	.08655	.16344	1.000	-.5083	.6814
	3.0	.11359	.14337	1.000	-.4111	.6383
	4.0	.22378	.14196	.996	-.2964	.7440
	5.0	.12065	.13346	1.000	-.3742	.6155
	6.0	.07858	.13899	1.000	-.4328	.5900
	7.0	-.05083	.13283	1.000	-.5434	.4417
	8.0	.18386	.13390	1.000	-.3122	.6800
	9.0	.16430	.13735	1.000	-.3421	.6707
	10.0	-.33009	.16395	.909	-.9298	.2696
	11.0	-.30921	.15396	.913	-.8693	.2509
	12.0	.12673	.15276	1.000	-.4310	.6845
2.0	1.0	-.08655	.16344	1.000	-.6814	.5083
	3.0	.02704	.14405	1.000	-.5003	.5544
	4.0	.13723	.14264	1.000	-.3857	.6601
	5.0	.03410	.13419	1.000	-.4636	.5319
	6.0	-.00797	.13969	1.000	-.5221	.5062
	7.0	-.13738	.13356	1.000	-.6329	.3581
	8.0	.09731	.13463	1.000	-.4017	.5963
	9.0	.07774	.13806	1.000	-.4314	.5869
	10.0	-.41664	.16454	.553	-1.0185	.1852
	11.0	-.39576	.15459	.530	-.9582	.1667
	12.0	.04018	.15340	1.000	-.5200	.6003
3.0	1.0	-.11359	.14337	1.000	-.6383	.4111
	2.0	-.02704	.14405	1.000	-.5544	.5003
	4.0	.11019	.11912	1.000	-.3216	.5420
	5.0	.00706	.10886	1.000	-.3896	.4037
	6.0	-.03501	.11557	1.000	-.4549	.3849
	7.0	-.16442	.10809	.998	-.5576	.2288
	8.0	.07026	.10940	1.000	-.3282	.4687
	9.0	.05070	.11360	1.000	-.3622	.4636
	10.0	-.44368	.14463	.215	-.9777	.0903
	11.0	-.42280	.13320	.159	-.9067	.0611
	12.0	.01314	.13181	1.000	-.4684	.4946

Station 18: Dunnett T3

(I) MON		Mean Difference (I-J)	Std. Error	Sig.	95% Confidence Interval	
					Lower Bound	Upper Bound
4.0	1.0	-.22378	.14196	.996	-.7440	.2964
	2.0	-.13723	.14264	1.000	-.6601	.3857
	3.0	-.11019	.11912	1.000	-.5420	.3216
	5.0	-.10313	.10699	1.000	-.4926	.2864
	6.0	-.14520	.11381	1.000	-.5586	.2682
	7.0	-.27461	.10620	.509	-.6605	.1113
	8.0	-.03992	.10753	1.000	-.4313	.3515
	9.0	-.05948	.11181	1.000	-.4658	.3468
	10.0	-.55387*	.14322	.033	-1.0835	-.0242
	11.0	-.53299*	.13167	.016	-1.0118	-.0542
	12.0	-.09705	.13027	1.000	-.5734	.3793
5.0	1.0	-.12065	.13346	1.000	-.6155	.3742
	2.0	-.03410	.13419	1.000	-.5319	.4636
	3.0	-.00706	.10886	1.000	-.4037	.3896
	4.0	.10313	.10699	1.000	-.2864	.4926
	6.0	-.04207	.10302	1.000	-.4176	.3335
	7.0	-.17148	.09455	.974	-.5143	.1714
	8.0	.06320	.09604	1.000	-.2864	.4128
	9.0	.04364	.10080	1.000	-.3236	.4108
	10.0	-.45074	.13481	.127	-.9564	.0549
	11.0	-.42986	.12246	.075	-.8792	.0195
	12.0	.00608	.12096	1.000	-.4410	.4532
6.0	1.0	-.07858	.13899	1.000	-.5900	.4328
	2.0	.00797	.13969	1.000	-.5062	.5221
	3.0	.03501	.11557	1.000	-.3849	.4549
	4.0	.14520	.11381	1.000	-.2682	.5586
	5.0	.04207	.10302	1.000	-.3335	.4176
	7.0	-.12941	.10220	1.000	-.5011	.2423
	8.0	.10527	.10359	1.000	-.2722	.4828
	9.0	.08571	.10802	1.000	-.3075	.4789
	10.0	-.40867	.14028	.297	-.9299	.1126
	11.0	-.38779	.12847	.228	-.8564	.0808
	12.0	.04815	.12703	1.000	-.4181	.5144

Station 18: Dunnett T3

(I) MON		Mean Difference (I-J)	Std. Error	Sig.	95% Confidence Interval	
					Lower Bound	Upper Bound
7.0	1.0	.05083	.13283	1.000	-.4417	.5434
	2.0	.13738	.13356	1.000	-.3581	.6329
	3.0	.16442	.10809	.998	-.2288	.5576
	4.0	.27461	.10620	.509	-.1113	.6605
	5.0	.17148	.09455	.974	-.1714	.5143
	6.0	.12941	.10220	1.000	-.2423	.5011
	8.0	.23469	.09516	.605	-.1104	.5798
	9.0	.21512	.09997	.838	-.1481	.5783
	10.0	-.27926	.13418	.867	-.7827	.2242
	11.0	-.25838	.12178	.853	-.7050	.1882
	12.0	.17756	.12026	.999	-.2668	.6219
8.0	1.0	-.18386	.13390	1.000	-.6800	.3122
	2.0	-.09731	.13463	1.000	-.5963	.4017
	3.0	-.07026	.10940	1.000	-.4687	.3282
	4.0	.03992	.10753	1.000	-.3515	.4313
	5.0	-.06320	.09604	1.000	-.4128	.2864
	6.0	-.10527	.10359	1.000	-.4828	.2722
	7.0	-.23469	.09516	.605	-.5798	.1104
	9.0	-.01956	.10138	1.000	-.3888	.3497
	10.0	-.51394*	.13524	.044	-1.0208	-.0071
	11.0	-.49307*	.12294	.020	-.9439	-.0423
	12.0	-.05712	.12144	1.000	-.5057	.3914
9.0	1.0	-.16430	.13735	1.000	-.6707	.3421
	2.0	-.07774	.13806	1.000	-.5869	.4314
	3.0	-.05070	.11360	1.000	-.4636	.3622
	4.0	.05948	.11181	1.000	-.3468	.4658
	5.0	-.04364	.10080	1.000	-.4108	.3236
	6.0	-.08571	.10802	1.000	-.4789	.3075
	7.0	-.21512	.09997	.838	-.5783	.1481
	8.0	.01956	.10138	1.000	-.3497	.3888
	10.0	-.49438	.13866	.073	-1.0109	.0221
	11.0	-.47350*	.12670	.040	-.9363	-.0107
	12.0	-.03756	.12524	1.000	-.4980	.4229

Station 18: Dunnett T3

(I) MON		Mean Difference (I-J)	Std. Error	Sig.	95% Confidence Interval	
					Lower Bound	Upper Bound
10.0	1.0	.33009	.16395	.909	-.2696	.9298
	2.0	.41664	.16454	.553	-.1852	1.0185
	3.0	.44368	.14463	.215	-.0903	.9777
	4.0	.55387*	.14322	.033	.0242	1.0835
	5.0	.45074	.13481	.127	-.0549	.9564
	6.0	.40867	.14028	.297	-.1126	.9299
	7.0	.27926	.13418	.867	-.2242	.7827
	8.0	.51394*	.13524	.044	.0071	1.0208
	9.0	.49438	.13866	.073	-.0221	1.0109
	11.0	.02088	.15513	1.000	-.5472	.5889
	12.0	.45682	.15394	.260	-.1090	1.0226
11.0	1.0	.30921	.15396	.913	-.2509	.8693
	2.0	.39576	.15459	.530	-.1667	.9582
	3.0	.42280	.13320	.159	-.0611	.9067
	4.0	.53299*	.13167	.016	.0542	1.0118
	5.0	.42986	.12246	.075	-.0195	.8792
	6.0	.38779	.12847	.228	-.0808	.8564
	7.0	.25838	.12178	.853	-.1882	.7050
	8.0	.49307*	.12294	.020	.0423	.9439
	9.0	.47350*	.12670	.040	.0107	.9363
	10.0	-.02088	.15513	1.000	-.5889	.5472
	12.0	.43594	.14325	.215	-.0855	.9574
12.0	1.0	-.12673	.15276	1.000	-.6845	.4310
	2.0	-.04018	.15340	1.000	-.6003	.5200
	3.0	-.01314	.13181	1.000	-.4946	.4684
	4.0	.09705	.13027	1.000	-.3793	.5734
	5.0	-.00608	.12096	1.000	-.4532	.4410
	6.0	-.04815	.12703	1.000	-.5144	.4181
	7.0	-.17756	.12026	.999	-.6219	.2668
	8.0	.05712	.12144	1.000	-.3914	.5057
	9.0	.03756	.12524	1.000	-.4229	.4980
	10.0	-.45682	.15394	.260	-1.0226	.1090
	11.0	-.43594	.14325	.215	-.9574	.0855

*. The mean difference is significant at the 0.05 level.

Station 19: Tukey HSD

(I) MON		Mean Difference (I-J)	Std. Error	Sig.	95% Confidence Interval	
					Lower Bound	Upper Bound
1.0	2.0	.04410	.13473	1.000	-.4014	.4896
	3.0	.11866	.13473	.999	-.3269	.5642
	4.0	.32375	.13114	.366	-.1099	.7574
	5.0	.23707	.13285	.825	-.2022	.6764
	6.0	.10874	.13285	1.000	-.3306	.5481
	7.0	.06368	.12958	1.000	-.3648	.4922
	8.0	.17041	.13285	.980	-.2689	.6097
	9.0	.19304	.13114	.946	-.2406	.6267
	10.0	-.20470	.13682	.940	-.6571	.2478
	11.0	-.33832	.13114	.298	-.7720	.0953
	12.0	-.28457	.13682	.638	-.7370	.1679
2.0	1.0	-.04410	.13473	1.000	-.4896	.4014
	3.0	.07456	.13473	1.000	-.3710	.5201
	4.0	.27966	.13114	.600	-.1540	.7133
	5.0	.19297	.13285	.951	-.2463	.6323
	6.0	.06465	.13285	1.000	-.3747	.5040
	7.0	.01959	.12958	1.000	-.4089	.4481
	8.0	.12632	.13285	.998	-.3130	.5656
	9.0	.14895	.13114	.993	-.2847	.5826
	10.0	-.24879	.13682	.806	-.7012	.2037
	11.0	-.38242	.13114	.143	-.8161	.0512
	12.0	-.32867	.13682	.410	-.7811	.1238
3.0	1.0	-.11866	.13473	.999	-.5642	.3269
	2.0	-.07456	.13473	1.000	-.5201	.3710
	4.0	.20510	.13114	.920	-.2286	.6388
	5.0	.11841	.13285	.999	-.3209	.5577
	6.0	-.00991	.13285	1.000	-.4492	.4294
	7.0	-.05497	.12958	1.000	-.4835	.3735
	8.0	.05176	.13285	1.000	-.3876	.4911
	9.0	.07439	.13114	1.000	-.3593	.5081
	10.0	-.32335	.13682	.436	-.7758	.1291
	11.0	-.45698*	.13114	.029	-.8906	-.0233
	12.0	-.40323	.13682	.133	-.8557	.0492

Station 19: Tukey HSD

(I) MON		Mean Difference (I-J)	Std. Error	Sig.	95% Confidence Interval	
					Lower Bound	Upper Bound
4.0	1.0	-.32375	.13114	.366	-.7574	.1099
	2.0	-.27966	.13114	.600	-.7133	.1540
	3.0	-.20510	.13114	.920	-.6388	.2286
	5.0	-.08668	.12920	1.000	-.5139	.3406
	6.0	-.21501	.12920	.882	-.6423	.2122
	7.0	-.26007	.12584	.647	-.6762	.1561
	8.0	-.15334	.12920	.989	-.5806	.2739
	9.0	-.13071	.12745	.997	-.5522	.2907
	10.0	-.52845*	.13329	.006	-.9692	-.0877
	11.0	-.66207*	.12745	.000	-1.0835	-.2406
	12.0	-.60832*	.13329	.001	-1.0491	-.1676
5.0	1.0	-.23707	.13285	.825	-.6764	.2022
	2.0	-.19297	.13285	.951	-.6323	.2463
	3.0	-.11841	.13285	.999	-.5577	.3209
	4.0	.08668	.12920	1.000	-.3406	.5139
	6.0	-.12833	.13094	.998	-.5613	.3047
	7.0	-.17339	.12762	.970	-.5954	.2486
	8.0	-.06665	.13094	1.000	-.4996	.3663
	9.0	-.04402	.12920	1.000	-.4713	.3832
	10.0	-.44176	.13497	.055	-.8881	.0046
	11.0	-.57539*	.12920	.001	-1.0026	-.1481
	12.0	-.52164*	.13497	.008	-.9680	-.0753
6.0	1.0	-.10874	.13285	1.000	-.5481	.3306
	2.0	-.06465	.13285	1.000	-.5040	.3747
	3.0	.00991	.13285	1.000	-.4294	.4492
	4.0	.21501	.12920	.882	-.2122	.6423
	5.0	.12833	.13094	.998	-.3047	.5613
	7.0	-.04506	.12762	1.000	-.4671	.3770
	8.0	.06167	.13094	1.000	-.3713	.4947
	9.0	.08430	.12920	1.000	-.3430	.5116
	10.0	-.31344	.13497	.464	-.7598	.1329
	11.0	-.44706*	.12920	.031	-.8743	-.0198
	12.0	-.39331	.13497	.144	-.8396	.0530

Station 19: Tukey HSD

(I) MON		Mean Difference (I-J)	Std. Error	Sig.	95% Confidence Interval	
					Lower Bound	Upper Bound
7.0	1.0	-.06368	.12958	1.000	-.4922	.3648
	2.0	-.01959	.12958	1.000	-.4481	.4089
	3.0	.05497	.12958	1.000	-.3735	.4835
	4.0	.26007	.12584	.647	-.1561	.6762
	5.0	.17339	.12762	.970	-.2486	.5954
	6.0	.04506	.12762	1.000	-.3770	.4671
	8.0	.10673	.12762	1.000	-.3153	.5288
	9.0	.12936	.12584	.997	-.2868	.5455
	10.0	-.26838	.13175	.668	-.7041	.1673
	11.0	-.40200	.12584	.069	-.8181	.0141
	12.0	-.34825	.13175	.263	-.7839	.0874
8.0	1.0	-.17041	.13285	.980	-.6097	.2689
	2.0	-.12632	.13285	.998	-.5656	.3130
	3.0	-.05176	.13285	1.000	-.4911	.3876
	4.0	.15334	.12920	.989	-.2739	.5806
	5.0	.06665	.13094	1.000	-.3663	.4996
	6.0	-.06167	.13094	1.000	-.4947	.3713
	7.0	-.10673	.12762	1.000	-.5288	.3153
	9.0	.02263	.12920	1.000	-.4046	.4499
	10.0	-.37511	.13497	.197	-.8214	.0712
	11.0	-.50873*	.12920	.006	-.9360	-.0815
	12.0	-.45498*	.13497	.041	-.9013	-.0087
9.0	1.0	-.19304	.13114	.946	-.6267	.2406
	2.0	-.14895	.13114	.993	-.5826	.2847
	3.0	-.07439	.13114	1.000	-.5081	.3593
	4.0	.13071	.12745	.997	-.2907	.5522
	5.0	.04402	.12920	1.000	-.3832	.4713
	6.0	-.08430	.12920	1.000	-.5116	.3430
	7.0	-.12936	.12584	.997	-.5455	.2868
	8.0	-.02263	.12920	1.000	-.4499	.4046
	10.0	-.39774	.13329	.121	-.8385	.0430
	11.0	-.53137*	.12745	.003	-.9528	-.1099
	12.0	-.47761*	.13329	.021	-.9184	-.0369

Station 19: Tukey HSD

(I) MON		Mean Difference (I-J)	Std. Error	Sig.	95% Confidence Interval	
					Lower Bound	Upper Bound
10.0	1.0	.20470	.13682	.940	-.2478	.6571
	2.0	.24879	.13682	.806	-.2037	.7012
	3.0	.32335	.13682	.436	-.1291	.7758
	4.0	.52845*	.13329	.006	.0877	.9692
	5.0	.44176	.13497	.055	-.0046	.8881
	6.0	.31344	.13497	.464	-.1329	.7598
	7.0	.26838	.13175	.668	-.1673	.7041
	8.0	.37511	.13497	.197	-.0712	.8214
	9.0	.39774	.13329	.121	-.0430	.8385
	11.0	-.13363	.13329	.998	-.5744	.3071
	12.0	-.07987	.13888	1.000	-.5391	.3794
11.0	1.0	.33832	.13114	.298	-.0953	.7720
	2.0	.38242	.13114	.143	-.0512	.8161
	3.0	.45698*	.13114	.029	.0233	.8906
	4.0	.66207*	.12745	.000	.2406	1.0835
	5.0	.57539*	.12920	.001	.1481	1.0026
	6.0	.44706*	.12920	.031	.0198	.8743
	7.0	.40200	.12584	.069	-.0141	.8181
	8.0	.50873*	.12920	.006	.0815	.9360
	9.0	.53137*	.12745	.003	.1099	.9528
	10.0	.13363	.13329	.998	-.3071	.5744
	12.0	.05375	.13329	1.000	-.3870	.4945
12.0	1.0	.28457	.13682	.638	-.1679	.7370
	2.0	.32867	.13682	.410	-.1238	.7811
	3.0	.40323	.13682	.133	-.0492	.8557
	4.0	.60832*	.13329	.001	.1676	1.0491
	5.0	.52164*	.13497	.008	.0753	.9680
	6.0	.39331	.13497	.144	-.0530	.8396
	7.0	.34825	.13175	.263	-.0874	.7839
	8.0	.45498*	.13497	.041	.0087	.9013
	9.0	.47761*	.13329	.021	.0369	.9184
	10.0	.07987	.13888	1.000	-.3794	.5391
	11.0	-.05375	.13329	1.000	-.4945	.3870

*. The mean difference is significant at the 0.05 level.

Station 20: Tukey HSD

(I) MON		Mean Difference (I-J)	Std. Error	Sig.	95% Confidence Interval	
					Lower Bound	Upper Bound
1.0	2.0	.00647	.12637	1.000	-.4114	.4243
	3.0	.15439	.12460	.985	-.2576	.5664
	4.0	.29211	.12300	.428	-.1146	.6988
	5.0	.19226	.12460	.927	-.2197	.6043
	6.0	.07558	.12460	1.000	-.3364	.4876
	7.0	.07229	.12154	1.000	-.3296	.4742
	8.0	.10973	.12460	.999	-.3023	.5217
	9.0	.12088	.12300	.998	-.2858	.5276
	10.0	-.04444	.12833	1.000	-.4688	.3799
	11.0	-.08421	.12300	1.000	-.4909	.3225
	12.0	-.11260	.12833	.999	-.5369	.3117
2.0	1.0	-.00647	.12637	1.000	-.4243	.4114
	3.0	.14792	.12460	.989	-.2641	.5599
	4.0	.28564	.12300	.464	-.1211	.6923
	5.0	.18579	.12460	.942	-.2262	.5978
	6.0	.06912	.12460	1.000	-.3429	.4811
	7.0	.06582	.12154	1.000	-.3361	.4677
	8.0	.10326	.12460	1.000	-.3087	.5153
	9.0	.11442	.12300	.999	-.2923	.5211
	10.0	-.05091	.12833	1.000	-.4752	.3734
	11.0	-.09068	.12300	1.000	-.4974	.3160
	12.0	-.11907	.12833	.999	-.5434	.3053
3.0	1.0	-.15439	.12460	.985	-.5664	.2576
	2.0	-.14792	.12460	.989	-.5599	.2641
	4.0	.13772	.12118	.993	-.2630	.5384
	5.0	.03787	.12281	1.000	-.3682	.4439
	6.0	-.07880	.12281	1.000	-.4849	.3273
	7.0	-.08210	.11970	1.000	-.4779	.3137
	8.0	-.04466	.12281	1.000	-.4507	.3614
	9.0	-.03350	.12118	1.000	-.4342	.3672
	10.0	-.19883	.12659	.918	-.6174	.2197
	11.0	-.23860	.12118	.714	-.6393	.1621
	12.0	-.26699	.12659	.617	-.6856	.1516

Station 20: Tukey HSD

(I) MON		Mean Difference (I-J)	Std. Error	Sig.	95% Confidence Interval	
					Lower Bound	Upper Bound
4.0	1.0	-.29211	.12300	.428	-.6988	.1146
	2.0	-.28564	.12300	.464	-.6923	.1211
	3.0	-.13772	.12118	.993	-.5384	.2630
	5.0	-.09985	.12118	1.000	-.5005	.3008
	6.0	-.21652	.12118	.823	-.6172	.1842
	7.0	-.21982	.11803	.781	-.6101	.1705
	8.0	-.18238	.12118	.938	-.5831	.2183
	9.0	-.17122	.11953	.956	-.5665	.2240
	10.0	-.33655	.12501	.238	-.7499	.0768
	11.0	-.37632	.11953	.078	-.7716	.0189
	12.0	-.40471	.12501	.061	-.8181	.0087
5.0	1.0	-.19226	.12460	.927	-.6043	.2197
	2.0	-.18579	.12460	.942	-.5978	.2262
	3.0	-.03787	.12281	1.000	-.4439	.3682
	4.0	.09985	.12118	1.000	-.3008	.5005
	6.0	-.11667	.12281	.998	-.5227	.2894
	7.0	-.11997	.11970	.998	-.5158	.2758
	8.0	-.08253	.12281	1.000	-.4886	.3235
	9.0	-.07137	.12118	1.000	-.4721	.3293
	10.0	-.23670	.12659	.776	-.6553	.1819
	11.0	-.27647	.12118	.493	-.6772	.1242
	12.0	-.30486	.12659	.405	-.7234	.1137
6.0	1.0	-.07558	.12460	1.000	-.4876	.3364
	2.0	-.06912	.12460	1.000	-.4811	.3429
	3.0	.07880	.12281	1.000	-.3273	.4849
	4.0	.21652	.12118	.823	-.1842	.6172
	5.0	.11667	.12281	.998	-.2894	.5227
	7.0	-.00330	.11970	1.000	-.3991	.3925
	8.0	.03414	.12281	1.000	-.3719	.4402
	9.0	.04530	.12118	1.000	-.3554	.4460
	10.0	-.12002	.12659	.998	-.5386	.2986
	11.0	-.15980	.12118	.976	-.5605	.2409
	12.0	-.18818	.12659	.943	-.6068	.2304

Station 20: Tukey HSD

(I) MON		Mean Difference (I-J)	Std. Error	Sig.	95% Confidence Interval	
					Lower Bound	Upper Bound
7.0	1.0	-.07229	.12154	1.000	-.4742	.3296
	2.0	-.06582	.12154	1.000	-.4677	.3361
	3.0	.08210	.11970	1.000	-.3137	.4779
	4.0	.21982	.11803	.781	-.1705	.6101
	5.0	.11997	.11970	.998	-.2758	.5158
	6.0	.00330	.11970	1.000	-.3925	.3991
	8.0	.03744	.11970	1.000	-.3584	.4332
	9.0	.04860	.11803	1.000	-.3417	.4389
	10.0	-.11673	.12357	.999	-.5253	.2919
	11.0	-.15650	.11803	.975	-.5468	.2338
	12.0	-.18489	.12357	.940	-.5935	.2237
8.0	1.0	-.10973	.12460	.999	-.5217	.3023
	2.0	-.10326	.12460	1.000	-.5153	.3087
	3.0	.04466	.12281	1.000	-.3614	.4507
	4.0	.18238	.12118	.938	-.2183	.5831
	5.0	.08253	.12281	1.000	-.3235	.4886
	6.0	-.03414	.12281	1.000	-.4402	.3719
	7.0	-.03744	.11970	1.000	-.4332	.3584
	9.0	.01116	.12118	1.000	-.3895	.4119
	10.0	-.15417	.12659	.987	-.5727	.2644
	11.0	-.19394	.12118	.907	-.5946	.2068
	12.0	-.22233	.12659	.839	-.6409	.1962
9.0	1.0	-.12088	.12300	.998	-.5276	.2858
	2.0	-.11442	.12300	.999	-.5211	.2923
	3.0	.03350	.12118	1.000	-.3672	.4342
	4.0	.17122	.11953	.956	-.2240	.5665
	5.0	.07137	.12118	1.000	-.3293	.4721
	6.0	-.04530	.12118	1.000	-.4460	.3554
	7.0	-.04860	.11803	1.000	-.4389	.3417
	8.0	-.01116	.12118	1.000	-.4119	.3895
	10.0	-.16532	.12501	.975	-.5787	.2480
	11.0	-.20510	.11953	.859	-.6003	.1901
	12.0	-.23348	.12501	.778	-.6468	.1799

Station 20: Tukey HSD

(I) MON		Mean Difference (I-J)	Std. Error	Sig.	95% Confidence Interval	
					Lower Bound	Upper Bound
10.0	1.0	.04444	.12833	1.000	-.3799	.4688
	2.0	.05091	.12833	1.000	-.3734	.4752
	3.0	.19883	.12659	.918	-.2197	.6174
	4.0	.33655	.12501	.238	-.0768	.7499
	5.0	.23670	.12659	.776	-.1819	.6553
	6.0	.12002	.12659	.998	-.2986	.5386
	7.0	.11673	.12357	.999	-.2919	.5253
	8.0	.15417	.12659	.987	-.2644	.5727
	9.0	.16532	.12501	.975	-.2480	.5787
	11.0	-.03977	.12501	1.000	-.4531	.3736
	12.0	-.06816	.13026	1.000	-.4989	.3626
11.0	1.0	.08421	.12300	1.000	-.3225	.4909
	2.0	.09068	.12300	1.000	-.3160	.4974
	3.0	.23860	.12118	.714	-.1621	.6393
	4.0	.37632	.11953	.078	-.0189	.7716
	5.0	.27647	.12118	.493	-.1242	.6772
	6.0	.15980	.12118	.976	-.2409	.5605
	7.0	.15650	.11803	.975	-.2338	.5468
	8.0	.19394	.12118	.907	-.2068	.5946
	9.0	.20510	.11953	.859	-.1901	.6003
	10.0	.03977	.12501	1.000	-.3736	.4531
	12.0	-.02839	.12501	1.000	-.4417	.3850
12.0	1.0	.11260	.12833	.999	-.3117	.5369
	2.0	.11907	.12833	.999	-.3053	.5434
	3.0	.26699	.12659	.617	-.1516	.6856
	4.0	.40471	.12501	.061	-.0087	.8181
	5.0	.30486	.12659	.405	-.1137	.7234
	6.0	.18818	.12659	.943	-.2304	.6068
	7.0	.18489	.12357	.940	-.2237	.5935
	8.0	.22233	.12659	.839	-.1962	.6409
	9.0	.23348	.12501	.778	-.1799	.6468
	10.0	.06816	.13026	1.000	-.3626	.4989
	11.0	.02839	.12501	1.000	-.3850	.4417

*. The mean difference is significant at the 0.05 level.

Station 27: Tukey HSD

(I) MON		Mean Difference (I-J)	Std. Error	Sig.	95% Confidence Interval	
					Lower Bound	Upper Bound
1.0	2.0	.21526	.12775	.873	-.2076	.6381
	3.0	.21904	.12775	.859	-.2038	.6419
	4.0	.29348	.12586	.458	-.1231	.7101
	5.0	.37970	.12775	.125	-.0432	.8026
	6.0	.26780	.12775	.626	-.1551	.6907
	7.0	.18077	.12415	.950	-.2302	.5917
	8.0	.21016	.12415	.869	-.2008	.6211
	9.0	.19292	.12415	.923	-.2180	.6039
	10.0	-.02690	.12987	1.000	-.4568	.4030
	11.0	-.13565	.12415	.995	-.5466	.2753
	12.0	.07085	.12987	1.000	-.3590	.5007
2.0	1.0	-.21526	.12775	.873	-.6381	.2076
	3.0	.00378	.12775	1.000	-.4191	.4266
	4.0	.07822	.12586	1.000	-.3384	.4948
	5.0	.16444	.12775	.980	-.2584	.5873
	6.0	.05255	.12775	1.000	-.3703	.4754
	7.0	-.03449	.12415	1.000	-.4454	.3765
	8.0	-.00510	.12415	1.000	-.4161	.4058
	9.0	-.02234	.12415	1.000	-.4333	.3886
	10.0	-.24216	.12987	.779	-.6720	.1877
	11.0	-.35091	.12415	.178	-.7619	.0600
	12.0	-.14440	.12987	.994	-.5743	.2855
3.0	1.0	-.21904	.12775	.859	-.6419	.2038
	2.0	-.00378	.12775	1.000	-.4266	.4191
	4.0	.07444	.12586	1.000	-.3422	.4910
	5.0	.16066	.12775	.983	-.2622	.5835
	6.0	.04877	.12775	1.000	-.3741	.4716
	7.0	-.03827	.12415	1.000	-.4492	.3727
	8.0	-.00888	.12415	1.000	-.4198	.4021
	9.0	-.02612	.12415	1.000	-.4371	.3848
	10.0	-.24594	.12987	.762	-.6758	.1839
	11.0	-.35469	.12415	.166	-.7656	.0563
	12.0	-.14818	.12987	.992	-.5780	.2817

Station 27: Tukey HSD

(I) MON		Mean Difference (I-J)	Std. Error	Sig.	95% Confidence Interval	
					Lower Bound	Upper Bound
4.0	1.0	-.29348	.12586	.458	-.7101	.1231
	2.0	-.07822	.12586	1.000	-.4948	.3384
	3.0	-.07444	.12586	1.000	-.4910	.3422
	5.0	.08622	.12586	1.000	-.3304	.5028
	6.0	-.02568	.12586	1.000	-.4423	.3909
	7.0	-.11271	.12221	.999	-.5172	.2918
	8.0	-.08333	.12221	1.000	-.4878	.3212
	9.0	-.10056	.12221	1.000	-.5051	.3039
	10.0	-.32038	.12800	.345	-.7441	.1033
	11.0	-.42914*	.12221	.027	-.8336	-.0246
	12.0	-.22263	.12800	.848	-.6463	.2011
5.0	1.0	-.37970	.12775	.125	-.8026	.0432
	2.0	-.16444	.12775	.980	-.5873	.2584
	3.0	-.16066	.12775	.983	-.5835	.2622
	4.0	-.08622	.12586	1.000	-.5028	.3304
	6.0	-.11190	.12775	.999	-.5348	.3110
	7.0	-.19893	.12415	.906	-.6099	.2120
	8.0	-.16955	.12415	.969	-.5805	.2414
	9.0	-.18678	.12415	.938	-.5977	.2242
	10.0	-.40660	.12987	.083	-.8365	.0233
	11.0	-.51536*	.12415	.003	-.9263	-.1044
	12.0	-.30885	.12987	.426	-.7387	.1210
6.0	1.0	-.26780	.12775	.626	-.6907	.1551
	2.0	-.05255	.12775	1.000	-.4754	.3703
	3.0	-.04877	.12775	1.000	-.4716	.3741
	4.0	.02568	.12586	1.000	-.3909	.4423
	5.0	.11190	.12775	.999	-.3110	.5348
	7.0	-.08704	.12415	1.000	-.4980	.3239
	8.0	-.05765	.12415	1.000	-.4686	.3533
	9.0	-.07489	.12415	1.000	-.4858	.3361
	10.0	-.29470	.12987	.502	-.7246	.1352
	11.0	-.40346	.12415	.060	-.8144	.0075
	12.0	-.19695	.12987	.934	-.6268	.2329

Station 27: Tukey HSD

(I) MON		Mean Difference (I-J)	Std. Error	Sig.	95% Confidence Interval	
					Lower Bound	Upper Bound
7.0	1.0	-.18077	.12415	.950	-.5917	.2302
	2.0	.03449	.12415	1.000	-.3765	.4454
	3.0	.03827	.12415	1.000	-.3727	.4492
	4.0	.11271	.12221	.999	-.2918	.5172
	5.0	.19893	.12415	.906	-.2120	.6099
	6.0	.08704	.12415	1.000	-.3239	.4980
	8.0	.02939	.12045	1.000	-.3693	.4281
	9.0	.01215	.12045	1.000	-.3865	.4108
	10.0	-.20767	.12633	.890	-.6258	.2105
	11.0	-.31642	.12045	.272	-.7151	.0823
	12.0	-.10991	.12633	.999	-.5281	.3082
8.0	1.0	-.21016	.12415	.869	-.6211	.2008
	2.0	.00510	.12415	1.000	-.4058	.4161
	3.0	.00888	.12415	1.000	-.4021	.4198
	4.0	.08333	.12221	1.000	-.3212	.4878
	5.0	.16955	.12415	.969	-.2414	.5805
	6.0	.05765	.12415	1.000	-.3533	.4686
	7.0	-.02939	.12045	1.000	-.4281	.3693
	9.0	-.01724	.12045	1.000	-.4159	.3814
	10.0	-.23705	.12633	.772	-.6552	.1811
	11.0	-.34581	.12045	.160	-.7445	.0529
	12.0	-.13930	.12633	.994	-.5574	.2788
9.0	1.0	-.19292	.12415	.923	-.6039	.2180
	2.0	.02234	.12415	1.000	-.3886	.4333
	3.0	.02612	.12415	1.000	-.3848	.4371
	4.0	.10056	.12221	1.000	-.3039	.5051
	5.0	.18678	.12415	.938	-.2242	.5977
	6.0	.07489	.12415	1.000	-.3361	.4858
	7.0	-.01215	.12045	1.000	-.4108	.3865
	8.0	.01724	.12045	1.000	-.3814	.4159
	10.0	-.21982	.12633	.847	-.6380	.1983
	11.0	-.32857	.12045	.221	-.7273	.0701
	12.0	-.12206	.12633	.998	-.5402	.2961

Station 27: Tukey HSD

(I) MON		Mean Difference (I-J)	Std. Error	Sig.	95% Confidence Interval	
					Lower Bound	Upper Bound
10.0	1.0	.02690	.12987	1.000	-.4030	.4568
	2.0	.24216	.12987	.779	-.1877	.6720
	3.0	.24594	.12987	.762	-.1839	.6758
	4.0	.32038	.12800	.345	-.1033	.7441
	5.0	.40660	.12987	.083	-.0233	.8365
	6.0	.29470	.12987	.502	-.1352	.7246
	7.0	.20767	.12633	.890	-.2105	.6258
	8.0	.23705	.12633	.772	-.1811	.6552
	9.0	.21982	.12633	.847	-.1983	.6380
	11.0	-.10876	.12633	.999	-.5269	.3094
	12.0	.09775	.13194	1.000	-.3390	.5345
11.0	1.0	.13565	.12415	.995	-.2753	.5466
	2.0	.35091	.12415	.178	-.0600	.7619
	3.0	.35469	.12415	.166	-.0563	.7656
	4.0	.42914*	.12221	.027	.0246	.8336
	5.0	.51536*	.12415	.003	.1044	.9263
	6.0	.40346	.12415	.060	-.0075	.8144
	7.0	.31642	.12045	.272	-.0823	.7151
	8.0	.34581	.12045	.160	-.0529	.7445
	9.0	.32857	.12045	.221	-.0701	.7273
	10.0	.10876	.12633	.999	-.3094	.5269
	12.0	.20651	.12633	.894	-.2116	.6246
12.0	1.0	-.07085	.12987	1.000	-.5007	.3590
	2.0	.14440	.12987	.994	-.2855	.5743
	3.0	.14818	.12987	.992	-.2817	.5780
	4.0	.22263	.12800	.848	-.2011	.6463
	5.0	.30885	.12987	.426	-.1210	.7387
	6.0	.19695	.12987	.934	-.2329	.6268
	7.0	.10991	.12633	.999	-.3082	.5281
	8.0	.13930	.12633	.994	-.2788	.5574
	9.0	.12206	.12633	.998	-.2961	.5402
	10.0	-.09775	.13194	1.000	-.5345	.3390
	11.0	-.20651	.12633	.894	-.6246	.2116

*. The mean difference is significant at the 0.05 level.

Station 28: Dunnett T3

(I) MON		Mean Difference (I-J)	Std. Error	Sig.	95% Confidence Interval	
					Lower Bound	Upper Bound
1.0	2.0	.09212	.15255	1.000	-.4735	.6577
	3.0	.23753	.13485	.979	-.2611	.7362
	4.0	.37514	.12175	.214	-.0777	.8280
	5.0	.35879	.12183	.282	-.0950	.8126
	6.0	.23195	.13315	.981	-.2605	.7244
	7.0	.06723	.13396	1.000	-.4258	.5603
	8.0	.15298	.12695	1.000	-.3161	.6221
	9.0	.13571	.13082	1.000	-.3464	.6178
	10.0	-.03226	.13756	1.000	-.5424	.4779
	11.0	.05473	.12540	1.000	-.4093	.5187
	12.0	-.10831	.16098	1.000	-.7103	.4937
2.0	1.0	-.09212	.15255	1.000	-.6577	.4735
	3.0	.14541	.14952	1.000	-.4100	.7008
	4.0	.28302	.13781	.880	-.2353	.8014
	5.0	.26667	.13789	.930	-.2524	.7857
	6.0	.13983	.14798	1.000	-.4104	.6901
	7.0	-.02488	.14871	1.000	-.5758	.5261
	8.0	.06086	.14243	1.000	-.4705	.5922
	9.0	.04359	.14589	1.000	-.4984	.5856
	10.0	-.12438	.15196	1.000	-.6892	.4404
	11.0	-.03739	.14105	1.000	-.5647	.4899
	12.0	-.20043	.17345	1.000	-.8446	.4437
3.0	1.0	-.23753	.13485	.979	-.7362	.2611
	2.0	-.14541	.14952	1.000	-.7008	.4100
	4.0	.13761	.11793	1.000	-.3000	.5752
	5.0	.12126	.11802	1.000	-.3173	.5599
	6.0	-.00558	.12966	1.000	-.4849	.4738
	7.0	-.17029	.13050	1.000	-.6502	.3096
	8.0	-.08455	.12329	1.000	-.5392	.3702
	9.0	-.10182	.12727	1.000	-.5702	.3666
	10.0	-.26979	.13419	.905	-.7677	.2281
	11.0	-.18280	.12170	.998	-.6321	.2665
	12.0	-.34584	.15811	.805	-.9388	.2471

Station 28: Dunnett T3

(I) MON		Mean Difference (I-J)	Std. Error	Sig.	95% Confidence Interval	
					Lower Bound	Upper Bound
4.0	1.0	-.37514	.12175	.214	-.8280	.0777
	2.0	-.28302	.13781	.880	-.8014	.2353
	3.0	-.13761	.11793	1.000	-.5752	.3000
	5.0	-.01635	.10278	1.000	-.3952	.3625
	6.0	-.14319	.11597	1.000	-.5730	.2866
	7.0	-.30790	.11690	.476	-.7378	.1220
	8.0	-.22215	.10880	.895	-.6212	.1769
	9.0	-.23942	.11329	.857	-.6555	.1766
	10.0	-.40740	.12101	.119	-.8597	.0449
	11.0	-.32041	.10699	.244	-.7127	.0719
	12.0	-.48345	.14709	.155	-1.0442	.0773
5.0	1.0	-.35879	.12183	.282	-.8126	.0950
	2.0	-.26667	.13789	.930	-.7857	.2524
	3.0	-.12126	.11802	1.000	-.5599	.3173
	4.0	.01635	.10278	1.000	-.3625	.3952
	6.0	-.12684	.11606	1.000	-.5577	.3040
	7.0	-.29155	.11700	.586	-.7226	.1395
	8.0	-.20580	.10890	.952	-.6061	.1945
	9.0	-.22307	.11338	.925	-.6403	.1941
	10.0	-.39105	.12110	.161	-.8443	.0622
	11.0	-.30406	.10709	.334	-.6977	.0895
	12.0	-.46710	.14716	.194	-1.0285	.0943
6.0	1.0	-.23195	.13315	.981	-.7244	.2605
	2.0	-.13983	.14798	1.000	-.6901	.4104
	3.0	.00558	.12966	1.000	-.4738	.4849
	4.0	.14319	.11597	1.000	-.2866	.5730
	5.0	.12684	.11606	1.000	-.3040	.5577
	7.0	-.16471	.12873	1.000	-.6379	.3085
	8.0	-.07897	.12142	1.000	-.5264	.3684
	9.0	-.09624	.12546	1.000	-.5577	.3653
	10.0	-.26421	.13247	.911	-.7560	.2275
	11.0	-.17722	.11980	.999	-.6191	.2647
	12.0	-.34026	.15665	.814	-.9287	.2482

Station 28: Dunnett T3

(I) MON		Mean Difference (I-J)	Std. Error	Sig.	95% Confidence Interval	
					Lower Bound	Upper Bound
7.0	1.0	-.06723	.13396	1.000	-.5603	.4258
	2.0	.02488	.14871	1.000	-.5261	.5758
	3.0	.17029	.13050	1.000	-.3096	.6502
	4.0	.30790	.11690	.476	-.1220	.7378
	5.0	.29155	.11700	.586	-.1395	.7226
	6.0	.16471	.12873	1.000	-.3085	.6379
	8.0	.08575	.12232	1.000	-.3620	.5335
	9.0	.06848	.12632	1.000	-.3935	.5305
	10.0	-.09950	.13329	1.000	-.5918	.3928
	11.0	-.01251	.12071	1.000	-.4547	.4297
	12.0	-.17555	.15735	1.000	-.7647	.4136
8.0	1.0	-.15298	.12695	1.000	-.6221	.3161
	2.0	-.06086	.14243	1.000	-.5922	.4705
	3.0	.08455	.12329	1.000	-.3702	.5392
	4.0	.22215	.10880	.895	-.1769	.6212
	5.0	.20580	.10890	.952	-.1945	.6061
	6.0	.07897	.12142	1.000	-.3684	.5264
	7.0	-.08575	.12232	1.000	-.5335	.3620
	9.0	-.01727	.11886	1.000	-.4521	.4175
	10.0	-.18524	.12624	.999	-.6537	.2832
	11.0	-.09826	.11288	1.000	-.5110	.3145
	12.0	-.26129	.15142	.980	-.8333	.3107
9.0	1.0	-.13571	.13082	1.000	-.6178	.3464
	2.0	-.04359	.14589	1.000	-.5856	.4984
	3.0	.10182	.12727	1.000	-.3666	.5702
	4.0	.23942	.11329	.857	-.1766	.6555
	5.0	.22307	.11338	.925	-.1941	.6403
	6.0	.09624	.12546	1.000	-.3653	.5577
	7.0	-.06848	.12632	1.000	-.5305	.3935
	8.0	.01727	.11886	1.000	-.4175	.4521
	10.0	-.16798	.13013	1.000	-.6494	.3134
	11.0	-.08099	.11721	1.000	-.5099	.3479
	12.0	-.24402	.15468	.995	-.8253	.3372

Station 28: Dunnett T3

(I) MON		Mean Difference (I-J)	Std. Error	Sig.	95% Confidence Interval	
					Lower Bound	Upper Bound
10.0	1.0	.03226	.13756	1.000	-.4779	.5424
	2.0	.12438	.15196	1.000	-.4404	.6892
	3.0	.26979	.13419	.905	-.2281	.7677
	4.0	.40740	.12101	.119	-.0449	.8597
	5.0	.39105	.12110	.161	-.0622	.8443
	6.0	.26421	.13247	.911	-.2275	.7560
	7.0	.09950	.13329	1.000	-.3928	.5918
	8.0	.18524	.12624	.999	-.2832	.6537
	9.0	.16798	.13013	1.000	-.3134	.6494
	11.0	.08699	.12469	1.000	-.3764	.5503
	12.0	-.07605	.16042	1.000	-.6773	.5252
11.0	1.0	-.05473	.12540	1.000	-.5187	.4093
	2.0	.03739	.14105	1.000	-.4899	.5647
	3.0	.18280	.12170	.998	-.2665	.6321
	4.0	.32041	.10699	.244	-.0719	.7127
	5.0	.30406	.10709	.334	-.0895	.6977
	6.0	.17722	.11980	.999	-.2647	.6191
	7.0	.01251	.12071	1.000	-.4297	.4547
	8.0	.09826	.11288	1.000	-.3145	.5110
	9.0	.08099	.11721	1.000	-.3479	.5099
	10.0	-.08699	.12469	1.000	-.5503	.3764
	12.0	-.16304	.15013	1.000	-.7315	.4054
12.0	1.0	.10831	.16098	1.000	-.4937	.7103
	2.0	.20043	.17345	1.000	-.4437	.8446
	3.0	.34584	.15811	.805	-.2471	.9388
	4.0	.48345	.14709	.155	-.0773	1.0442
	5.0	.46710	.14716	.194	-.0943	1.0285
	6.0	.34026	.15665	.814	-.2482	.9287
	7.0	.17555	.15735	1.000	-.4136	.7647
	8.0	.26129	.15142	.980	-.3107	.8333
	9.0	.24402	.15468	.995	-.3372	.8253
	10.0	.07605	.16042	1.000	-.5252	.6773
	11.0	.16304	.15013	1.000	-.4054	.7315

*. The mean difference is significant at the 0.05 level.

Appendix C By month ANOVA for Log-transformed Chl-a

Month	Anova F	Sig	Equal Variance
Jan	3.582	0.000	No
Feb	3.803	0.000	No
Mar	6.881	0.000	Yes
Apr	10.228	0.000	No
May	10.169	0.000	No
Jun	6.226	0.000	Yes
Jul	3.760	0.000	No
Aug	11.975	0.000	Yes
Sep	12.812	0.000	Yes
Oct	5.694	0.000	Yes
Nov	6.613	0.000	No
Dec	6.605	0.000	No

Appendix D Across Station Comparison of Log-transformed Chl-a

January: Dunnet T3

Station		Mean Difference (I-J)	Std. Error	Sig.	95% Confidence Interval	
					Lower Bound	Upper Bound
12.0	13.0	-.15592	.19891	1.000	-.8744	.5626
	14.0	-.33749	.18035	.936	-.9912	.3162
	15.0	-.25236	.17176	.997	-.8771	.3724
	16.0	-.31306	.15444	.856	-.8906	.2644
	17.0	.02885	.17424	1.000	-.6035	.6612
	18.0	.08677	.18116	1.000	-.5676	.7412
	25.0	-.33562	.15695	.793	-.9197	.2484
	26.0	-.25390	.15924	.988	-.8440	.3362
	27.0	-.02520	.16392	1.000	-.6283	.5779
	28.0	.26299	.17062	.994	-.3603	.8863
13.0	12.0	.15592	.19891	1.000	-.5626	.8744
	14.0	-.18158	.18158	1.000	-.8400	.4769
	15.0	-.09644	.17305	1.000	-.7262	.5333
	16.0	-.15714	.15587	1.000	-.7404	.4261
	17.0	.18477	.17551	1.000	-.4525	.8221
	18.0	.24269	.18238	1.000	-.4164	.9018
	25.0	-.17971	.15836	1.000	-.7694	.4100
	26.0	-.09798	.16063	1.000	-.6936	.4977
	27.0	.13071	.16526	1.000	-.4778	.7392
	28.0	.41891	.17192	.579	-.2095	1.0473
14.0	12.0	.33749	.18035	.936	-.3162	.9912
	13.0	.18158	.18158	1.000	-.4769	.8400
	15.0	.08514	.15135	1.000	-.4604	.6307
	16.0	.02444	.13136	1.000	-.4603	.5092
	17.0	.36634	.15416	.625	-.1887	.9214
	18.0	.42427	.16194	.436	-.1579	1.0064
	25.0	.00187	.13431	1.000	-.4917	.4954
	26.0	.08360	.13698	1.000	-.4179	.5851
	27.0	.31229	.14239	.761	-.2062	.8308
	28.0	.60048*	.15006	.019	.0563	1.1447

January: Dunnet T3

Station		Mean Difference (I-J)	Std. Error	Sig.	95% Confidence Interval	
					Lower Bound	Upper Bound
15.0	12.0	.25236	.17176	.997	-.3724	.8771
	13.0	.09644	.17305	1.000	-.5333	.7262
	14.0	-.08514	.15135	1.000	-.6307	.4604
	16.0	-.06070	.11929	1.000	-.4934	.3720
	17.0	.28121	.14401	.908	-.2341	.7965
	18.0	.33913	.15231	.741	-.2067	.8849
	25.0	-.08327	.12252	1.000	-.5267	.3602
	26.0	-.00154	.12545	1.000	-.4546	.4515
	27.0	.22715	.13133	.974	-.2461	.7005
	28.0	.51534*	.13961	.040	.0122	1.0185
16.0	12.0	.31306	.15444	.856	-.2644	.8906
	13.0	.15714	.15587	1.000	-.4261	.7404
	14.0	-.02444	.13136	1.000	-.5092	.4603
	15.0	.06070	.11929	1.000	-.3720	.4934
	17.0	.34191	.12283	.332	-.1045	.7883
	18.0	.39983	.13247	.213	-.0842	.8838
	25.0	-.02256	.09676	1.000	-.3734	.3283
	26.0	.05916	.10043	1.000	-.3057	.4240
	27.0	.28785	.10769	.406	-.1051	.6809
	28.0	.57605*	.11764	.002	.1435	1.0086
17.0	12.0	-.02885	.17424	1.000	-.6612	.6035
	13.0	-.18477	.17551	1.000	-.8221	.4525
	14.0	-.36634	.15416	.625	-.9214	.1887
	15.0	-.28121	.14401	.908	-.7965	.2341
	16.0	-.34191	.12283	.332	-.7883	.1045
	18.0	.05792	.15510	1.000	-.4975	.6133
	25.0	-.36447	.12598	.268	-.8211	.0922
	26.0	-.28275	.12882	.762	-.7486	.1831
	27.0	-.05405	.13456	1.000	-.5392	.4311
	28.0	.23414	.14265	.987	-.2798	.7481

January: Dunnet T3

Station		Mean Difference (I-J)	Std. Error	Sig.	95% Confidence Interval	
					Lower Bound	Upper Bound
18.0	12.0	-.08677	.18116	1.000	-.7412	.5676
	13.0	-.24269	.18238	1.000	-.9018	.4164
	14.0	-.42427	.16194	.436	-1.0064	.1579
	15.0	-.33913	.15231	.741	-.8849	.2067
	16.0	-.39983	.13247	.213	-.8838	.0842
	17.0	-.05792	.15510	1.000	-.6133	.4975
	25.0	-.42240	.13539	.170	-.9153	.0706
	26.0	-.34067	.13804	.554	-.8418	.1604
	27.0	-.11198	.14341	1.000	-.6303	.4064
	28.0	.17622	.15103	1.000	-.3681	.7206
25.0	12.0	.33562	.15695	.793	-.2484	.9197
	13.0	.17971	.15836	1.000	-.4100	.7694
	14.0	-.00187	.13431	1.000	-.4954	.4917
	15.0	.08327	.12252	1.000	-.3602	.5267
	16.0	.02256	.09676	1.000	-.3283	.3734
	17.0	.36447	.12598	.268	-.0922	.8211
	18.0	.42240	.13539	.170	-.0706	.9153
	26.0	.08173	.10425	1.000	-.2971	.4606
	27.0	.31042	.11126	.330	-.0950	.7158
	28.0	.59861*	.12092	.002	.1556	1.0416
26.0	12.0	.25390	.15924	.988	-.3362	.8440
	13.0	.09798	.16063	1.000	-.4977	.6936
	14.0	-.08360	.13698	1.000	-.5851	.4179
	15.0	.00154	.12545	1.000	-.4515	.4546
	16.0	-.05916	.10043	1.000	-.4240	.3057
	17.0	.28275	.12882	.762	-.1831	.7486
	18.0	.34067	.13804	.554	-.1604	.8418
	25.0	-.08173	.10425	1.000	-.4606	.2971
	27.0	.22869	.11447	.881	-.1876	.6450
	28.0	.51689*	.12388	.013	.0644	.9694

January: Dunnet T3

Station		Mean Difference (I-J)	Std. Error	Sig.	95% Confidence Interval	
					Lower Bound	Upper Bound
27.0	12.0	.02520	.16392	1.000	-.5779	.6283
	13.0	-.13071	.16526	1.000	-.7392	.4778
	14.0	-.31229	.14239	.761	-.8308	.2062
	15.0	-.22715	.13133	.974	-.7005	.2461
	16.0	-.28785	.10769	.406	-.6809	.1051
	17.0	.05405	.13456	1.000	-.4311	.5392
	18.0	.11198	.14341	1.000	-.4064	.6303
	25.0	-.31042	.11126	.330	-.7158	.0950
	26.0	-.22869	.11447	.881	-.6450	.1876
	28.0	.28819	.12984	.743	-.1842	.7606
28.0	12.0	-.26299	.17062	.994	-.8863	.3603
	13.0	-.41891	.17192	.579	-1.0473	.2095
	14.0	-.60048*	.15006	.019	-1.1447	-.0563
	15.0	-.51534*	.13961	.040	-1.0185	-.0122
	16.0	-.57605*	.11764	.002	-1.0086	-.1435
	17.0	-.23414	.14265	.987	-.7481	.2798
	18.0	-.17622	.15103	1.000	-.7206	.3681
	25.0	-.59861*	.12092	.002	-1.0416	-.1556
	26.0	-.51689*	.12388	.013	-.9694	-.0644
	27.0	-.28819	.12984	.743	-.7606	.1842

*. The mean difference is significant at the 0.05 level.

February: Dunnet T3

Station		Mean Difference (I-J)	Std. Error	Sig.	95% Confidence Interval	
					Lower Bound	Upper Bound
12.0	13.0	-.09096	.18593	1.000	-.7626	.5806
	14.0	-.20513	.17092	1.000	-.8243	.4140
	15.0	-.04005	.18239	1.000	-.6961	.6160
	16.0	-.26394	.14974	.961	-.8184	.2905
	17.0	.21182	.17514	1.000	-.4194	.8430
	18.0	.19568	.17528	1.000	-.4360	.8273
	25.0	-.25904	.14181	.939	-.7941	.2760
	26.0	-.11999	.15619	1.000	-.6931	.4531
	27.0	.21240	.17042	1.000	-.4062	.8310
	28.0	.37746	.17604	.796	-.2606	1.0155
13.0	12.0	.09096	.18593	1.000	-.5806	.7626
	14.0	-.11417	.17101	1.000	-.7337	.5053
	15.0	.05091	.18247	1.000	-.6054	.7072
	16.0	-.17298	.14984	1.000	-.7278	.3818
	17.0	.30277	.17523	.975	-.3288	.9343
	18.0	.28663	.17537	.988	-.3454	.9186
	25.0	-.16808	.14191	1.000	-.7036	.3674
	26.0	-.02903	.15629	1.000	-.6025	.5444
	27.0	.30336	.17051	.962	-.3156	.9223
	28.0	.46842	.17613	.412	-.1699	1.1067
14.0	12.0	.20513	.17092	1.000	-.4140	.8243
	13.0	.11417	.17101	1.000	-.5053	.7337
	15.0	.16508	.16715	1.000	-.4360	.7662
	16.0	-.05881	.13075	1.000	-.5375	.4199
	17.0	.41694	.15922	.437	-.1553	.9892
	18.0	.40080	.15937	.515	-.1720	.9736
	25.0	-.05391	.12159	1.000	-.5076	.3998
	26.0	.08514	.13809	1.000	-.4172	.5875
	27.0	.41753	.15400	.376	-.1403	.9754
	28.0	.58259*	.16020	.049	.0018	1.1634

February: Dunnet T3

Station		Mean Difference (I-J)	Std. Error	Sig.	95% Confidence Interval	
					Lower Bound	Upper Bound
15.0	12.0	.04005	.18239	1.000	-.6160	.6961
	13.0	-.05091	.18247	1.000	-.7072	.6054
	14.0	-.16508	.16715	1.000	-.7662	.4360
	16.0	-.22389	.14542	.994	-.7553	.3075
	17.0	.25186	.17147	.998	-.3620	.8657
	18.0	.23572	.17161	.999	-.3786	.8501
	25.0	-.21899	.13724	.988	-.7288	.2908
	26.0	-.07994	.15205	1.000	-.6317	.4718
	27.0	.25245	.16664	.996	-.3481	.8530
	28.0	.41751	.17238	.589	-.2036	1.0386
16.0	12.0	.26394	.14974	.961	-.2905	.8184
	13.0	.17298	.14984	1.000	-.3818	.7278
	14.0	.05881	.13075	1.000	-.4199	.5375
	15.0	.22389	.14542	.994	-.3075	.7553
	17.0	.47575	.13622	.071	-.0197	.9712
	18.0	.45961	.13640	.096	-.0366	.9558
	25.0	.00490	.08938	1.000	-.3207	.3305
	26.0	.14395	.11079	1.000	-.2587	.5466
	27.0	.47634	.13009	.052	-.0023	.9550
	28.0	.64140*	.13737	.005	.1334	1.1494
17.0	12.0	-.21182	.17514	1.000	-.8430	.4194
	13.0	-.30277	.17523	.975	-.9343	.3288
	14.0	-.41694	.15922	.437	-.9892	.1553
	15.0	-.25186	.17147	.998	-.8657	.3620
	16.0	-.47575	.13622	.071	-.9712	.0197
	18.0	-.01614	.16389	1.000	-.6025	.5702
	25.0	-.47085	.12745	.050	-.9421	.0004
	26.0	-.33180	.14328	.672	-.8500	.1864
	27.0	.00059	.15867	1.000	-.5711	.5723
	28.0	.16564	.16470	1.000	-.4282	.7595

February: Dunnet T3

Station		Mean Difference (I-J)	Std. Error	Sig.	95% Confidence Interval	
					Lower Bound	Upper Bound
18.0	12.0	-.19568	.17528	1.000	-.8273	.4360
	13.0	-.28663	.17537	.988	-.9186	.3454
	14.0	-.40080	.15937	.515	-.9736	.1720
	15.0	-.23572	.17161	.999	-.8501	.3786
	16.0	-.45961	.13640	.096	-.9558	.0366
	17.0	.01614	.16389	1.000	-.5702	.6025
	25.0	-.45471	.12764	.069	-.9267	.0173
	26.0	-.31566	.14345	.758	-.8345	.2032
	27.0	.01673	.15883	1.000	-.5555	.5890
	28.0	.18178	.16485	1.000	-.4126	.7762
25.0	12.0	.25904	.14181	.939	-.2760	.7941
	13.0	.16808	.14191	1.000	-.3674	.7036
	14.0	.05391	.12159	1.000	-.3998	.5076
	15.0	.21899	.13724	.988	-.2908	.7288
	16.0	-.00490	.08938	1.000	-.3305	.3207
	17.0	.47085	.12745	.050	-.0004	.9421
	18.0	.45471	.12764	.069	-.0173	.9267
	26.0	.13905	.09982	.999	-.2297	.5078
	27.0	.47144*	.12088	.036	.0173	.9256
	28.0	.63650*	.12868	.003	.1506	1.1224
26.0	12.0	.11999	.15619	1.000	-.4531	.6931
	13.0	.02903	.15629	1.000	-.5444	.6025
	14.0	-.08514	.13809	1.000	-.5875	.4172
	15.0	.07994	.15205	1.000	-.4718	.6317
	16.0	-.14395	.11079	1.000	-.5466	.2587
	17.0	.33180	.14328	.672	-.1864	.8500
	18.0	.31566	.14345	.758	-.2032	.8345
	25.0	-.13905	.09982	.999	-.5078	.2297
	27.0	.33239	.13747	.593	-.1697	.8345
	28.0	.49745	.14438	.085	-.0318	1.0267

February: Dunnet T3

Station		Mean Difference (I-J)	Std. Error	Sig.	95% Confidence Interval	
					Lower Bound	Upper Bound
27.0	12.0	-.21240	.17042	1.000	-.8310	.4062
	13.0	-.30336	.17051	.962	-.9223	.3156
	14.0	-.41753	.15400	.376	-.9754	.1403
	15.0	-.25245	.16664	.996	-.8530	.3481
	16.0	-.47634	.13009	.052	-.9550	.0023
	17.0	-.00059	.15867	1.000	-.5723	.5711
	18.0	-.01673	.15883	1.000	-.5890	.5555
	25.0	-.47144*	.12088	.036	-.9256	-.0173
	26.0	-.33239	.13747	.593	-.8345	.1697
	28.0	.16506	.15967	1.000	-.4153	.7454
28.0	12.0	-.37746	.17604	.796	-1.0155	.2606
	13.0	-.46842	.17613	.412	-1.1067	.1699
	14.0	-.58259*	.16020	.049	-1.1634	-.0018
	15.0	-.41751	.17238	.589	-1.0386	.2036
	16.0	-.64140*	.13737	.005	-1.1494	-.1334
	17.0	-.16564	.16470	1.000	-.7595	.4282
	18.0	-.18178	.16485	1.000	-.7762	.4126
	25.0	-.63650*	.12868	.003	-1.1224	-.1506
	26.0	-.49745	.14438	.085	-1.0267	.0318
	27.0	-.16506	.15967	1.000	-.7454	.4153

*. The mean difference is significant at the 0.05 level.

March: Tukey HSD

Station		Mean Difference (I-J)	Std. Error	Sig.	95% Confidence Interval	
					Lower Bound	Upper Bound
12.0	13.0	-.01639	.12501	1.000	-.4239	.3911
	14.0	-.16035	.12683	.974	-.5738	.2531
	15.0	-.00778	.12184	1.000	-.4049	.3894
	16.0	-.37458	.12501	.103	-.7821	.0329
	17.0	.15389	.12184	.974	-.2433	.5511
	18.0	.19935	.12184	.865	-.1978	.5965
	25.0	-.21755	.12886	.840	-.6376	.2025
	26.0	-.09652	.12886	1.000	-.5166	.3235
	27.0	.19281	.12886	.919	-.2272	.6128
	28.0	.49949*	.12886	.007	.0795	.9195
13.0	12.0	.01639	.12501	1.000	-.3911	.4239
	14.0	-.14395	.12683	.988	-.5574	.2695
	15.0	.00862	.12184	1.000	-.3886	.4058
	16.0	-.35819	.12501	.143	-.7657	.0493
	17.0	.17028	.12184	.948	-.2269	.5675
	18.0	.21574	.12184	.796	-.1814	.6129
	25.0	-.20116	.12886	.896	-.6212	.2189
	26.0	-.08013	.12886	1.000	-.5002	.3399
	27.0	.20920	.12886	.870	-.2108	.6292
	28.0	.51589*	.12886	.004	.0959	.9359
14.0	12.0	.16035	.12683	.974	-.2531	.5738
	13.0	.14395	.12683	.988	-.2695	.5574
	15.0	.15257	.12372	.978	-.2507	.5558
	16.0	-.21424	.12683	.839	-.6277	.1992
	17.0	.31424	.12372	.289	-.0890	.7175
	18.0	.35969	.12372	.129	-.0436	.7630
	25.0	-.05721	.13063	1.000	-.4830	.3686
	26.0	.06383	.13063	1.000	-.3620	.4896
	27.0	.35316	.13063	.207	-.0726	.7790
	28.0	.65984*	.13063	.000	.2340	1.0856

March: Tukey HSD

Station		Mean Difference (I-J)	Std. Error	Sig.	95% Confidence Interval	
					Lower Bound	Upper Bound
15.0	12.0	.00778	.12184	1.000	-.3894	.4049
	13.0	-.00862	.12184	1.000	-.4058	.3886
	14.0	-.15257	.12372	.978	-.5558	.2507
	16.0	-.36681	.12184	.099	-.7640	.0304
	17.0	.16167	.11859	.956	-.2249	.5482
	18.0	.20712	.11859	.809	-.1795	.5937
	25.0	-.20978	.12579	.850	-.6198	.2003
	26.0	-.08874	.12579	1.000	-.4988	.3213
	27.0	.20059	.12579	.883	-.2094	.6106
	28.0	.50727*	.12579	.004	.0972	.9173
16.0	12.0	.37458	.12501	.103	-.0329	.7821
	13.0	.35819	.12501	.143	-.0493	.7657
	14.0	.21424	.12683	.839	-.1992	.6277
	15.0	.36681	.12184	.099	-.0304	.7640
	17.0	.52847*	.12184	.001	.1313	.9256
	18.0	.57393*	.12184	.000	.1768	.9711
	25.0	.15703	.12886	.980	-.2630	.5771
	26.0	.27806	.12886	.538	-.1420	.6981
	27.0	.56739*	.12886	.001	.1474	.9874
	28.0	.87408*	.12886	.000	.4540	1.2941
17.0	12.0	-.15389	.12184	.974	-.5511	.2433
	13.0	-.17028	.12184	.948	-.5675	.2269
	14.0	-.31424	.12372	.289	-.7175	.0890
	15.0	-.16167	.11859	.956	-.5482	.2249
	16.0	-.52847*	.12184	.001	-.9256	-.1313
	18.0	.04545	.11859	1.000	-.3411	.4320
	25.0	-.37145	.12579	.115	-.7815	.0386
	26.0	-.25041	.12579	.656	-.6604	.1596
	27.0	.03892	.12579	1.000	-.3711	.4489
	28.0	.34560	.12579	.187	-.0644	.7556

March: Tukey HSD

Station		Mean Difference (I-J)	Std. Error	Sig.	95% Confidence Interval	
					Lower Bound	Upper Bound
18.0	12.0	-.19935	.12184	.865	-.5965	.1978
	13.0	-.21574	.12184	.796	-.6129	.1814
	14.0	-.35969	.12372	.129	-.7630	.0436
	15.0	-.20712	.11859	.809	-.5937	.1795
	16.0	-.57393*	.12184	.000	-.9711	-.1768
	17.0	-.04545	.11859	1.000	-.4320	.3411
	25.0	-.41690*	.12579	.043	-.8269	-.0069
	26.0	-.29587	.12579	.404	-.7059	.1142
	27.0	-.00654	.12579	1.000	-.4166	.4035
	28.0	.30015	.12579	.381	-.1099	.7102
25.0	12.0	.21755	.12886	.840	-.2025	.6376
	13.0	.20116	.12886	.896	-.2189	.6212
	14.0	.05721	.13063	1.000	-.3686	.4830
	15.0	.20978	.12579	.850	-.2003	.6198
	16.0	-.15703	.12886	.980	-.5771	.2630
	17.0	.37145	.12579	.115	-.0386	.7815
	18.0	.41690*	.12579	.043	.0069	.8269
	26.0	.12103	.13259	.998	-.3112	.5532
	27.0	.41036	.13259	.079	-.0218	.8426
	28.0	.71705*	.13259	.000	.2848	1.1493
26.0	12.0	.09652	.12886	1.000	-.3235	.5166
	13.0	.08013	.12886	1.000	-.3399	.5002
	14.0	-.06383	.13063	1.000	-.4896	.3620
	15.0	.08874	.12579	1.000	-.3213	.4988
	16.0	-.27806	.12886	.538	-.6981	.1420
	17.0	.25041	.12579	.656	-.1596	.6604
	18.0	.29587	.12579	.404	-.1142	.7059
	25.0	-.12103	.13259	.998	-.5532	.3112
	27.0	.28933	.13259	.520	-.1429	.7215
	28.0	.59602*	.13259	.001	.1638	1.0282

March: Tukey HSD

Station		Mean Difference (I-J)	Std. Error	Sig.	95% Confidence Interval	
					Lower Bound	Upper Bound
27.0	12.0	-.19281	.12886	.919	-.6128	.2272
	13.0	-.20920	.12886	.870	-.6292	.2108
	14.0	-.35316	.13063	.207	-.7790	.0726
	15.0	-.20059	.12579	.883	-.6106	.2094
	16.0	-.56739*	.12886	.001	-.9874	-.1474
	17.0	-.03892	.12579	1.000	-.4489	.3711
	18.0	.00654	.12579	1.000	-.4035	.4166
	25.0	-.41036	.13259	.079	-.8426	.0218
	26.0	-.28933	.13259	.520	-.7215	.1429
	28.0	.30668	.13259	.430	-.1255	.7389
28.0	12.0	-.49949*	.12886	.007	-.9195	-.0795
	13.0	-.51589*	.12886	.004	-.9359	-.0959
	14.0	-.65984*	.13063	.000	-1.0856	-.2340
	15.0	-.50727*	.12579	.004	-.9173	-.0972
	16.0	-.87408*	.12886	.000	-1.2941	-.4540
	17.0	-.34560	.12579	.187	-.7556	.0644
	18.0	-.30015	.12579	.381	-.7102	.1099
	25.0	-.71705*	.13259	.000	-1.1493	-.2848
	26.0	-.59602*	.13259	.001	-1.0282	-.1638
	27.0	-.30668	.13259	.430	-.7389	.1255

*. The mean difference is significant at the 0.05 level.

April: Dunnet T3

Station		Mean Difference (I-J)	Std. Error	Sig.	95% Confidence Interval	
					Lower Bound	Upper Bound
12.0	13.0	.09979	.14034	1.000	-.4209	.6204
	14.0	-.06044	.15209	1.000	-.6138	.4929
	15.0	.06096	.14978	1.000	-.4848	.6067
	16.0	-.41527	.14261	.270	-.9417	.1111
	17.0	.10863	.15512	1.000	-.4529	.6702
	18.0	.25117	.15159	.984	-.2999	.8022
	25.0	-.30488	.14597	.827	-.8409	.2311
	26.0	-.13332	.15029	1.000	-.6818	.4151
	27.0	.20889	.15461	.999	-.3527	.7705
	28.0	.57874*	.14615	.024	.0423	1.1152
13.0	12.0	-.09979	.14034	1.000	-.6204	.4209
	14.0	-.16023	.10321	.994	-.5339	.2134
	15.0	-.03883	.09977	1.000	-.3967	.3190
	16.0	-.51506*	.08865	.000	-.8324	-.1977
	17.0	.00885	.10762	1.000	-.3789	.3966
	18.0	.15138	.10247	.998	-.2167	.5195
	25.0	-.40467*	.09396	.008	-.7439	-.0654
	26.0	-.23311	.10054	.670	-.5979	.1317
	27.0	.10911	.10688	1.000	-.2807	.4989
	28.0	.47895*	.09423	.001	.1386	.8193
14.0	12.0	.06044	.15209	1.000	-.4929	.6138
	13.0	.16023	.10321	.994	-.2134	.5339
	15.0	.12140	.11572	1.000	-.2930	.5358
	16.0	-.35482	.10628	.098	-.7382	.0286
	17.0	.16908	.12255	.999	-.2694	.6075
	18.0	.31161	.11806	.419	-.1109	.7341
	25.0	-.24444	.11074	.754	-.6439	.1550
	26.0	-.07287	.11638	1.000	-.4922	.3464
	27.0	.26934	.12190	.752	-.1701	.7088
	28.0	.63919*	.11098	.000	.2389	1.0394

April: Dunnet T3

Station		Mean Difference (I-J)	Std. Error	Sig.	95% Confidence Interval	
					Lower Bound	Upper Bound
15.0	12.0	-.06096	.14978	1.000	-.6067	.4848
	13.0	.03883	.09977	1.000	-.3190	.3967
	14.0	-.12140	.11572	1.000	-.5358	.2930
	16.0	-.47622*	.10295	.003	-.8446	-.1079
	17.0	.04768	.11967	1.000	-.3792	.4745
	18.0	.19021	.11506	.987	-.2199	.6003
	25.0	-.36584	.10755	.080	-.7515	.0198
	26.0	-.19427	.11334	.978	-.6010	.2125
	27.0	.14794	.11901	1.000	-.2800	.5759
	28.0	.51779*	.10779	.002	.1313	.9043
16.0	12.0	.41527	.14261	.270	-.1111	.9417
	13.0	.51506*	.08865	.000	.1977	.8324
	14.0	.35482	.10628	.098	-.0286	.7382
	15.0	.47622*	.10295	.003	.1079	.8446
	17.0	.52390*	.11057	.002	.1268	.9210
	18.0	.66644*	.10557	.000	.2883	1.0446
	25.0	.11039	.09732	1.000	-.2401	.4609
	26.0	.28195	.10369	.370	-.0929	.6568
	27.0	.62416*	.10985	.000	.2253	1.0230
	28.0	.99401*	.09759	.000	.6425	1.3455
17.0	12.0	-.10863	.15512	1.000	-.6702	.4529
	13.0	-.00885	.10762	1.000	-.3966	.3789
	14.0	-.16908	.12255	.999	-.6075	.2694
	15.0	-.04768	.11967	1.000	-.4745	.3792
	16.0	-.52390*	.11057	.002	-.9210	-.1268
	18.0	.14254	.12193	1.000	-.2921	.5772
	25.0	-.41351*	.11487	.049	-.8259	-.0011
	26.0	-.24195	.12031	.879	-.6734	.1895
	27.0	.10026	.12566	1.000	-.3505	.5510
	28.0	.47011*	.11509	.013	.0570	.8832

April: Dunnet T3

Station		Mean Difference (I-J)	Std. Error	Sig.	95% Confidence Interval	
					Lower Bound	Upper Bound
18.0	12.0	-.25117	.15159	.984	-.8022	.2999
	13.0	-.15138	.10247	.998	-.5195	.2167
	14.0	-.31161	.11806	.419	-.7341	.1109
	15.0	-.19021	.11506	.987	-.6003	.2199
	16.0	-.66644*	.10557	.000	-1.0446	-.2883
	17.0	-.14254	.12193	1.000	-.5772	.2921
	25.0	-.55605*	.11006	.001	-.9508	-.1613
	26.0	-.38449	.11573	.098	-.7996	.0306
	27.0	-.04228	.12128	1.000	-.4779	.3934
	28.0	.32757	.11029	.221	-.0680	.7231
25.0	12.0	.30488	.14597	.827	-.2311	.8409
	13.0	.40467*	.09396	.008	.0654	.7439
	14.0	.24444	.11074	.754	-.1550	.6439
	15.0	.36584	.10755	.080	-.0198	.7515
	16.0	-.11039	.09732	1.000	-.4609	.2401
	17.0	.41351*	.11487	.049	.0011	.8259
	18.0	.55605*	.11006	.001	.1613	.9508
	26.0	.17156	.10826	.992	-.2199	.5630
	27.0	.51378*	.11418	.005	.1000	.9276
	28.0	.88362*	.10243	.000	.5136	1.2536
26.0	12.0	.13332	.15029	1.000	-.4151	.6818
	13.0	.23311	.10054	.670	-.1317	.5979
	14.0	.07287	.11638	1.000	-.3464	.4922
	15.0	.19427	.11334	.978	-.2125	.6010
	16.0	-.28195	.10369	.370	-.6568	.0929
	17.0	.24195	.12031	.879	-.1895	.6734
	18.0	.38449	.11573	.098	-.0306	.7996
	25.0	-.17156	.10826	.992	-.5630	.2199
	27.0	.34221	.11965	.284	-.0903	.7747
	28.0	.71206*	.10850	.000	.3198	1.1043

April: Dunnet T3

Station		Mean Difference (I-J)	Std. Error	Sig.	95% Confidence Interval	
					Lower Bound	Upper Bound
27.0	12.0	-.20889	.15461	.999	-.7705	.3527
	13.0	-.10911	.10688	1.000	-.4989	.2807
	14.0	-.26934	.12190	.752	-.7088	.1701
	15.0	-.14794	.11901	1.000	-.5759	.2800
	16.0	-.62416*	.10985	.000	-1.0230	-.2253
	17.0	-.10026	.12566	1.000	-.5510	.3505
	18.0	.04228	.12128	1.000	-.3934	.4779
	25.0	-.51378*	.11418	.005	-.9276	-.1000
	26.0	-.34221	.11965	.284	-.7747	.0903
	28.0	.36985	.11440	.129	-.0447	.7844
28.0	12.0	-.57874*	.14615	.024	-1.1152	-.0423
	13.0	-.47895*	.09423	.001	-.8193	-.1386
	14.0	-.63919*	.11098	.000	-1.0394	-.2389
	15.0	-.51779*	.10779	.002	-.9043	-.1313
	16.0	-.99401*	.09759	.000	-1.3455	-.6425
	17.0	-.47011*	.11509	.013	-.8832	-.0570
	18.0	-.32757	.11029	.221	-.7231	.0680
	25.0	-.88362*	.10243	.000	-1.2536	-.5136
	26.0	-.71206*	.10850	.000	-1.1043	-.3198
	27.0	-.36985	.11440	.129	-.7844	.0447

*. The mean difference is significant at the 0.05 level.

May: Dunnet T3

Station		Mean Difference (I-J)	Std. Error	Sig.	95% Confidence Interval	
					Lower Bound	Upper Bound
12	13	-.08852	.14376	1.000	-.6137	.4367
	14	-.20030	.16167	1.000	-.7824	.3818
	15	-.07373	.14626	1.000	-.6058	.4584
	16	-.50810*	.13550	.046	-1.0110	-.0052
	17	.01072	.13919	1.000	-.5015	.5229
	18	.05803	.13983	1.000	-.4559	.5720
	25	-.30500	.13410	.700	-.8047	.1947
	26	-.26946	.14003	.911	-.7848	.2459
	27	.20510	.15128	.999	-.3442	.7544
	28	.47238	.14245	.114	-.0498	.9946
13	12	.08852	.14376	1.000	-.4367	.6137
	14	-.11177	.12963	1.000	-.5817	.3581
	15	.01480	.10982	1.000	-.3790	.4086
	16	-.41958*	.09502	.006	-.7629	-.0763
	17	.09924	.10021	1.000	-.2608	.4593
	18	.14655	.10110	.998	-.2165	.5096
	25	-.21647	.09301	.663	-.5542	.1212
	26	-.18093	.10138	.962	-.5472	.1853
	27	.29362	.11642	.512	-.1287	.7160
	28	.56090*	.10469	.000	.1827	.9391
14	12	.20030	.16167	1.000	-.3818	.7824
	13	.11177	.12963	1.000	-.3581	.5817
	15	.12657	.13240	1.000	-.3515	.6047
	16	-.30781	.12041	.491	-.7506	.1350
	17	.21101	.12454	.978	-.2432	.6652
	18	.25832	.12526	.845	-.1979	.7146
	25	-.10470	.11882	1.000	-.5437	.3343
	26	-.06916	.12548	1.000	-.5272	.3889
	27	.40539	.13792	.242	-.0933	.9041
	28	.67267*	.12818	.001	.2063	1.1391

May: Dunnet T3

Station		Mean Difference (I-J)	Std. Error	Sig.	95% Confidence Interval	
					Lower Bound	Upper Bound
15	12	.07373	.14626	1.000	-.4584	.6058
	13	-.01480	.10982	1.000	-.4086	.3790
	14	-.12657	.13240	1.000	-.6047	.3515
	16	-.43438*	.09876	.006	-.7907	-.0780
	17	.08444	.10377	1.000	-.2878	.4567
	18	.13175	.10463	1.000	-.2434	.5069
	25	-.23127	.09683	.616	-.5823	.1197
	26	-.19573	.10489	.939	-.5738	.1823
	27	.27882	.11950	.659	-.1531	.7107
	28	.54610*	.10810	.001	.1566	.9356
16	12	.50810*	.13550	.046	.0052	1.0110
	13	.41958*	.09502	.006	.0763	.7629
	14	.30781	.12041	.491	-.1350	.7506
	15	.43438*	.09876	.006	.0780	.7907
	17	.51882*	.08795	.000	.2032	.8344
	18	.56613*	.08896	.000	.2468	.8855
	25	.20311	.07964	.490	-.0846	.4908
	26	.23865	.08927	.402	-.0851	.5624
	27	.71320*	.10605	.000	.3230	1.1034
	28	.98048*	.09303	.000	.6421	1.3189
17	12	-.01072	.13919	1.000	-.5229	.5015
	13	-.09924	.10021	1.000	-.4593	.2608
	14	-.21101	.12454	.978	-.6652	.2432
	15	-.08444	.10377	1.000	-.4567	.2878
	16	-.51882*	.08795	.000	-.8344	-.2032
	18	.04731	.09449	1.000	-.2908	.3854
	25	-.31571*	.08577	.041	-.6250	-.0065
	26	-.28017	.09478	.232	-.6220	.0617
	27	.19438	.11073	.967	-.2093	.5981
	28	.46166*	.09832	.003	.1064	.8169

May: Dunnet T3

Station		Mean Difference (I-J)	Std. Error	Sig.	95% Confidence Interval	
					Lower Bound	Upper Bound
18	12	-.05803	.13983	1.000	-.5720	.4559
	13	-.14655	.10110	.998	-.5096	.2165
	14	-.25832	.12526	.845	-.7146	.1979
	15	-.13175	.10463	1.000	-.5069	.2434
	16	-.56613*	.08896	.000	-.8855	-.2468
	17	-.04731	.09449	1.000	-.3854	.2908
	25	-.36302*	.08681	.011	-.6761	-.0499
	26	-.32748	.09572	.080	-.6726	.0176
	27	.14707	.11153	1.000	-.2591	.5532
	28	.41435*	.09923	.011	.0560	.7727
25	12	.30500	.13410	.700	-.1947	.8047
	13	.21647	.09301	.663	-.1212	.5542
	14	.10470	.11882	1.000	-.3343	.5437
	15	.23127	.09683	.616	-.1197	.5823
	16	-.20311	.07964	.490	-.4908	.0846
	17	.31571*	.08577	.041	.0065	.6250
	18	.36302*	.08681	.011	.0499	.6761
	26	.03554	.08713	1.000	-.2823	.3534
	27	.51009*	.10425	.003	.1244	.8958
	28	.77737*	.09097	.000	.4446	1.1102
26	12	.26946	.14003	.911	-.2459	.7848
	13	.18093	.10138	.962	-.1853	.5472
	14	.06916	.12548	1.000	-.3889	.5272
	15	.19573	.10489	.939	-.1823	.5738
	16	-.23865	.08927	.402	-.5624	.0851
	17	.28017	.09478	.232	-.0617	.6220
	18	.32748	.09572	.080	-.0176	.6726
	25	-.03554	.08713	1.000	-.3534	.2823
	27	.47455*	.11178	.011	.0660	.8832
	28	.74183*	.09951	.000	.3802	1.1035

May: Dunnet T3

Station		Mean Difference (I-J)	Std. Error	Sig.	95% Confidence Interval	
					Lower Bound	Upper Bound
27	12	-.20510	.15128	.999	-.7544	.3442
	13	-.29362	.11642	.512	-.7160	.1287
	14	-.40539	.13792	.242	-.9041	.0933
	15	-.27882	.11950	.659	-.7107	.1531
	16	-.71320*	.10605	.000	-1.1034	-.3230
	17	-.19438	.11073	.967	-.5981	.2093
	18	-.14707	.11153	1.000	-.5532	.2591
	25	-.51009*	.10425	.003	-.8958	-.1244
	26	-.47455*	.11178	.011	-.8832	-.0660
	28	.26728	.11480	.662	-.1512	.6858
28	12	-.47238	.14245	.114	-.9946	.0498
	13	-.56090*	.10469	.000	-.9391	-.1827
	14	-.67267*	.12818	.001	-1.1391	-.2063
	15	-.54610*	.10810	.001	-.9356	-.1566
	16	-.98048*	.09303	.000	-1.3189	-.6421
	17	-.46166*	.09832	.003	-.8169	-.1064
	18	-.41435*	.09923	.011	-.7727	-.0560
	25	-.77737*	.09097	.000	-1.1102	-.4446
	26	-.74183*	.09951	.000	-1.1035	-.3802
	27	-.26728	.11480	.662	-.6858	.1512

*. The mean difference is significant at the 0.05 level.

June: Tukey HSD

Station		Mean Difference (I-J)	Std. Error	Sig.	95% Confidence Interval	
					Lower Bound	Upper Bound
12	13	.11362	.11146	.995	-.2498	.4770
	14	-.17961	.11146	.876	-.5430	.1838
	15	.01732	.10999	1.000	-.3413	.3759
	16	-.14333	.11146	.970	-.5067	.2201
	17	.10814	.10999	.996	-.2504	.4667
	18	.20685	.10999	.729	-.1517	.5654
	25	-.04566	.11490	1.000	-.4202	.3289
	26	.01455	.11490	1.000	-.3600	.3891
	27	.28409	.11490	.328	-.0905	.6587
	28	.53643*	.11490	.000	.1619	.9110
13	12	-.11362	.11146	.995	-.4770	.2498
	14	-.29323	.11146	.241	-.6566	.0702
	15	-.09631	.10999	.999	-.4549	.2623
	16	-.25695	.11146	.435	-.6203	.1064
	17	-.00548	.10999	1.000	-.3641	.3531
	18	.09323	.10999	.999	-.2653	.4518
	25	-.15928	.11490	.950	-.5339	.2153
	26	-.09907	.11490	.999	-.4736	.2755
	27	.17047	.11490	.923	-.2041	.5450
	28	.42281*	.11490	.013	.0482	.7974
14	12	.17961	.11146	.876	-.1838	.5430
	13	.29323	.11146	.241	-.0702	.6566
	15	.19692	.10999	.784	-.1617	.5555
	16	.03628	.11146	1.000	-.3271	.3997
	17	.28775	.10999	.248	-.0708	.6463
	18	.38646*	.10999	.023	.0279	.7450
	25	.13395	.11490	.985	-.2406	.5085
	26	.19416	.11490	.839	-.1804	.5687
	27	.46370*	.11490	.004	.0891	.8383
	28	.71604*	.11490	.000	.3415	1.0906

June: Tukey HSD

Station		Mean Difference (I-J)	Std. Error	Sig.	95% Confidence Interval	
					Lower Bound	Upper Bound
15	12	-.01732	.10999	1.000	-.3759	.3413
	13	.09631	.10999	.999	-.2623	.4549
	14	-.19692	.10999	.784	-.5555	.1617
	16	-.16065	.10999	.931	-.5192	.1979
	17	.09082	.10849	.999	-.2629	.4445
	18	.18953	.10849	.809	-.1642	.5432
	25	-.06297	.11346	1.000	-.4329	.3069
	26	-.00276	.11346	1.000	-.3727	.3671
	27	.26678	.11346	.404	-.1031	.6367
	28	.51912*	.11346	.000	.1492	.8890
16	12	.14333	.11146	.970	-.2201	.5067
	13	.25695	.11146	.435	-.1064	.6203
	14	-.03628	.11146	1.000	-.3997	.3271
	15	.16065	.10999	.931	-.1979	.5192
	17	.25147	.10999	.448	-.1071	.6100
	18	.35018	.10999	.062	-.0084	.7088
	25	.09767	.11490	.999	-.2769	.4722
	26	.15788	.11490	.953	-.2167	.5325
	27	.42742*	.11490	.012	.0528	.8020
	28	.67976*	.11490	.000	.3052	1.0543
17	12	-.10814	.10999	.996	-.4667	.2504
	13	.00548	.10999	1.000	-.3531	.3641
	14	-.28775	.10999	.248	-.6463	.0708
	15	-.09082	.10849	.999	-.4445	.2629
	16	-.25147	.10999	.448	-.6100	.1071
	18	.09871	.10849	.998	-.2550	.4524
	25	-.15380	.11346	.957	-.5237	.2161
	26	-.09359	.11346	.999	-.4635	.2763
	27	.17595	.11346	.900	-.1940	.5459
	28	.42829*	.11346	.010	.0584	.7982

June: Tukey HSD

Station		Mean Difference (I-J)	Std. Error	Sig.	95% Confidence Interval	
					Lower Bound	Upper Bound
18	12	-.20685	.10999	.729	-.5654	.1517
	13	-.09323	.10999	.999	-.4518	.2653
	14	-.38646*	.10999	.023	-.7450	-.0279
	15	-.18953	.10849	.809	-.5432	.1642
	16	-.35018	.10999	.062	-.7088	.0084
	17	-.09871	.10849	.998	-.4524	.2550
	25	-.25251	.11346	.490	-.6224	.1174
	26	-.19230	.11346	.836	-.5622	.1776
	27	.07724	.11346	1.000	-.2927	.4471
	28	.32958	.11346	.130	-.0403	.6995
25	12	.04566	.11490	1.000	-.3289	.4202
	13	.15928	.11490	.950	-.2153	.5339
	14	-.13395	.11490	.985	-.5085	.2406
	15	.06297	.11346	1.000	-.3069	.4329
	16	-.09767	.11490	.999	-.4722	.2769
	17	.15380	.11346	.957	-.2161	.5237
	18	.25251	.11346	.490	-.1174	.6224
	26	.06021	.11823	1.000	-.3252	.4456
	27	.32975	.11823	.171	-.0557	.7152
	28	.58209*	.11823	.000	.1967	.9675
26	12	-.01455	.11490	1.000	-.3891	.3600
	13	.09907	.11490	.999	-.2755	.4736
	14	-.19416	.11490	.839	-.5687	.1804
	15	.00276	.11346	1.000	-.3671	.3727
	16	-.15788	.11490	.953	-.5325	.2167
	17	.09359	.11346	.999	-.2763	.4635
	18	.19230	.11346	.836	-.1776	.5622
	25	-.06021	.11823	1.000	-.4456	.3252
	27	.26954	.11823	.452	-.1159	.6550
	28	.52188*	.11823	.001	.1364	.9073

June: Tukey HSD

Station		Mean Difference (I-J)	Std. Error	Sig.	95% Confidence Interval	
					Lower Bound	Upper Bound
27	12	-.28409	.11490	.328	-.6587	.0905
	13	-.17047	.11490	.923	-.5450	.2041
	14	-.46370*	.11490	.004	-.8383	-.0891
	15	-.26678	.11346	.404	-.6367	.1031
	16	-.42742*	.11490	.012	-.8020	-.0528
	17	-.17595	.11346	.900	-.5459	.1940
	18	-.07724	.11346	1.000	-.4471	.2927
	25	-.32975	.11823	.171	-.7152	.0557
	26	-.26954	.11823	.452	-.6550	.1159
	28	.25234	.11823	.554	-.1331	.6378
28	12	-.53643*	.11490	.000	-.9110	-.1619
	13	-.42281*	.11490	.013	-.7974	-.0482
	14	-.71604*	.11490	.000	-1.0906	-.3415
	15	-.51912*	.11346	.000	-.8890	-.1492
	16	-.67976*	.11490	.000	-1.0543	-.3052
	17	-.42829*	.11346	.010	-.7982	-.0584
	18	-.32958	.11346	.130	-.6995	.0403
	25	-.58209*	.11823	.000	-.9675	-.1967
	26	-.52188*	.11823	.001	-.9073	-.1364
	27	-.25234	.11823	.554	-.6378	.1331

*. The mean difference is significant at the 0.05 level.

July: Dunnet T3

Station		Mean Difference (I-J)	Std. Error	Sig.	95% Confidence Interval	
					Lower Bound	Upper Bound
12.0	13.0	.04229	.12050	1.000	-.3935	.4780
	14.0	-.10780	.15632	1.000	-.6684	.4528
	15.0	-.14072	.14827	1.000	-.6691	.3877
	16.0	-.07479	.12812	1.000	-.5344	.3848
	17.0	.09540	.13013	1.000	-.3703	.5611
	18.0	.12861	.12022	1.000	-.3060	.5632
	25.0	-.15729	.13603	1.000	-.6452	.3306
	26.0	-.02514	.12834	1.000	-.4867	.4364
	27.0	.24823	.12829	.914	-.2132	.7096
	28.0	.42289	.13588	.161	-.0645	.9103
13.0	12.0	-.04229	.12050	1.000	-.4780	.3935
	14.0	-.15009	.13719	1.000	-.6512	.3510
	15.0	-.18301	.12794	.999	-.6441	.2780
	16.0	-.11708	.10392	1.000	-.4882	.2541
	17.0	.05311	.10640	1.000	-.3263	.4325
	18.0	.08632	.09401	1.000	-.2481	.4207
	25.0	-.19958	.11353	.968	-.6099	.2107
	26.0	-.06743	.10419	1.000	-.4418	.3069
	27.0	.20594	.10414	.895	-.1682	.5801
	28.0	.38060	.11335	.095	-.0290	.7902
14.0	12.0	.10780	.15632	1.000	-.4528	.6684
	13.0	.15009	.13719	1.000	-.3510	.6512
	15.0	-.03291	.16212	1.000	-.6115	.5457
	16.0	.03301	.14392	1.000	-.4874	.5535
	17.0	.20320	.14572	.999	-.3223	.7287
	18.0	.23641	.13694	.972	-.2638	.7366
	25.0	-.04949	.15101	1.000	-.5932	.4943
	26.0	.08267	.14412	1.000	-.4392	.6046
	27.0	.35603	.14408	.551	-.1657	.8778
	28.0	.53069	.15087	.062	-.0126	1.0740

July: Dunnet T3

Station		Mean Difference (I-J)	Std. Error	Sig.	95% Confidence Interval	
					Lower Bound	Upper Bound
15.0	12.0	.14072	.14827	1.000	-.3877	.6691
	13.0	.18301	.12794	.999	-.2780	.6441
	14.0	.03291	.16212	1.000	-.5457	.6115
	16.0	.06593	.13514	1.000	-.4174	.5493
	17.0	.23611	.13705	.978	-.2529	.7252
	18.0	.26933	.12768	.820	-.1907	.7294
	25.0	-.01657	.14266	1.000	-.5263	.4931
	26.0	.11558	.13535	1.000	-.3694	.6006
	27.0	.38895	.13531	.270	-.0959	.8738
	28.0	.56361*	.14252	.017	.0544	1.0728
16.0	12.0	.07479	.12812	1.000	-.3848	.5344
	13.0	.11708	.10392	1.000	-.2541	.4882
	14.0	-.03301	.14392	1.000	-.5535	.4874
	15.0	-.06593	.13514	1.000	-.5493	.4174
	17.0	.17019	.11495	.998	-.2387	.5791
	18.0	.20340	.10359	.904	-.1662	.5730
	25.0	-.08250	.12158	1.000	-.5188	.3538
	26.0	.04965	.11291	1.000	-.3544	.4538
	27.0	.32302	.11286	.276	-.0809	.7269
	28.0	.49768*	.12141	.012	.0620	.9333
17.0	12.0	-.09540	.13013	1.000	-.5611	.3703
	13.0	-.05311	.10640	1.000	-.4325	.3263
	14.0	-.20320	.14572	.999	-.7287	.3223
	15.0	-.23611	.13705	.978	-.7252	.2529
	16.0	-.17019	.11495	.998	-.5791	.2387
	18.0	.03321	.10608	1.000	-.3447	.4111
	25.0	-.25269	.12370	.863	-.6955	.1901
	26.0	-.12053	.11520	1.000	-.5319	.2908
	27.0	.15283	.11515	1.000	-.2584	.5640
	28.0	.32749	.12354	.411	-.1147	.7697

July: Dunnet T3

Station		Mean Difference (I-J)	Std. Error	Sig.	95% Confidence Interval	
					Lower Bound	Upper Bound
18.0	12.0	-.12861	.12022	1.000	-.5632	.3060
	13.0	-.08632	.09401	1.000	-.4207	.2481
	14.0	-.23641	.13694	.972	-.7366	.2638
	15.0	-.26933	.12768	.820	-.7294	.1907
	16.0	-.20340	.10359	.904	-.5730	.1662
	17.0	-.03321	.10608	1.000	-.4111	.3447
	25.0	-.28590	.11323	.509	-.6950	.1232
	26.0	-.15375	.10387	.997	-.5266	.2191
	27.0	.11962	.10381	1.000	-.2530	.4923
	28.0	.29428	.11305	.450	-.1141	.7026
25.0	12.0	.15729	.13603	1.000	-.3306	.6452
	13.0	.19958	.11353	.968	-.2107	.6099
	14.0	.04949	.15101	1.000	-.4943	.5932
	15.0	.01657	.14266	1.000	-.4931	.5263
	16.0	.08250	.12158	1.000	-.3538	.5188
	17.0	.25269	.12370	.863	-.1901	.6955
	18.0	.28590	.11323	.509	-.1232	.6950
	26.0	.13215	.12181	1.000	-.3063	.5706
	27.0	.40552	.12177	.098	-.0328	.8438
	28.0	.58018*	.12973	.004	.1139	1.0464
26.0	12.0	.02514	.12834	1.000	-.4364	.4867
	13.0	.06743	.10419	1.000	-.3069	.4418
	14.0	-.08267	.14412	1.000	-.6046	.4392
	15.0	-.11558	.13535	1.000	-.6006	.3694
	16.0	-.04965	.11291	1.000	-.4538	.3544
	17.0	.12053	.11520	1.000	-.2908	.5319
	18.0	.15375	.10387	.997	-.2191	.5266
	25.0	-.13215	.12181	1.000	-.5706	.3063
	27.0	.27337	.11311	.593	-.1332	.6799
	28.0	.44803*	.12165	.040	.0102	.8859

July: Dunnet T3

Station		Mean Difference (I-J)	Std. Error	Sig.	95% Confidence Interval	
					Lower Bound	Upper Bound
27.0	12.0	-.24823	.12829	.914	-.7096	.2132
	13.0	-.20594	.10414	.895	-.5801	.1682
	14.0	-.35603	.14408	.551	-.8778	.1657
	15.0	-.38895	.13531	.270	-.8738	.0959
	16.0	-.32302	.11286	.276	-.7269	.0809
	17.0	-.15283	.11515	1.000	-.5640	.2584
	18.0	-.11962	.10381	1.000	-.4923	.2530
	25.0	-.40552	.12177	.098	-.8438	.0328
	26.0	-.27337	.11311	.593	-.6799	.1332
	28.0	.17466	.12160	.998	-.2630	.6123
28.0	12.0	-.42289	.13588	.161	-.9103	.0645
	13.0	-.38060	.11335	.095	-.7902	.0290
	14.0	-.53069	.15087	.062	-1.0740	.0126
	15.0	-.56361*	.14252	.017	-1.0728	-.0544
	16.0	-.49768*	.12141	.012	-.9333	-.0620
	17.0	-.32749	.12354	.411	-.7697	.1147
	18.0	-.29428	.11305	.450	-.7026	.1141
	25.0	-.58018*	.12973	.004	-1.0464	-.1139
	26.0	-.44803*	.12165	.040	-.8859	-.0102
	27.0	-.17466	.12160	.998	-.6123	.2630

*. The mean difference is significant at the 0.05 level.

August: Tukey HSD

Station		Mean Difference (I-J)	Std. Error	Sig.	95% Confidence Interval	
					Lower Bound	Upper Bound
12.0	13.0	-.06937	.11599	1.000	-.4474	.3086
	14.0	-.45190*	.11764	.008	-.8353	-.0685
	15.0	-.12331	.11450	.992	-.4964	.2498
	16.0	-.11384	.11599	.996	-.4918	.2642
	17.0	.21014	.11450	.758	-.1630	.5833
	18.0	.38283*	.11450	.039	.0097	.7560
	25.0	-.07341	.11599	1.000	-.4514	.3046
	26.0	-.09323	.11599	.999	-.4712	.2848
	27.0	.29715	.11599	.277	-.0808	.6751
	28.0	.52817*	.11599	.000	.1502	.9062
13.0	12.0	.06937	.11599	1.000	-.3086	.4474
	14.0	-.38253*	.11599	.045	-.7605	-.0045
	15.0	-.05394	.11281	1.000	-.4216	.3137
	16.0	-.04447	.11432	1.000	-.4170	.3281
	17.0	.27951	.11281	.324	-.0881	.6471
	18.0	.45220*	.11281	.004	.0846	.8198
	25.0	-.00404	.11432	1.000	-.3766	.3685
	26.0	-.02386	.11432	1.000	-.3964	.3487
	27.0	.36652	.11432	.058	-.0060	.7391
	28.0	.59754*	.11432	.000	.2250	.9701
14.0	12.0	.45190*	.11764	.008	.0685	.8353
	13.0	.38253*	.11599	.045	.0045	.7605
	15.0	.32859	.11450	.141	-.0445	.7017
	16.0	.33807	.11599	.126	-.0399	.7161
	17.0	.66205*	.11450	.000	.2889	1.0352
	18.0	.83473*	.11450	.000	.4616	1.2079
	25.0	.37849*	.11599	.049	.0005	.7565
	26.0	.35867	.11599	.080	-.0193	.7367
	27.0	.74905*	.11599	.000	.3711	1.1271
	28.0	.98007*	.11599	.000	.6021	1.3581

August: Tukey HSD

Station		Mean Difference (I-J)	Std. Error	Sig.	95% Confidence Interval	
					Lower Bound	Upper Bound
15.0	12.0	.12331	.11450	.992	-.2498	.4964
	13.0	.05394	.11281	1.000	-.3137	.4216
	14.0	-.32859	.11450	.141	-.7017	.0445
	16.0	.00947	.11281	1.000	-.3582	.3771
	17.0	.33345	.11127	.103	-.0292	.6961
	18.0	.50614*	.11127	.000	.1435	.8688
	25.0	.04990	.11281	1.000	-.3177	.4175
	26.0	.03008	.11281	1.000	-.3375	.3977
	27.0	.42046*	.11281	.011	.0528	.7881
	28.0	.65148*	.11281	.000	.2839	1.0191
16.0	12.0	.11384	.11599	.996	-.2642	.4918
	13.0	.04447	.11432	1.000	-.3281	.4170
	14.0	-.33807	.11599	.126	-.7161	.0399
	15.0	-.00947	.11281	1.000	-.3771	.3582
	17.0	.32398	.11281	.140	-.0436	.6916
	18.0	.49667*	.11281	.001	.1290	.8643
	25.0	.04043	.11432	1.000	-.3321	.4130
	26.0	.02061	.11432	1.000	-.3520	.3932
	27.0	.41099*	.11432	.018	.0384	.7835
	28.0	.64201*	.11432	.000	.2694	1.0146
17.0	12.0	-.21014	.11450	.758	-.5833	.1630
	13.0	-.27951	.11281	.324	-.6471	.0881
	14.0	-.66205*	.11450	.000	-1.0352	-.2889
	15.0	-.33345	.11127	.103	-.6961	.0292
	16.0	-.32398	.11281	.140	-.6916	.0436
	18.0	.17269	.11127	.900	-.1899	.5353
	25.0	-.28355	.11281	.304	-.6512	.0841
	26.0	-.30337	.11281	.213	-.6710	.0643
	27.0	.08701	.11281	1.000	-.2806	.4546
	28.0	.31803	.11281	.159	-.0496	.6857

August: Tukey HSD

Station		Mean Difference (I-J)	Std. Error	Sig.	95% Confidence Interval	
					Lower Bound	Upper Bound
18.0	12.0	-.38283*	.11450	.039	-.7560	-.0097
	13.0	-.45220*	.11281	.004	-.8198	-.0846
	14.0	-.83473*	.11450	.000	-1.2079	-.4616
	15.0	-.50614*	.11127	.000	-.8688	-.1435
	16.0	-.49667*	.11281	.001	-.8643	-.1290
	17.0	-.17269	.11127	.900	-.5353	.1899
	25.0	-.45624*	.11281	.004	-.8239	-.0886
	26.0	-.47606*	.11281	.002	-.8437	-.1084
	27.0	-.08568	.11281	1.000	-.4533	.2819
	28.0	.14534	.11281	.970	-.2223	.5130
25.0	12.0	.07341	.11599	1.000	-.3046	.4514
	13.0	.00404	.11432	1.000	-.3685	.3766
	14.0	-.37849*	.11599	.049	-.7565	-.0005
	15.0	-.04990	.11281	1.000	-.4175	.3177
	16.0	-.04043	.11432	1.000	-.4130	.3321
	17.0	.28355	.11281	.304	-.0841	.6512
	18.0	.45624*	.11281	.004	.0886	.8239
	26.0	-.01982	.11432	1.000	-.3924	.3527
	27.0	.37056	.11432	.053	-.0020	.7431
	28.0	.60158*	.11432	.000	.2290	.9741
26.0	12.0	.09323	.11599	.999	-.2848	.4712
	13.0	.02386	.11432	1.000	-.3487	.3964
	14.0	-.35867	.11599	.080	-.7367	.0193
	15.0	-.03008	.11281	1.000	-.3977	.3375
	16.0	-.02061	.11432	1.000	-.3932	.3520
	17.0	.30337	.11281	.213	-.0643	.6710
	18.0	.47606*	.11281	.002	.1084	.8437
	25.0	.01982	.11432	1.000	-.3527	.3924
	27.0	.39038*	.11432	.031	.0178	.7629
	28.0	.62140*	.11432	.000	.2488	.9940

August: Tukey HSD

Station		Mean Difference (I-J)	Std. Error	Sig.	95% Confidence Interval	
					Lower Bound	Upper Bound
27.0	12.0	-.29715	.11599	.277	-.6751	.0808
	13.0	-.36652	.11432	.058	-.7391	.0060
	14.0	-.74905*	.11599	.000	-1.1271	-.3711
	15.0	-.42046*	.11281	.011	-.7881	-.0528
	16.0	-.41099*	.11432	.018	-.7835	-.0384
	17.0	-.08701	.11281	1.000	-.4546	.2806
	18.0	.08568	.11281	1.000	-.2819	.4533
	25.0	-.37056	.11432	.053	-.7431	.0020
	26.0	-.39038*	.11432	.031	-.7629	-.0178
	28.0	.23102	.11432	.635	-.1415	.6036
28.0	12.0	-.52817*	.11599	.000	-.9062	-.1502
	13.0	-.59754*	.11432	.000	-.9701	-.2250
	14.0	-.98007*	.11599	.000	-1.3581	-.6021
	15.0	-.65148*	.11281	.000	-1.0191	-.2839
	16.0	-.64201*	.11432	.000	-1.0146	-.2694
	17.0	-.31803	.11281	.159	-.6857	.0496
	18.0	-.14534	.11281	.970	-.5130	.2223
	25.0	-.60158*	.11432	.000	-.9741	-.2290
	26.0	-.62140*	.11432	.000	-.9940	-.2488
	27.0	-.23102	.11432	.635	-.6036	.1415

*. The mean difference is significant at the 0.05 level.

September: Tukey HSD

Station		Mean Difference (I-J)	Std. Error	Sig.	95% Confidence Interval	
					Lower Bound	Upper Bound
12.0	13.0	.00630	.11435	1.000	-.3663	.3789
	14.0	-.21083	.11435	.752	-.5834	.1618
	15.0	-.07155	.11283	1.000	-.4392	.2961
	16.0	-.11807	.11435	.994	-.4907	.2545
	17.0	.34790	.11283	.082	-.0197	.7156
	18.0	.48414*	.11283	.001	.1165	.8518
	25.0	-.11732	.11435	.995	-.4899	.2553
	26.0	.00216	.11435	1.000	-.3704	.3748
	27.0	.40078*	.11435	.024	.0282	.7734
	28.0	.63177*	.11435	.000	.2592	1.0044
13.0	12.0	-.00630	.11435	1.000	-.3789	.3663
	14.0	-.21713	.11435	.717	-.5897	.1555
	15.0	-.07785	.11283	1.000	-.4455	.2898
	16.0	-.12437	.11435	.991	-.4970	.2482
	17.0	.34160	.11283	.095	-.0261	.7093
	18.0	.47784*	.11283	.002	.1102	.8455
	25.0	-.12362	.11435	.992	-.4962	.2490
	26.0	-.00414	.11435	1.000	-.3767	.3684
	27.0	.39448*	.11435	.028	.0219	.7671
	28.0	.62547*	.11435	.000	.2529	.9981
14.0	12.0	.21083	.11435	.752	-.1618	.5834
	13.0	.21713	.11435	.717	-.1555	.5897
	15.0	.13928	.11283	.978	-.2284	.5069
	16.0	.09276	.11435	.999	-.2798	.4653
	17.0	.55873*	.11283	.000	.1911	.9264
	18.0	.69497*	.11283	.000	.3273	1.0626
	25.0	.09351	.11435	.999	-.2791	.4661
	26.0	.21299	.11435	.741	-.1596	.5856
	27.0	.61161*	.11435	.000	.2390	.9842
	28.0	.84260*	.11435	.000	.4700	1.2152

September: Tukey HSD

Station		Mean Difference (I-J)	Std. Error	Sig.	95% Confidence Interval	
					Lower Bound	Upper Bound
15.0	12.0	.07155	.11283	1.000	-.2961	.4392
	13.0	.07785	.11283	1.000	-.2898	.4455
	14.0	-.13928	.11283	.978	-.5069	.2284
	16.0	-.04652	.11283	1.000	-.4142	.3211
	17.0	.41945*	.11130	.010	.0568	.7821
	18.0	.55569*	.11130	.000	.1930	.9183
	25.0	-.04577	.11283	1.000	-.4134	.3219
	26.0	.07371	.11283	1.000	-.2939	.4414
	27.0	.47233*	.11283	.002	.1047	.8400
	28.0	.70332*	.11283	.000	.3357	1.0710
16.0	12.0	.11807	.11435	.994	-.2545	.4907
	13.0	.12437	.11435	.991	-.2482	.4970
	14.0	-.09276	.11435	.999	-.4653	.2798
	15.0	.04652	.11283	1.000	-.3211	.4142
	17.0	.46597*	.11283	.003	.0983	.8336
	18.0	.60221*	.11283	.000	.2346	.9699
	25.0	.00075	.11435	1.000	-.3718	.3733
	26.0	.12023	.11435	.993	-.2524	.4928
	27.0	.51885*	.11435	.001	.1463	.8914
	28.0	.74984*	.11435	.000	.3773	1.1224
17.0	12.0	-.34790	.11283	.082	-.7156	.0197
	13.0	-.34160	.11283	.095	-.7093	.0261
	14.0	-.55873*	.11283	.000	-.9264	-.1911
	15.0	-.41945*	.11130	.010	-.7821	-.0568
	16.0	-.46597*	.11283	.003	-.8336	-.0983
	18.0	.13623	.11130	.979	-.2264	.4989
	25.0	-.46522*	.11283	.003	-.8329	-.0976
	26.0	-.34574	.11283	.086	-.7134	.0219
	27.0	.05288	.11283	1.000	-.3148	.4205
	28.0	.28387	.11283	.302	-.0838	.6515

September: Tukey HSD

Station		Mean Difference (I-J)	Std. Error	Sig.	95% Confidence Interval	
					Lower Bound	Upper Bound
18.0	12.0	-.48414*	.11283	.001	-.8518	-.1165
	13.0	-.47784*	.11283	.002	-.8455	-.1102
	14.0	-.69497*	.11283	.000	-1.0626	-.3273
	15.0	-.55569*	.11130	.000	-.9183	-.1930
	16.0	-.60221*	.11283	.000	-.9699	-.2346
	17.0	-.13623	.11130	.979	-.4989	.2264
	25.0	-.60146*	.11283	.000	-.9691	-.2338
	26.0	-.48198*	.11283	.002	-.8496	-.1143
	27.0	-.08336	.11283	1.000	-.4510	.2843
	28.0	.14763	.11283	.966	-.2200	.5153
25.0	12.0	.11732	.11435	.995	-.2553	.4899
	13.0	.12362	.11435	.992	-.2490	.4962
	14.0	-.09351	.11435	.999	-.4661	.2791
	15.0	.04577	.11283	1.000	-.3219	.4134
	16.0	-.00075	.11435	1.000	-.3733	.3718
	17.0	.46522*	.11283	.003	.0976	.8329
	18.0	.60146*	.11283	.000	.2338	.9691
	26.0	.11948	.11435	.994	-.2531	.4921
	27.0	.51810*	.11435	.001	.1455	.8907
	28.0	.74909*	.11435	.000	.3765	1.1217
26.0	12.0	-.00216	.11435	1.000	-.3748	.3704
	13.0	.00414	.11435	1.000	-.3684	.3767
	14.0	-.21299	.11435	.741	-.5856	.1596
	15.0	-.07371	.11283	1.000	-.4414	.2939
	16.0	-.12023	.11435	.993	-.4928	.2524
	17.0	.34574	.11283	.086	-.0219	.7134
	18.0	.48198*	.11283	.002	.1143	.8496
	25.0	-.11948	.11435	.994	-.4921	.2531
	27.0	.39862*	.11435	.025	.0260	.7712
	28.0	.62961*	.11435	.000	.2570	1.0022

September: Tukey HSD

Station		Mean Difference (I-J)	Std. Error	Sig.	95% Confidence Interval	
					Lower Bound	Upper Bound
27.0	12.0	-.40078*	.11435	.024	-.7734	-.0282
	13.0	-.39448*	.11435	.028	-.7671	-.0219
	14.0	-.61161*	.11435	.000	-.9842	-.2390
	15.0	-.47233*	.11283	.002	-.8400	-.1047
	16.0	-.51885*	.11435	.001	-.8914	-.1463
	17.0	-.05288	.11283	1.000	-.4205	.3148
	18.0	.08336	.11283	1.000	-.2843	.4510
	25.0	-.51810*	.11435	.001	-.8907	-.1455
	26.0	-.39862*	.11435	.025	-.7712	-.0260
	28.0	.23099	.11435	.635	-.1416	.6036
28.0	12.0	-.63177*	.11435	.000	-1.0044	-.2592
	13.0	-.62547*	.11435	.000	-.9981	-.2529
	14.0	-.84260*	.11435	.000	-1.2152	-.4700
	15.0	-.70332*	.11283	.000	-1.0710	-.3357
	16.0	-.74984*	.11435	.000	-1.1224	-.3773
	17.0	-.28387	.11283	.302	-.6515	.0838
	18.0	-.14763	.11283	.966	-.5153	.2200
	25.0	-.74909*	.11435	.000	-1.1217	-.3765
	26.0	-.62961*	.11435	.000	-1.0022	-.2570
	27.0	-.23099	.11435	.635	-.6036	.1416

*. The mean difference is significant at the 0.05 level.

October: Tukey HSD

Station		Mean Difference (I-J)	Std. Error	Sig.	95% Confidence Interval	
					Lower Bound	Upper Bound
12.0	13.0	-.08910	.14573	1.000	-.5649	.3868
	14.0	-.36144	.14573	.324	-.8373	.1144
	15.0	-.20228	.14357	.945	-.6711	.2665
	16.0	-.14708	.14814	.996	-.6308	.3366
	17.0	.10216	.14573	1.000	-.3737	.5780
	18.0	.09455	.14357	1.000	-.3743	.5633
	25.0	-.06956	.14814	1.000	-.5533	.4142
	26.0	.01782	.14814	1.000	-.4659	.5015
	27.0	.28576	.14814	.697	-.1980	.7695
	28.0	.56859*	.14814	.008	.0849	1.0523
13.0	12.0	.08910	.14573	1.000	-.3868	.5649
	14.0	-.27234	.14573	.736	-.7482	.2035
	15.0	-.11319	.14357	.999	-.5820	.3556
	16.0	-.05798	.14814	1.000	-.5417	.4257
	17.0	.19126	.14573	.965	-.2846	.6671
	18.0	.18364	.14357	.971	-.2852	.6524
	25.0	.01954	.14814	1.000	-.4642	.5033
	26.0	.10692	.14814	1.000	-.3768	.5906
	27.0	.37485	.14814	.295	-.1089	.8586
	28.0	.65768*	.14814	.001	.1740	1.1414
14.0	12.0	.36144	.14573	.324	-.1144	.8373
	13.0	.27234	.14573	.736	-.2035	.7482
	15.0	.15915	.14357	.990	-.3096	.6280
	16.0	.21436	.14814	.934	-.2694	.6981
	17.0	.46360	.14573	.063	-.0123	.9394
	18.0	.45598	.14357	.064	-.0128	.9248
	25.0	.29188	.14814	.670	-.1918	.7756
	26.0	.37926	.14814	.279	-.1045	.8630
	27.0	.64719*	.14814	.001	.1635	1.1309
	28.0	.93002*	.14814	.000	.4463	1.4137

October: Tukey HSD

Station		Mean Difference (I-J)	Std. Error	Sig.	95% Confidence Interval	
					Lower Bound	Upper Bound
15.0	12.0	.20228	.14357	.945	-.2665	.6711
	13.0	.11319	.14357	.999	-.3556	.5820
	14.0	-.15915	.14357	.990	-.6280	.3096
	16.0	.05521	.14601	1.000	-.4216	.5320
	17.0	.30445	.14357	.564	-.1644	.7732
	18.0	.29683	.14138	.579	-.1648	.7585
	25.0	.13273	.14601	.998	-.3441	.6095
	26.0	.22010	.14601	.915	-.2567	.6969
	27.0	.48804*	.14601	.040	.0113	.9648
	28.0	.77087*	.14601	.000	.2941	1.2477
16.0	12.0	.14708	.14814	.996	-.3366	.6308
	13.0	.05798	.14814	1.000	-.4257	.5417
	14.0	-.21436	.14814	.934	-.6981	.2694
	15.0	-.05521	.14601	1.000	-.5320	.4216
	17.0	.24924	.14814	.842	-.2345	.7330
	18.0	.24162	.14601	.856	-.2352	.7184
	25.0	.07752	.15051	1.000	-.4139	.5690
	26.0	.16490	.15051	.991	-.3266	.6563
	27.0	.43283	.15051	.140	-.0586	.9243
	28.0	.71566*	.15051	.000	.2242	1.2071
17.0	12.0	-.10216	.14573	1.000	-.5780	.3737
	13.0	-.19126	.14573	.965	-.6671	.2846
	14.0	-.46360	.14573	.063	-.9394	.0123
	15.0	-.30445	.14357	.564	-.7732	.1644
	16.0	-.24924	.14814	.842	-.7330	.2345
	18.0	-.00761	.14357	1.000	-.4764	.4612
	25.0	-.17172	.14814	.986	-.6554	.3120
	26.0	-.08434	.14814	1.000	-.5681	.3994
	27.0	.18359	.14814	.977	-.3001	.6673
	28.0	.46642	.14814	.069	-.0173	.9501

October: Tukey HSD

Station		Mean Difference (I-J)	Std. Error	Sig.	95% Confidence Interval	
					Lower Bound	Upper Bound
18.0	12.0	-.09455	.14357	1.000	-.5633	.3743
	13.0	-.18364	.14357	.971	-.6524	.2852
	14.0	-.45598	.14357	.064	-.9248	.0128
	15.0	-.29683	.14138	.579	-.7585	.1648
	16.0	-.24162	.14601	.856	-.7184	.2352
	17.0	.00761	.14357	1.000	-.4612	.4764
	25.0	-.16410	.14601	.989	-.6409	.3127
	26.0	-.07673	.14601	1.000	-.5535	.4001
	27.0	.19121	.14601	.966	-.2856	.6680
	28.0	.47404	.14601	.053	-.0027	.9508
25.0	12.0	.06956	.14814	1.000	-.4142	.5533
	13.0	-.01954	.14814	1.000	-.5033	.4642
	14.0	-.29188	.14814	.670	-.7756	.1918
	15.0	-.13273	.14601	.998	-.6095	.3441
	16.0	-.07752	.15051	1.000	-.5690	.4139
	17.0	.17172	.14814	.986	-.3120	.6554
	18.0	.16410	.14601	.989	-.3127	.6409
	26.0	.08738	.15051	1.000	-.4041	.5788
	27.0	.35531	.15051	.399	-.1361	.8468
	28.0	.63814*	.15051	.002	.1467	1.1296
26.0	12.0	-.01782	.14814	1.000	-.5015	.4659
	13.0	-.10692	.14814	1.000	-.5906	.3768
	14.0	-.37926	.14814	.279	-.8630	.1045
	15.0	-.22010	.14601	.915	-.6969	.2567
	16.0	-.16490	.15051	.991	-.6563	.3266
	17.0	.08434	.14814	1.000	-.3994	.5681
	18.0	.07673	.14601	1.000	-.4001	.5535
	25.0	-.08738	.15051	1.000	-.5788	.4041
	27.0	.26794	.15051	.790	-.2235	.7594
	28.0	.55077*	.15051	.015	.0593	1.0422

October: Tukey HSD

Station		Mean Difference (I-J)	Std. Error	Sig.	95% Confidence Interval	
					Lower Bound	Upper Bound
27.0	12.0	-.28576	.14814	.697	-.7695	.1980
	13.0	-.37485	.14814	.295	-.8586	.1089
	14.0	-.64719*	.14814	.001	-1.1309	-.1635
	15.0	-.48804*	.14601	.040	-.9648	-.0113
	16.0	-.43283	.15051	.140	-.9243	.0586
	17.0	-.18359	.14814	.977	-.6673	.3001
	18.0	-.19121	.14601	.966	-.6680	.2856
	25.0	-.35531	.15051	.399	-.8468	.1361
	26.0	-.26794	.15051	.790	-.7594	.2235
	28.0	.28283	.15051	.730	-.2086	.7743
28.0	12.0	-.56859*	.14814	.008	-1.0523	-.0849
	13.0	-.65768*	.14814	.001	-1.1414	-.1740
	14.0	-.93002*	.14814	.000	-1.4137	-.4463
	15.0	-.77087*	.14601	.000	-1.2477	-.2941
	16.0	-.71566*	.15051	.000	-1.2071	-.2242
	17.0	-.46642	.14814	.069	-.9501	.0173
	18.0	-.47404	.14601	.053	-.9508	.0027
	25.0	-.63814*	.15051	.002	-1.1296	-.1467
	26.0	-.55077*	.15051	.015	-1.0422	-.0593
	27.0	-.28283	.15051	.730	-.7743	.2086

*. The mean difference is significant at the 0.05 level.

November: Dunnet T3

Station		Mean Difference (I-J)	Std. Error	Sig.	95% Confidence Interval	
					Lower Bound	Upper Bound
12.0	13.0	-.23204	.11854	.905	-.6570	.1930
	14.0	-.55104*	.13204	.011	-1.0273	-.0748
	15.0	-.41419	.14343	.268	-.9325	.1041
	16.0	-.46984*	.10903	.006	-.8600	-.0797
	17.0	-.15077	.13708	1.000	-.6446	.3431
	18.0	-.21484	.12777	.983	-.6732	.2435
	25.0	-.34507	.10369	.097	-.7170	.0269
	26.0	-.34195	.10429	.109	-.7160	.0321
	27.0	-.15327	.11902	1.000	-.5814	.2748
	28.0	.32531	.10980	.225	-.0685	.7191
13.0	12.0	.23204	.11854	.905	-.1930	.6570
	14.0	-.31900	.14044	.707	-.8226	.1846
	15.0	-.18216	.15121	1.000	-.7247	.3604
	16.0	-.23780	.11908	.886	-.6646	.1890
	17.0	.08127	.14520	1.000	-.4387	.6012
	18.0	.01719	.13644	1.000	-.4703	.5047
	25.0	-.11303	.11420	1.000	-.5242	.2981
	26.0	-.10991	.11475	1.000	-.5228	.3030
	27.0	.07877	.12828	1.000	-.3813	.5388
	28.0	.55734*	.11978	.002	.1274	.9873
14.0	12.0	.55104*	.13204	.011	.0748	1.0273
	13.0	.31900	.14044	.707	-.1846	.8226
	15.0	.13684	.16200	1.000	-.4420	.7157
	16.0	.08120	.13252	1.000	-.3966	.5589
	17.0	.40026	.15641	.479	-.1582	.9588
	18.0	.33619	.14831	.712	-.1936	.8660
	25.0	.20597	.12816	.990	-.2587	.6707
	26.0	.20909	.12864	.988	-.2571	.6753
	27.0	.39777	.14085	.300	-.1080	.9035
	28.0	.87634*	.13315	.000	.3961	1.3566

November: Dunnet T3

Station		Mean Difference (I-J)	Std. Error	Sig.	95% Confidence Interval	
					Lower Bound	Upper Bound
15.0	12.0	.41419	.14343	.268	-.1041	.9325
	13.0	.18216	.15121	1.000	-.3604	.7247
	14.0	-.13684	.16200	1.000	-.7157	.4420
	16.0	-.05565	.14388	1.000	-.5753	.4640
	17.0	.26342	.16614	.993	-.3288	.8557
	18.0	.19935	.15855	1.000	-.3668	.7655
	25.0	.06912	.13987	1.000	-.4390	.5772
	26.0	.07224	.14032	1.000	-.4371	.5816
	27.0	.26093	.15158	.977	-.2835	.8053
	28.0	.73950*	.14446	.001	.2177	1.2613
16.0	12.0	.46984*	.10903	.006	.0797	.8600
	13.0	.23780	.11908	.886	-.1890	.6646
	14.0	-.08120	.13252	1.000	-.5589	.3966
	15.0	.05565	.14388	1.000	-.4640	.5753
	17.0	.31907	.13755	.670	-.1762	.8144
	18.0	.25500	.12827	.891	-.2050	.7150
	25.0	.12477	.10430	1.000	-.2494	.4989
	26.0	.12789	.10490	1.000	-.2484	.5042
	27.0	.31657	.11955	.416	-.1133	.7464
	28.0	.79515*	.11038	.000	.3993	1.1910
17.0	12.0	.15077	.13708	1.000	-.3431	.6446
	13.0	-.08127	.14520	1.000	-.6012	.4387
	14.0	-.40026	.15641	.479	-.9588	.1582
	15.0	-.26342	.16614	.993	-.8557	.3288
	16.0	-.31907	.13755	.670	-.8144	.1762
	18.0	-.06407	.15282	1.000	-.6091	.4810
	25.0	-.19430	.13335	.998	-.6772	.2886
	26.0	-.19118	.13382	.998	-.6755	.2931
	27.0	-.00250	.14559	1.000	-.5245	.5195
	28.0	.47608	.13816	.074	-.0216	.9737

November: Dunnet T3

Station		Mean Difference (I-J)	Std. Error	Sig.	95% Confidence Interval	
					Lower Bound	Upper Bound
18.0	12.0	.21484	.12777	.983	-.2435	.6732
	13.0	-.01719	.13644	1.000	-.5047	.4703
	14.0	-.33619	.14831	.712	-.8660	.1936
	15.0	-.19935	.15855	1.000	-.7655	.3668
	16.0	-.25500	.12827	.891	-.7150	.2050
	17.0	.06407	.15282	1.000	-.4810	.6091
	25.0	-.13023	.12375	1.000	-.5762	.3158
	26.0	-.12711	.12426	1.000	-.5747	.3205
	27.0	.06158	.13685	1.000	-.4282	.5514
	28.0	.54015*	.12892	.010	.0775	1.0028
25.0	12.0	.34507	.10369	.097	-.0269	.7170
	13.0	.11303	.11420	1.000	-.2981	.5242
	14.0	-.20597	.12816	.990	-.6707	.2587
	15.0	-.06912	.13987	1.000	-.5772	.4390
	16.0	-.12477	.10430	1.000	-.4989	.2494
	17.0	.19430	.13335	.998	-.2886	.6772
	18.0	.13023	.12375	1.000	-.3158	.5762
	26.0	.00312	.09933	1.000	-.3539	.3601
	27.0	.19180	.11470	.983	-.2227	.6063
	28.0	.67038*	.10510	.000	.2922	1.0485
26.0	12.0	.34195	.10429	.109	-.0321	.7160
	13.0	.10991	.11475	1.000	-.3030	.5228
	14.0	-.20909	.12864	.988	-.6753	.2571
	15.0	-.07224	.14032	1.000	-.5816	.4371
	16.0	-.12789	.10490	1.000	-.5042	.2484
	17.0	.19118	.13382	.998	-.2931	.6755
	18.0	.12711	.12426	1.000	-.3205	.5747
	25.0	-.00312	.09933	1.000	-.3601	.3539
	27.0	.18868	.11524	.987	-.2275	.6049
	28.0	.66726*	.10570	.000	.2870	1.0475

November: Dunnet T3

Station		Mean Difference (I-J)	Std. Error	Sig.	95% Confidence Interval	
					Lower Bound	Upper Bound
27.0	12.0	.15327	.11902	1.000	-.2748	.5814
	13.0	-.07877	.12828	1.000	-.5388	.3813
	14.0	-.39777	.14085	.300	-.9035	.1080
	15.0	-.26093	.15158	.977	-.8053	.2835
	16.0	-.31657	.11955	.416	-.7464	.1133
	17.0	.00250	.14559	1.000	-.5195	.5245
	18.0	-.06158	.13685	1.000	-.5514	.4282
	25.0	-.19180	.11470	.983	-.6063	.2227
	26.0	-.18868	.11524	.987	-.6049	.2275
	28.0	.47857*	.12025	.018	.0457	.9115
28.0	12.0	-.32531	.10980	.225	-.7191	.0685
	13.0	-.55734*	.11978	.002	-.9873	-.1274
	14.0	-.87634*	.13315	.000	-1.3566	-.3961
	15.0	-.73950*	.14446	.001	-1.2613	-.2177
	16.0	-.79515*	.11038	.000	-1.1910	-.3993
	17.0	-.47608	.13816	.074	-.9737	.0216
	18.0	-.54015*	.12892	.010	-1.0028	-.0775
	25.0	-.67038*	.10510	.000	-1.0485	-.2922
	26.0	-.66726*	.10570	.000	-1.0475	-.2870
	27.0	-.47857*	.12025	.018	-.9115	-.0457

*. The mean difference is significant at the 0.05 level.

December: Dunnet T3

Station		Mean Difference (I-J)	Std. Error	Sig.	95% Confidence Interval	
					Lower Bound	Upper Bound
12.0	13.0	-.22505	.16301	.999	-.8162	.3661
	14.0	-.55933	.15970	.070	-1.1403	.0217
	15.0	-.36826	.16031	.686	-.9490	.2124
	16.0	-.44364	.13034	.113	-.9379	.0506
	17.0	.10312	.15971	1.000	-.4756	.6818
	18.0	.15571	.15642	1.000	-.4120	.7235
	25.0	-.39879	.14223	.329	-.9239	.1263
	26.0	-.28029	.13088	.786	-.7760	.2154
	27.0	-.01215	.15244	1.000	-.5698	.5455
	28.0	.09688	.17536	1.000	-.5427	.7365
13.0	12.0	.22505	.16301	.999	-.3661	.8162
	14.0	-.33428	.15265	.765	-.8872	.2186
	15.0	-.14321	.15328	1.000	-.6957	.4092
	16.0	-.21860	.12159	.950	-.6737	.2365
	17.0	.32816	.15266	.794	-.2221	.8784
	18.0	.38075	.14921	.488	-.1575	.9190
	25.0	-.17375	.13426	1.000	-.6644	.3169
	26.0	-.05524	.12217	1.000	-.5121	.4016
	27.0	.21290	.14503	.997	-.3143	.7401
	28.0	.32193	.16896	.921	-.2944	.9382
14.0	12.0	.55933	.15970	.070	-.0217	1.1403
	13.0	.33428	.15265	.765	-.2186	.8872
	15.0	.19107	.14976	1.000	-.3500	.7321
	16.0	.11569	.11711	1.000	-.3246	.5559
	17.0	.66245*	.14912	.005	.1236	1.2012
	18.0	.71504*	.14558	.001	.1886	1.2414
	25.0	.16054	.13022	1.000	-.3167	.6378
	26.0	.27904	.11771	.630	-.1631	.7212
	27.0	.54718*	.14130	.028	.0320	1.0624
	28.0	.65621*	.16577	.024	.0493	1.2632

December: Dunnet T3

Station		Mean Difference (I-J)	Std. Error	Sig.	95% Confidence Interval	
					Lower Bound	Upper Bound
15.0	12.0	.36826	.16031	.686	-.2124	.9490
	13.0	.14321	.15328	1.000	-.4092	.6957
	14.0	-.19107	.14976	1.000	-.7321	.3500
	16.0	-.07538	.11793	1.000	-.5129	.3621
	17.0	.47138	.14976	.150	-.0669	1.0096
	18.0	.52397	.14624	.052	-.0018	1.0497
	25.0	-.03053	.13096	1.000	-.5063	.4452
	26.0	.08797	.11853	1.000	-.3515	.5274
	27.0	.35611	.14198	.523	-.1582	.8704
	28.0	.46514	.16635	.327	-.1416	1.0719
16.0	12.0	.44364	.13034	.113	-.0506	.9379
	13.0	.21860	.12159	.950	-.2365	.6737
	14.0	-.11569	.11711	1.000	-.5559	.3246
	15.0	.07538	.11793	1.000	-.3621	.5129
	17.0	.54676*	.11712	.005	.1125	.9810
	18.0	.59935*	.11259	.001	.1831	1.0156
	25.0	.04485	.09187	1.000	-.2930	.3827
	26.0	.16335	.07306	.732	-.1023	.4290
	27.0	.43150*	.10699	.027	.0294	.8335
	28.0	.54052*	.13770	.042	.0113	1.0698
17.0	12.0	-.10312	.15971	1.000	-.6818	.4756
	13.0	-.32816	.15266	.794	-.8784	.2221
	14.0	-.66245*	.14912	.005	-1.2012	-.1236
	15.0	-.47138	.14976	.150	-1.0096	.0669
	16.0	-.54676*	.11712	.005	-.9810	-.1125
	18.0	.05259	.14559	1.000	-.4708	.5759
	25.0	-.50191*	.13023	.028	-.9748	-.0290
	26.0	-.38341	.11772	.137	-.8196	.0528
	27.0	-.11527	.14130	1.000	-.6271	.3966
	28.0	-.00624	.16578	1.000	-.6111	.5986

December: Dunnet T3

Station		Mean Difference (I-J)	Std. Error	Sig.	95% Confidence Interval	
					Lower Bound	Upper Bound
18.0	12.0	-.15571	.15642	1.000	-.7235	.4120
	13.0	-.38075	.14921	.488	-.9190	.1575
	14.0	-.71504*	.14558	.001	-1.2414	-.1886
	15.0	-.52397	.14624	.052	-1.0497	.0018
	16.0	-.59935*	.11259	.001	-1.0156	-.1831
	17.0	-.05259	.14559	1.000	-.5759	.4708
	25.0	-.55450*	.12617	.006	-1.0119	-.0971
	26.0	-.43600*	.11321	.034	-.8543	-.0177
	27.0	-.16786	.13757	1.000	-.6662	.3305
	28.0	-.05883	.16260	1.000	-.6537	.5360
25.0	12.0	.39879	.14223	.329	-.1263	.9239
	13.0	.17375	.13426	1.000	-.3169	.6644
	14.0	-.16054	.13022	1.000	-.6378	.3167
	15.0	.03053	.13096	1.000	-.4452	.5063
	16.0	-.04485	.09187	1.000	-.3827	.2930
	17.0	.50191*	.13023	.028	.0290	.9748
	18.0	.55450*	.12617	.006	.0971	1.0119
	26.0	.11850	.09264	1.000	-.2225	.4595
	27.0	.38665	.12120	.150	-.0574	.8307
	28.0	.49567	.14901	.123	-.0606	1.0519
26.0	12.0	.28029	.13088	.786	-.2154	.7760
	13.0	.05524	.12217	1.000	-.4016	.5121
	14.0	-.27904	.11771	.630	-.7212	.1631
	15.0	-.08797	.11853	1.000	-.5274	.3515
	16.0	-.16335	.07306	.732	-.4290	.1023
	17.0	.38341	.11772	.137	-.0528	.8196
	18.0	.43600*	.11321	.034	.0177	.8543
	25.0	-.11850	.09264	1.000	-.4595	.2225
	27.0	.26814	.10765	.543	-.1361	.6724
	28.0	.37717	.13821	.394	-.1533	.9077

December: Dunnet T3

Station		Mean Difference (I-J)	Std. Error	Sig.	95% Confidence Interval	
					Lower Bound	Upper Bound
27.0	12.0	.01215	.15244	1.000	-.5455	.5698
	13.0	-.21290	.14503	.997	-.7401	.3143
	14.0	-.54718*	.14130	.028	-1.0624	-.0320
	15.0	-.35611	.14198	.523	-.8704	.1582
	16.0	-.43150*	.10699	.027	-.8335	-.0294
	17.0	.11527	.14130	1.000	-.3966	.6271
	18.0	.16786	.13757	1.000	-.3305	.6662
	25.0	-.38665	.12120	.150	-.8307	.0574
	26.0	-.26814	.10765	.543	-.6724	.1361
	28.0	.10903	.15878	1.000	-.4765	.6946
28.0	12.0	-.09688	.17536	1.000	-.7365	.5427
	13.0	-.32193	.16896	.921	-.9382	.2944
	14.0	-.65621*	.16577	.024	-1.2632	-.0493
	15.0	-.46514	.16635	.327	-1.0719	.1416
	16.0	-.54052*	.13770	.042	-1.0698	-.0113
	17.0	.00624	.16578	1.000	-.5986	.6111
	18.0	.05883	.16260	1.000	-.5360	.6537
	25.0	-.49567	.14901	.123	-1.0519	.0606
	26.0	-.37717	.13821	.394	-.9077	.1533
	27.0	-.10903	.15878	1.000	-.6946	.4765

*. The mean difference is significant at the 0.05 level.

VITA

TARA BLAKEY

Born, Miami, Florida

2000-2004	B.S., Civil Engineering University of Florida Gainesville, Florida
2004-2006	M.S., Transportation Massachusetts Institute of Technology Cambridge, Massachusetts
2011-2013	NASA Waterscapes Fellow
2013-2015	Doctoral Candidate Florida International University Miami, Florida
2014	Teaching Assistant Florida International University Miami, Florida
2014-2015	McKnight Dissertation Fellow

PUBLICATIONS

Blakey T, Melesse A, Rousseaux C (2015). Toward connecting subtropical algal blooms to freshwater nutrient sources using a long-term, spatially distributed, in situ chlorophyll-*a* record. CATENA, 133, 119-127.

Blakey T, Melesse A, Hall M (2015). Supervised Classification of Benthic Reflectance in Shallow Subtropical Waters Using a Generalized Pixel-Based Classifier across a Time Series. Remote Sensing, 7, 5098-5116.